Notes: These are notes live-tex'd from a graduate course in Floer Homology taught by Akram Alishahi at the University of Georgia in Spring 2021. As such, any errors or inaccuracies are almost certainly my own.

Floer Homology

Lectures by Akram Alishahi. University of Georgia, Spring 2021

D. Zack Garza

D. Zack Garza
University of Georgia
[*dzackgarza@gmail.com*](dzackgarza@gmail.com)

Last updated: 2021-05-02

Table of Contents

Contents

1 | Lecture 1: Overview (Wednesday, January 13)

1.1 Course Logistics

> *Note (DZG): Everything in this section comes from Akram!*

1.1.1 Description

"I am teaching a topics course about Heegaard Floer homology next semester. Heegaard Floer homology was defined by Peter Ozsváth and Zoltan Szabó around 2000. It is a package of powerful invariants of smooth 3- and 4-manifolds, knots/links and contact structures. Over the last two decades, it has become a central tool in low-dimensional topology. It has been used extensively to study and resolve important questions concerning unknotting number, slice genus, knot concordance and Dehn surgery. It has been employed in critical ways to study taut foliations, contact structures and smooth 4-manifolds. There are also many rich connections between Heegaard Floer homology and other manifold and knot invariants coming from gauge theory as well as representation theory. We will learn the basic construction of Heegaard Floer homology, starting with the definition of the 3-manifold and knot invariants. In the second half of this course, we will turn to computations and applications of the theory to low-dimensional topology and knot theory. In particular, several numerical invariants have been defined using this homological invariants. At the end of the semester, I would expect each one of you to learn the construction of one of these invariants (of course with my help) and present it to the class."

1.1.2 Expository Papers

- [**G**] J. Greene, Heegaard Floer homology
- [**H**] J. Hom, Lecture notes on Heegaard Floer homology
- [**L**] R. Lipshitz, Heegaard Floer homologies
- [**M**] C. Manolescu, An introduction to knot Floer homology
- [**OS-1**] P. Ozsváth and Z. Szabó, An introduction to Heegaard Floer homology
- [**OS-2**] P. Ozsváth and Z. Szabó, Lectures on Heegaard Floer homology
- [**OS-3**] P. Ozsváth and Z. Szabó, Heegaard diagrams and holomorphic disks

1.1.3 Research Papers

- [**OSz04a**] Peter Ozsváth and Zoltán Szabó, Holomorphic disks and topological invariants for closed three-manifolds. Ann. of Math. (2) 159 (2004), no. 3, 1027–1158. arXiv:math/0101206

- [**OSz04b**] Peter Ozsváth and Zoltán Szabó, Holomorphic disks and three-manifold invariants: properties and applications. Ann. of Math. (2) 159 (2004), no. 3, 1159–1245. arXiv:math/0105202
- [**OSz04c**] Peter Ozsváth and Zoltán Szabó, Holomorphic disks and knot invariants. Adv. Math. 186 (2004), no. 1, 58–116. arXiv:math/0209056
- [**OSz06**] Peter Ozsváth and Zoltán Szabó, Holomorphic triangles and invariants for smooth four manifolds. Adv. Math. 202 (2006), no. 2, 326–400. arXiv:math/0110169
- [**Per08**] Timothy Perutz, Hamiltonian handleslides for Heegaard Floer homology. Proceedings of Gökova Geometry-Topology Conference 2007, 15–35, Gökova Geometry/Topology Conference (GGT), Gökova, 2008. arXiv:0801.0564

1.1.4 Basic Morse Theory, Symplectic Geometry and Floer Homology

- [**Mi-1**] Milnor, Morse theory
- [**Mi-2**] Milnor, Lectures on the h-cobordism theorem
- [**Ca**] A. Cannas da Silva. Lectures on Symplectic Geometry
- [**Mc**] D. McDuff, Floer theory and low-dimensional topology
- [**AD**] M. Audin and M. Damian, Morse theory and Floer homology
- [**Hu**] M. Hutchings, Lecture notes on Morse homology (with an eye towards Floer theory and pseudoholomorphic curves)

1.1.5 Low-dimensional Topology

- [**S**] N. Saveliev, Lectures on the topology of 3-manifolds
- [**R**] D. Rolfsen, Knots and links
- [**GS**] R. Gompf and A. Stipsicz, 4-manifolds and Kirby calculus
- [**L**] R. Lickorish, An introduction to knot theory

1.1.6 Suggested Topics for Presentations

- [**SW**] S. Sarkar and J. Wang, [An algorithm for computing some Heegaard Floer homologies, Ann. of Math., 171 (2010), 1213–1236, arXiv:math/0607777.

- Grid homology from:

  - C. Manolescu and P. Ozsváth and S. Sarkar, A combinatorial description of knot Floer homology, Ann. of Math., 169 (2009), 633–660, arXiv:math/0607691.

  - P. Ozsváth and A. Stipsicz and Z. Szabó, Grid Homology for Knots and Links,

    ◇ Also available here with comment: please go and buy a hard copy, too!

- J. Hom, A survey on Heegaard Floer homology and concordance J. of Knot Theo. and Its Ram.(2) 26 (2017) arXiv:1512.00383

- K. Honda and W. Kazez and G. Matić, On the contact class in Heegaard Floer homology, J. Differential Geom. (2) 83 (2009), 289-311, arXiv:math/0609734

- Sutured Floer homology from:

  - [**L**] Lipshitz expository paper listed above
  - A. Juhász Holomorphic discs and sutured manifolds Algebr. Geom. Topol., (3) 6 (2006), 1429-1457, arXiv:math/0601443
  - A. Juhász, Knot Floer homology and Seifert surfaces Algebr. Geom. Topol., (1) 8 (2008), 603-608 arxiv:math/0702514

> Convert to bibtex?

1.2 Intro and Motivation

Remark 1.2.1: We'll assume everything is smooth and oriented.

> **Proposition 1.2.2***(Osvath-Szabo (2000)).*
> To closed 3-manifolds M we can assign a graded abelian group $\widehat{HF}(M)$, which can be computed combinatorially [a] . There are several variants:
>
> - $HF^- \in \mathsf{grMod}(\mathbb{Z}_2[u])$, [b]
>
> - $HF^+ \in \mathsf{Mod}(\mathbb{Z}_2[u, u^{-1}]/u\mathbb{Z}_2[u])$.
>
> - $HF^\infty \in \mathsf{grMod}(\mathbb{Z}_2[u, u^{-1}])$,
>
> HF^+ and HF^∞ can be computed using HF^-. In general, we'll write HF^- to denote constructions that work with any of the above variants.
>
> ---
> [a] See Sarkour-Wang
> [b] This is the strongest variant.

Remark 1.2.3: Note that $\mathbb{Z}_2$ can be replaced with $\mathbb{Z}$, but it's technical and we won't discuss it here. For the first half of the course, we'll just discuss $\widehat{HF}$, and we'll discuss the latter 3 in the second half.

1.3 Geometric Information

Remark 1.3.1: These invariants can be used to compute the **Thurston seminorm** of a 3-manifold:

Definition 1.3.2 (Thurston Seminorm)
A homology class $\alpha \in H_2(M)$ can be represented as $\alpha \in [S]$ for S a closed surface whose fundamental class represents α where $S = \bigcup\limits_{i=1}^{n} S_i$ can be a union of closed embedded surfaces S_i. Then we first compute

$$\max\{0, -\chi(S_i)\} = \begin{cases} 0 & \text{if } S_i \cong \mathbb{S}^2, \mathbb{T}^2 \\ \\ -\chi(S_i) = 2g(S_i) - 2 & \text{else.} \end{cases}$$

Note that the max checks if χ is positive. Then define

$$\|\alpha\| := \min_S \left(\sum_{i=1}^{n} \max\{0, -\chi(S_i)\} \right),$$

where we sum over the embedded subsurfaces and check which overall surface gives the smallest norm.

Remark 1.3.3: Note that this can't be a norm, since if $\mathbb{S}^2, \mathbb{T}^2 \in [S] \implies \|\alpha\| = 0$.

Theorem 1.3.4 *(Osvath-Szabo).*
HF detects [a] the Thurston seminorm, and there is a splitting as groups/modules

$$HF^-(M) = \bigoplus_{\mathfrak{s} \in \operatorname{Spin}^c(M)} HF^-(M, S)$$

where $S \in \operatorname{Spin}^c(M)$ is a **spin^c structure**: an oriented 2-dimensional vector bundle on M (up to some equivalence).

---
[a]What does "detect" mean? This is slightly technical.

Remark 1.3.5: The Thurston norm $\|a\|$ can be computed from this data by considering a perturbed version of $\widehat{HF}$, denoted $\underline{\widehat{HF}}$, in the following way: taking the first Chern class $c_1(\mathfrak{s}) \in H^2(M)$ (which can be associated to every 2-dimensional vector bundle), we have

$$\|\alpha\| = \max_{\underline{\widehat{HF}}(M, \mathfrak{s}) \neq 0} |\langle c_1(\mathfrak{s}), \ \alpha \rangle|.$$

Slogan 1.3.6
Floer homology groups split over these spin^c structures and can be used to compute Thurston norms.

Theorem 1.3.7 *(Ni).*
Given $F \subseteq M$ with genus $g \geq 2$, HF detects if M *fibers* over S^1 with F as a fiber, i.e. there exists a fiber bundle

$$F \longleftrightarrow M$$
$$\downarrow \pi$$
$$S^1$$

This uses the existence of the splitting over spin^c structures and uses HF^+ in the following way: such a bundles exists if and only if

$$\bigoplus_{\langle c_1(\mathfrak{s}),\ [F] \rangle = 2g-2} HF^+(M, \mathfrak{s}) = \mathbb{Z}.$$

Definition 1.3.8 (Contact Structure)
Equivalently,

- A smooth oriented nowhere integrable 2-plane field ξ, or

- A 2-plane field $\xi := \ker(\alpha)$ where α is a 1-form such that $\alpha \wedge d\alpha > 0$. [a]

---
[a]Note that wedging to a nontrivial top form is equivalent to being nowhere integrable here.

Example 1.3.9*(?):* The standard contact structure on $\mathbb{R}^3$ is given by

$$\alpha := dz - ydz,$$

which yields the following 2-plane field $\xi := \ker \alpha$:
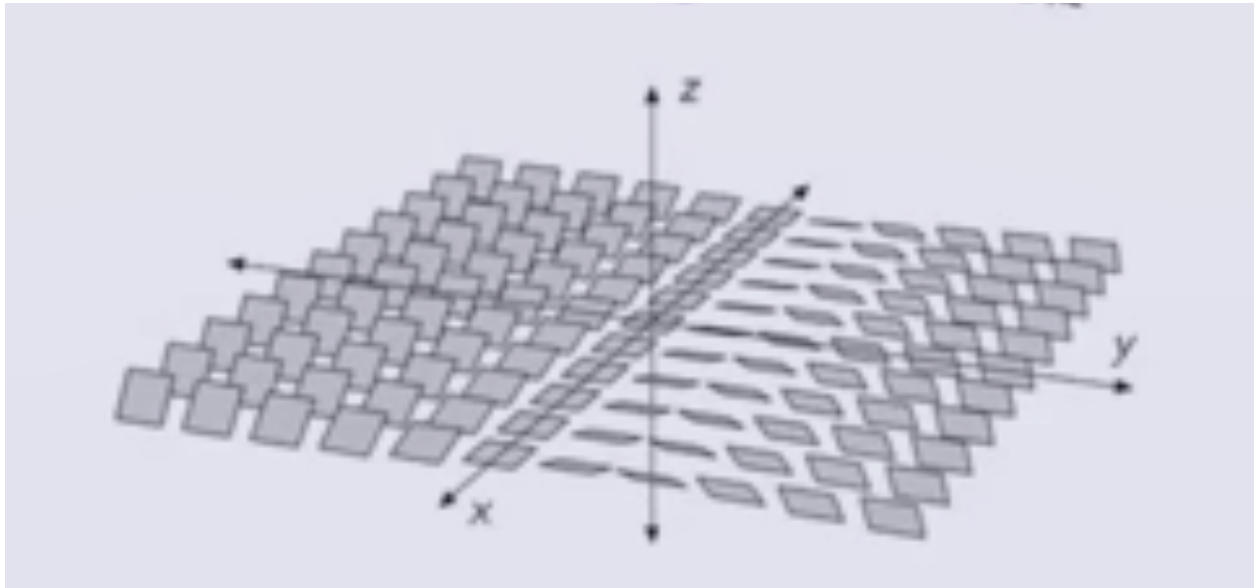

Figure 1: 2-Plane Field in $\mathbb{R}^3$

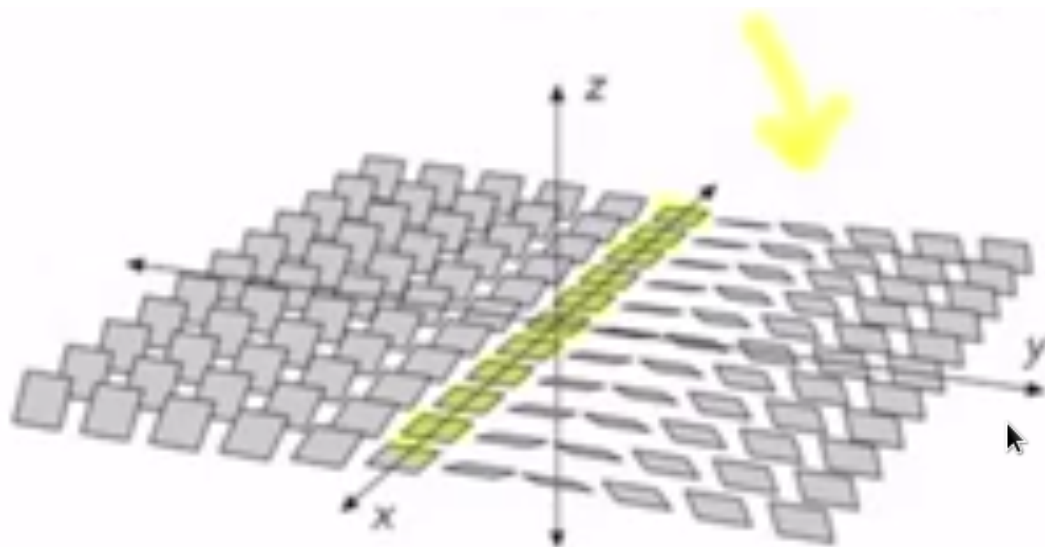You can see that $z = 0 \implies y = 0$, so the xy-plane is in the kernel, yielding the flat planes down the middle:

Figure 2: Flat Planes

Proposition 1.3.10*(Contact Class (Osvath-Szabo-Honda-Kazez-Matic)).*
To each such ξ one can associate a **contact class** $c(\xi) \in \widehat{HF}(-M)$, where $-M$ is M with the reversed orientation.

Remark 1.3.11: This gives obstructions for two of the following important properties of contact structures:

- Being **overtwisted**, or
- Being **Stein fillable**.

Theorem 1.3.12*(?).*

- If ξ is overtwisted, then $c(\xi) = 0$.
- If ξ is Stein fillable, then $c(\xi) \neq 0$.

Remark 1.3.13: We'll also discuss similar invariants for knots that were created after these invariants for manifolds.

Definition 1.3.14 (Knots)
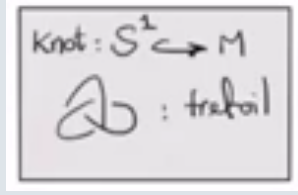Recall that a **knot** is an embedding $S^1 \hookrightarrow M$.

Figure 3: Example: the trefoil knot

Proposition 1.3.15 *(Knot Floer Homology (Ozsváth-Szabó)).*
Given a knot $K \subseteq M$ a 3-manifold (e.g. $M = S^3$), there is extra algebraic structure on $\widehat{CF}(M)$: a filtration. These allow defining a new bigraded abelian group $\widehat{HFK}(M, K)$ (which is also a $\mathbb{Z}_2$-vector space) that takes includes the information of K. This yields a decomposition

$$\widehat{HFK}(M, K) = \bigoplus_{m,a} \widehat{HFK}_m(M, K, a).$$

This similarly works for other variants: there is a filtration on $CF^-(M)$ which yields $HFK^-(M, K)$, a bigraded $\mathbb{Z}_2[u]$-module.

1.3.1 Some properties of Knot Floer Homology

Fact 1.3.16
$\widehat{HFK}(K)$ categorifies the Alexander polynomial $\Delta_K(t)$ of K, i.e. taking the graded Euler characteristic yields

$$\Delta_K(t) = \sum_{m,a} (-1)^m \left(\dim \widehat{HFK}_m(K, a) \right) t^a.$$

Fact 1.3.17
$\widehat{HFK}(K)$ detects the **Seifert genus** of a knot $g(K)$, defined as the smallest g such that there exists an embedded surface [1] F of genus g in S^3 that bounds K, so $\partial F = K$.

Example 1.3.18 *(The Unknot):* The unknot bounds a disc, so its genus is zero:

---

[1] These are referred to as **Seifert surfaces**.

Figure 4: The genus of the unknot

Exercise 1.3.19 (The Trefoil)
Using the "outside" disc on the trefoil, find 3 bands that show its genus is 1.

Figure 5: The genus of the trefoil

The genus can be computed by setting $\widehat{HFK}(K,a) := \bigoplus_m \widehat{HFK}_m(K,a)$, which yields

$$g(k) = \max\left\{a \mid \widehat{HFK}(K,a) \neq 0\right\}.$$

Note that the a grading here is referred to as the **Alexander grading**.

Fact 1.3.20
$\widehat{HFK}$ detects whether or not a knot is **fibered**, where K is fibered if and only if it admits an S^1 family F_t of Seifert surfaces such that $t \neq s \in S^1 \implies F_t \cap F_s = K$. I.e., there is a fibration on the knot complement where each fiber is a Seifert surface:

$$\Sigma_g \longrightarrow S^3 \setminus K$$
$$\downarrow \pi$$
$$K$$

Example 1.3.21 *(The Unknot):* The unknot is fibered by $\mathbb{D}^2$s:
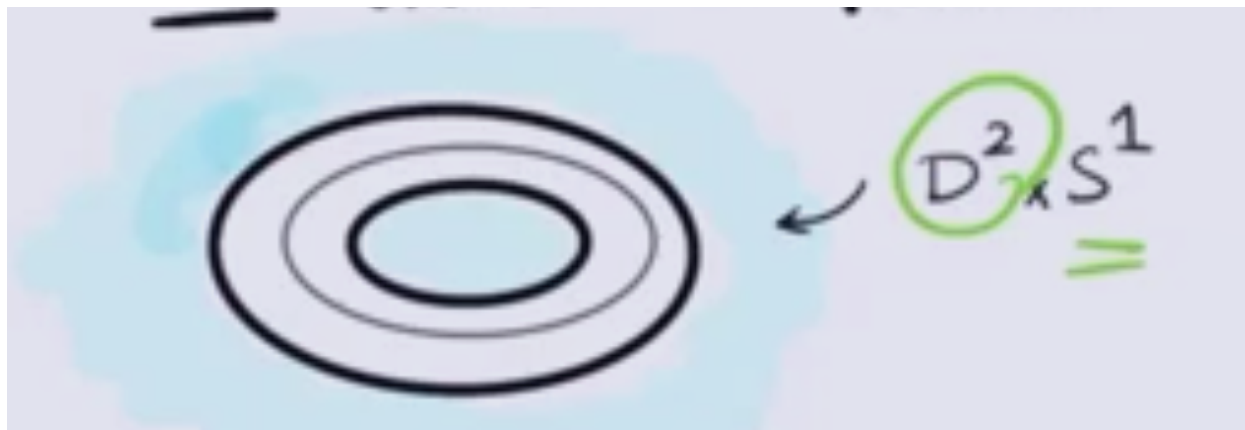

Figure 6: The unknot fibered by discs.

This is "detected" in the following sense: K is fibered if and only if

$$\widehat{HFK}(k, g(K)) = \mathbb{Z}_2.$$

Definition 1.3.22 (Slice Genus)
Let $K \subseteq S^3$. We know $S^3 = \partial B^4$, so we consider all of the smoothly properly embedded surfaces F in B^4 such that $\partial F = K$ and take the smallest genus:
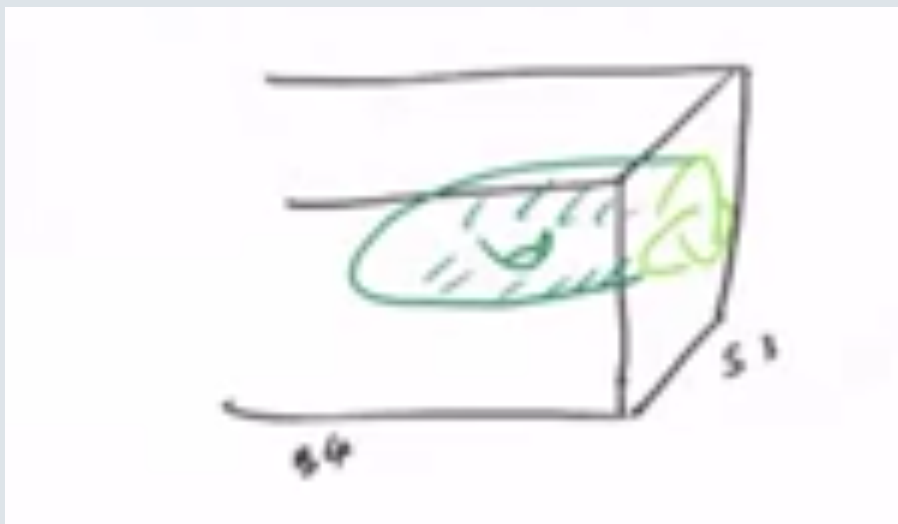

Figure 7: Knot in S^3 bounding a surface in B^4

We thus define the **slice genus** or **4-ball genus** as

$$g_S(K) := g_4(K) := \min \left\{ g(F) \ \middle| \ F \hookrightarrow B^4 \text{ smootherly, properly with } \partial F = K \right\}.$$

Exercise 1.3.23 (?)
Show that $g_4(K) \leq g(K)$.

Definition 1.3.24 (Unknotting number)
Define $u(K)$ the **unknotting number** of K as the minimum number of times that K must cross itself to become unknotted.

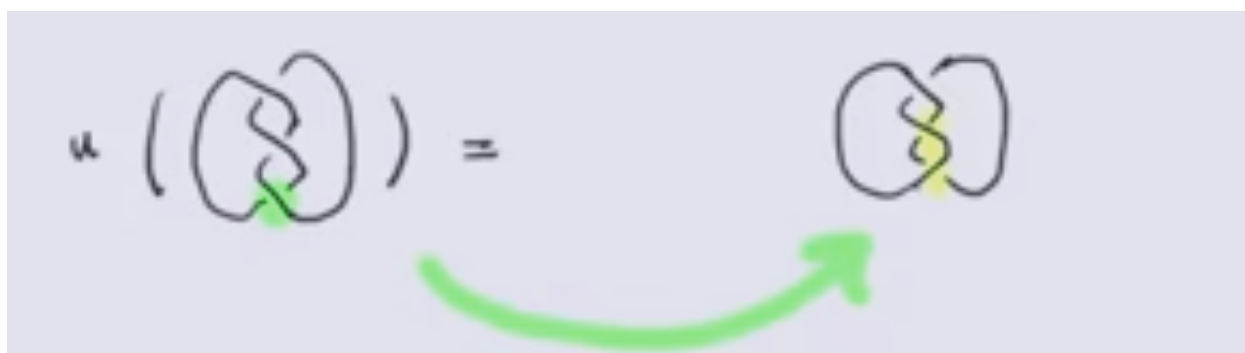**Example 1.3.25** *(The Trefoil):* Consider changing the bottom crossing of a trefoil:

Figure 8: Changing one crossing in the trefoil

This in fact produces the unknot:

Figure 9: Unkink to yield the unknot

Thus $u(K) = 1$, assuming that we know $K \neq 0$ is not the unknot.

Exercise 1.3.26 (?)
Show that $g_f(K) \leq u(K)$.

> *Hint: each crossing change $K \to K'$ yields some surface that is a cobordism from K to K' in B^4, and you can use each step to build your surface.*
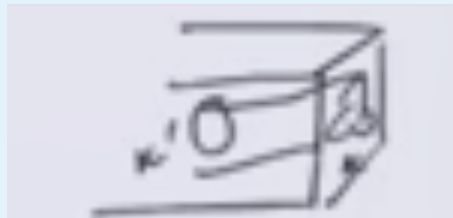

Figure 10: Surface between K and K'

Theorem 1.3.27 *(Ozsváth-Szabó).*
Define an invariant $\tau(K) \in \mathbb{Z}$ from $\widehat{HFK}$ such that $|\tau(K)| \leq g_4(K) \leq u(K)$.

Definition 1.3.28 (Torus Knots $T_{p,q}$)

Recall that we can view $\mathbb{T}^2 := \mathbb{R}^2/\mathbb{Z}^2$ where the action is $(x, y) \xrightarrow{(m,n)} (x + m, y + m)$, i.e. we module out by integer translations. Then for $p, q > 0$ coprime, $T_{p,q}$ is the image of the line $y = mx$ in $\mathbb{T}^2$ where $m = p/q$.

Example 1.3.29 *($T_{2,3}$):* The torus knot $T_{2,3}$ wraps 3 times around the torus in one direction and twice in the other:
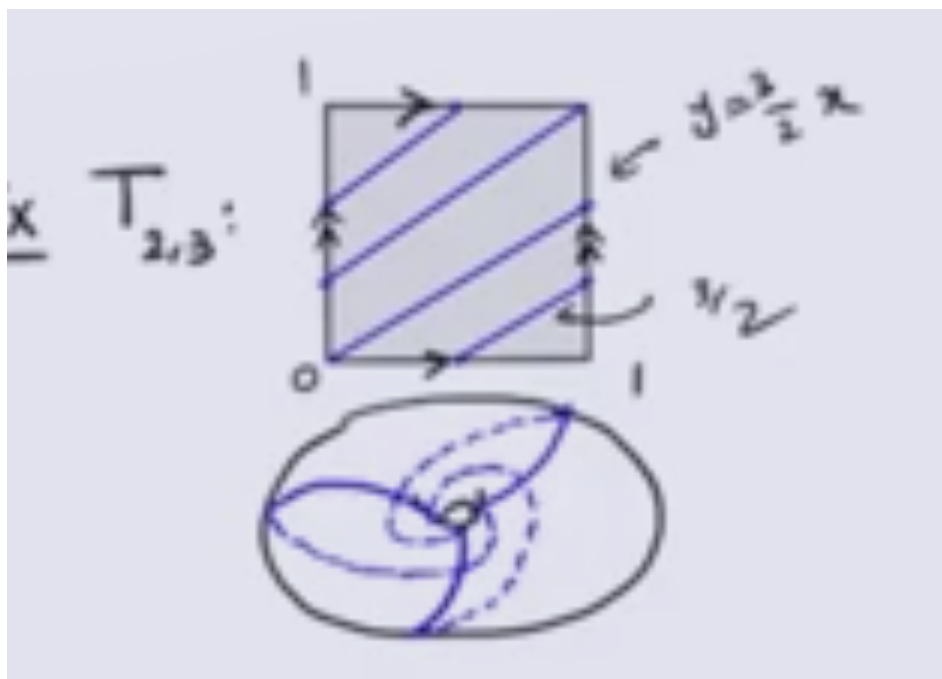
Figure 11: The torus knot $T_{2,3}$

Theorem 1.3.30 *(Milnor).*

$$g_4(T_{p,q}) = u(T_{p,q}) = \frac{(p-1)(1-q)}{2}.$$

- First proved by Kronheimer-Mrowka
- Another proof by Osvath-Szabó using Heegard Floer homology.

Exercise 1.3.31 (?)

Show that $u(T_{p,q}) \leq \dfrac{(p-1)(q-1)}{2}$, i.e. torus knots can be unknotted with this many crossing changes.

Theorem 1.3.32 *(Osvath-Szabó).*

$$\tau(T_{p,q}) = \frac{(p-1)(q-1)}{2},$$

which implies

$$\frac{(p-1)(q-1)}{2} \leq g_4(T_{p,q}) \leq u(T_{p,q}) \leq \frac{(p-1)(q-1)}{2},$$

making all of these equal.

Remark 1.3.33: There are better lower bounds for $u(K)$ defined using $\widehat{HFK}$ which are *not* lower bounds for the slice genus. There are also other lower bounds for the slice genus with different names (see Jen Hom's survey), some of which are stronger than τ.

Remark 1.3.34: Another application of having these lower bounds is that we can construct exotic (or *fake*) $\mathbb{R}^4$s, i.e. 4-manifolds X homeomorphic to $\mathbb{R}^4$ but not diffeomorphic to $\mathbb{R}^4$.

Remark 1.3.35: All of these invariants work nicely in a $(3+1)$-TQFT: we have invariants of 3-manifolds M_i and knots in them, so we can talk about **cobordisms** between them: W^4 a compact oriented 4-manifold with $\partial W^4 = -M_1 \coprod M_2$.
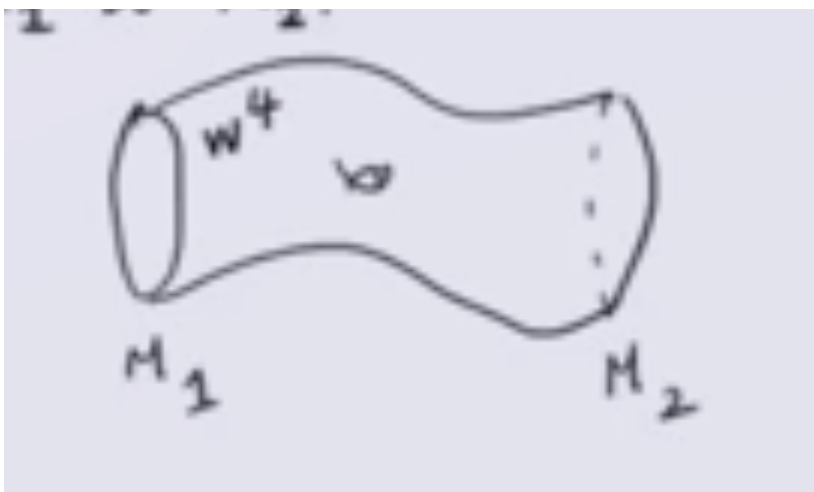

Figure 12: A cobordism

Osvath-Szabó define a map

$$F_{W,t}^- : HF^-(M_1, t|_{M_1}) \to HF^-(M_2, t|_{M_2})$$

using t coming from the splitting of spin^c structure which yields an invariant of closed 4-manifolds referred to as **mixed invariants**.

Similarly, if we have knots in 3-manifolds we can define a cobordism $(M_1, K_1) \to (M_2, K_2)$ as (W^4, F) where W^4 is a cobordism $M_1 \to M_2$ and $F \hookrightarrow W$ is a smoothly embedded surface that is a cobordism from $K_1 \to K_2$ with $F \cap M_i = K_i$ and $\partial F = -K_1 \coprod K_2$.

Figure 13: A cobordism including knots

This similarly yields a map

$$F_{W,Ft}^- : HF^-(M_1, K_1, t|_{M_1}) \to HF^-(M_2, K_2, t|_{M_2})$$

Remark 1.3.36: This smoothly embedded surface in the middle can be used to study other smoothly embedded surfaces in 4-manifolds, which has been done recently.

2 | Lecture 2 (Tuesday, January 19)

Copy in references recommended by Akram!

2.1 Constructing Heegard Floer

Remark 2.1.1: For Morse Theory, there are some good exercises in Audin's book – essentially anything other than the existence questions. The first 8 look good on p. 18.

Today:

1. Overview of the construction of HF, and

2. A discussion of Morse Theory.

First goal: discuss how the name "Heegard" fits in.

Definition 2.1.2 (Genus g handlebody)
A **genus g handlebody** H_g is a compact oriented 3-manifold with boundary obtained from B^3 by attaching g solid handles (a neighborhood of an arc).

Example 2.1.3*(Attaching $g = 2$ handles to a sphere):* For $g = 2$ attached to a sphere, we glue $D^2 \times I$ by its boundary to S^2.
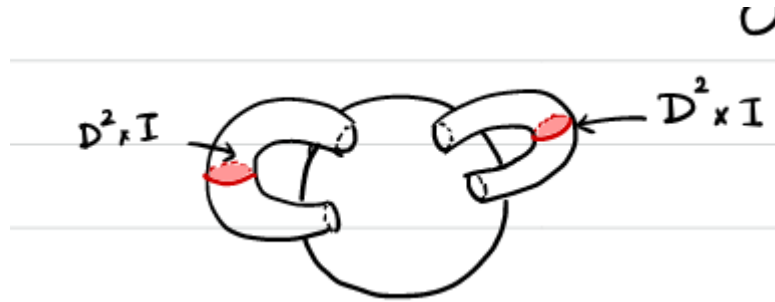

Figure 14: image__2021-01-19-00-35-48

In general, $\partial H_g = \Sigma_g$ is a genus g surface, and $H_g \setminus \coprod_{i=1}^g D_i = B^3$. We can keep track of the data by specifying $(\Sigma, \alpha_1, \alpha_2, \cdots, \alpha_g)$ where $\partial D_i = \alpha_i$.

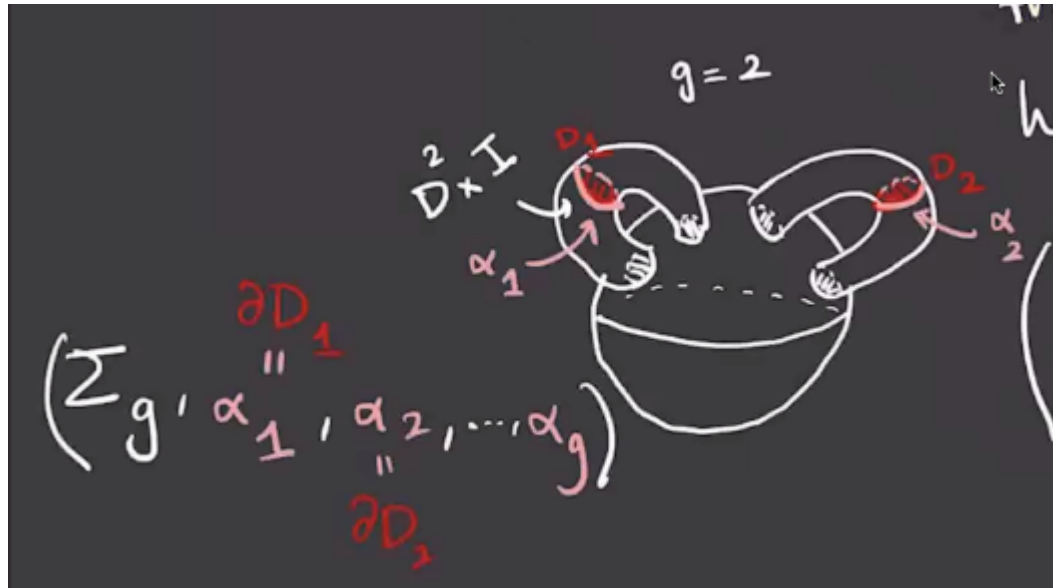Figure 15: Attaching a handlebody

Definition 2.1.4 (Heegard Decomposition)
A **Heegard diagram** is $M = H_1 \cup_\partial H_2$ where H_i are genus g handlebodies and there is a

diffeomorphism $\partial H_1 \to \partial H_2$.

Theorem 2.1.5 *(?)*.
Every closed 3-manifold has a Heegard decomposition, although it is not unique.

Definition 2.1.6 (Heegard Diagram)
A **Heegard diagram** is the data $(\Sigma_g, \alpha = \{\alpha_1, \cdots, \alpha_g\}, \beta = \{\beta_1, \cdots, \beta_g\})$ where the α correspond to H_1 and β to H_2 and $\Sigma_g = \partial H_1 = \partial H_2$.

2.2 Lagrangian Floer Homology

Remark 2.2.1: This is essentially an infinite-dimensional version of Morse homology.

Definition 2.2.2 (Symplectic Manifold)
A **symplectic manifold** is a pair (M^{2n}, ω) such that

- ω is *closed*, i.e. $d\omega = 0$, and
- ω is *nondegenerate*, i.e. $\wedge^n \omega \neq 0$.

Definition 2.2.3 (Lagrangian)
A **Lagrangian submanifold** is an $L^n \subseteq M$ such that $\omega|_L = 0$.

Remark 2.2.4: If $L_1 \cap L_2$ is finitely many points, case we can define a chain complex

$$CF(M^{2n}, L_1, L_2) := \mathbb{Z}_2[L_1 \cap L_2],$$

the $\mathbb{Z}_2$-vector space generated by the intersection points of the Lagrangian submanifolds. We'll define a differential by essentially counting discs between intersection points:

Figure 16: Two intersection points

We'll want to write $\partial x = c_y y + \cdots$ where c_y is some coefficient. How do we compute it? In this case, we have half of the boundary on L_1 and half is on L_2
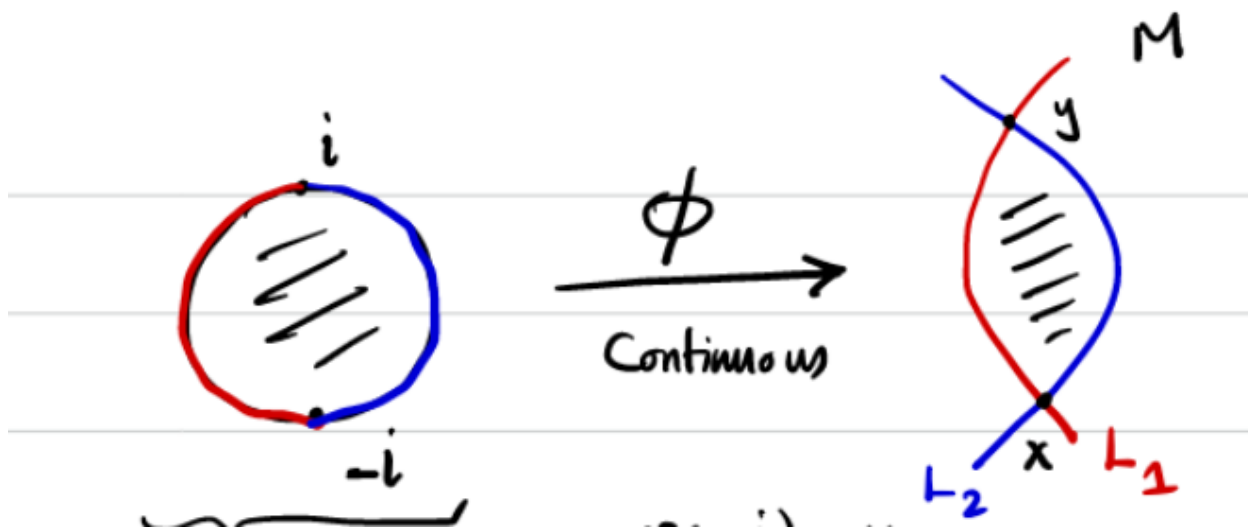
Figure 17: i

So we can the number of *holomorphic* discs from x to y. We'll get $\partial^2 = 0 \iff \operatorname{im}\partial \subset \ker\partial$, and HF will be kernels modulo images. In more detail, we'll have

$$\partial x = \sum_y \sum_{\mu(\varphi)=1} \#\widehat{\mathcal{M}}(\varphi)y \qquad\qquad \widehat{\mathcal{M}}(\varphi) = \mathcal{M}(\varphi)/\mathbb{R}$$

where $\widehat{\mathcal{M}}$ will (in good cases) be a 1-dimensional manifold with finitely many points. Note that it's not necessarily true that CF has a grading!

Given a 3-manifold M^3, we'll associate a Heegard diagram Σ, α, β. Note the g-element symmetric group acts on $\prod_{i=1}^{g} \Sigma$ by permuting the g coordinates, so we can define $\operatorname{Sym}^g(\Sigma) := \prod_{i=1}^{g} \Sigma/S_g$.

> **Theorem 2.2.5 *(?)*.**
> The space $\operatorname{Sym}^g(\Sigma)$ is a smooth complex manifold of $\mathbb{R}$-dimension $2g$.

Remark 2.2.6: Write $\mathbb{T}_\alpha := \prod_{i=1}^{g} \alpha_i \subseteq \prod_{i=1}^{g} \Sigma$ for a g-dimensional torus; this admits a quotient map to $\operatorname{Sym}^g(\Sigma)$. We can repeat this to obtain $\mathbb{T}_\beta$. Then $HF^-(M)$ will be a variation of Lagrangian Floer Homology for $(\operatorname{Sym}^g(\Sigma), \mathbb{T}_\alpha, \mathbb{T}_\beta)$.

Example 2.2.7 *(?)*: Consider constructing a genus $g = 1$ Heegard diagram. Recall that S^3 can be constructed by gluing two solid torii.
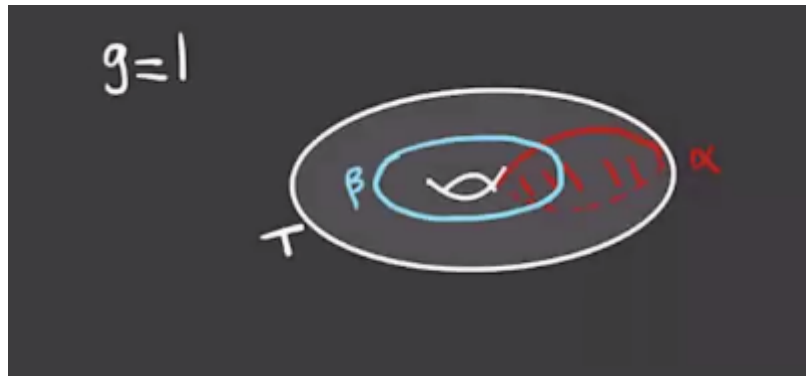
Figure 18: image_2021-01-19-12-20-16

Here (T, α, β) will be a Heegard diagram for S^3.

Exercise 2.2.8 (?)
Show that the following diagram with β defined as some perturbation of α is a Heegard diagram for $S^1 \times S^2$.
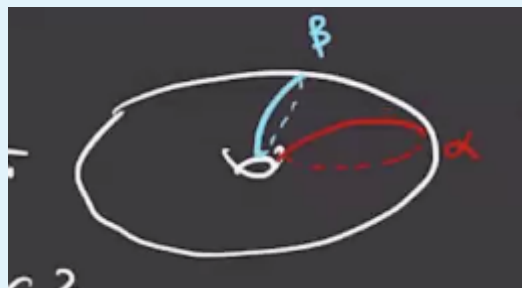

Figure 19: image_2021-01-19-12-21-56

Definition 2.2.9 (Dehn Surgery)
Consider M a 3-manifold containing a knot K, we can construct a new 3-manifold by first removing a neighborhood of K to yield $M \setminus N(K)$:
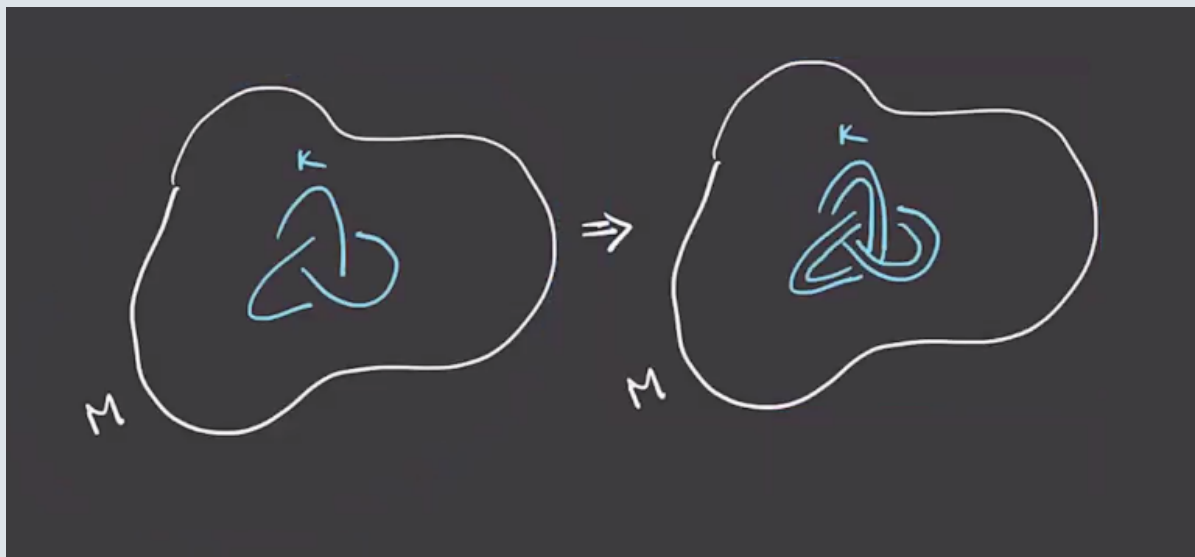
Figure 20: image_2021-01-19-12-23-16

Taking a new solid torus $S := \mathbb{D}^2 \times S^1$ and a diffeomorphism $i : \partial S \to \partial(M \setminus N(K))$, this yields a new manifold $M_\varphi(K)$, a **surgery** along K.
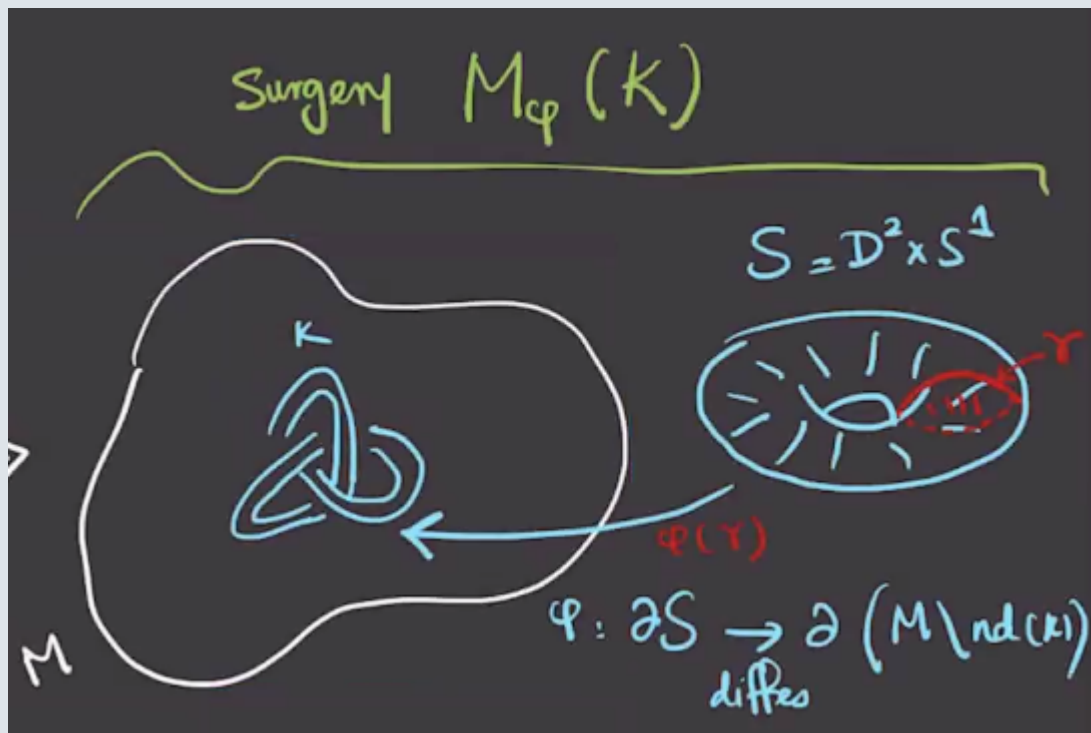

Figure 21: image_2021-01-19-12-25-25

Remark 2.2.10: Note that the diffeomorphism is entirely determined by the image of the curve

α . The Knot Floer chain complex of K will allow us to compute any flavor $HF^- M_\varphi(K)$ of Floer homology. Why is this important: any closed 3-manifold is surgery on a link in S^3. However there are many more computational tools available here and not in the other theories: combinatorial approaches to compute, exact sequences, bordered Floer homology.

Next time: we'll talk about "integer surgeries".

3 | Lecture 3: Morse Theory (Thursday, January 19)

3.1 Intro to Morse Theory

Remark 3.1.1: Let M^n be a smooth closed manifold, then the goal is to study the topology of M by studying smooth functions $f \in C^\infty(M, \mathbb{R})$. We'll need f to be *generic* in a sense we'll discuss later.
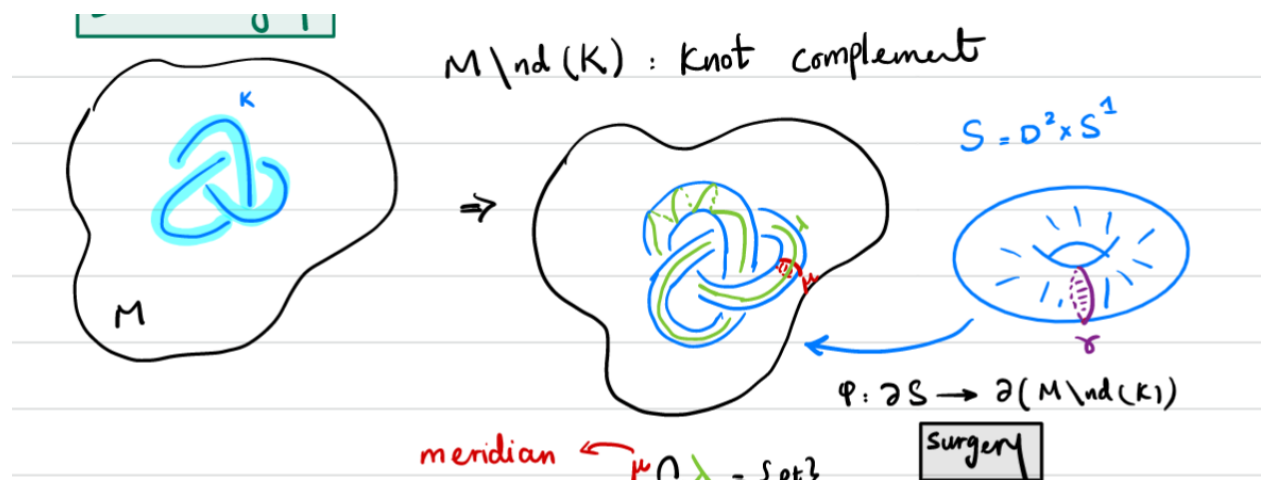

Figure 22: image_2021-01-19-00-41-55

> **Definition 3.1.2** (Critical Point)
> A point $p \in M$ is called a **critical point** if and only if $(df)_p = 0$.

> **Definition 3.1.3** (Hessian / Second Derivative)
> Fixing a critical point p for f, the **second derivative** or **Hessian** of f at p is a bilinear form on $T_p M$ which is defined in the following way: for $v, w \in T_p M$, extend w to a vector field $\tilde{w}$ in

a neighborhood of p and set

$$d^2 f_p(v, w) = v \cdot (\tilde{w} \cdot f)(p) := v \cdot (df)(\tilde{w})(p).$$

where we take the derivative of f with respect to $\tilde{w}$, then take the derivative with respect to v, then evaluate at the point to get a number.

Remark 3.1.4: This is only well-defined at critical points (check!). Note that we need $\tilde{w}$ so that $\tilde{w} \cdot f$ is again a function (and not a number) which can be differentiated again. You can also take e.g. $\tilde{v} \cdot (\tilde{w} \cdot f)$, differentiating with respect to the vector field instead of just the vector v, but we're plugging in p in either case.

Claim: The second derivative is

1. Well-defined, and

2. Symmetric

Remark 3.1.5: If you fix a coordinate chart in a neighborhood of p, then the bilinear form is represented by a matrix given by

$$(d^2 f)_p = H_p = \left(\frac{\partial^2}{\partial x_j \partial x_i}(p) \right)_{ij}.$$

> *Proof (of 2).*
> We can compute
>
> $$
> \begin{aligned}
> (d^2 f)_p(v, w) - (d^2 f)_p(w, v) &= v \cdot (\tilde{w} \cdot f)(p) - w \cdot (\tilde{v} \cdot f)(p) \\
> &:= df_p([\tilde{v}, \tilde{w}]) \\
> &= 0 \qquad\qquad\qquad \text{since } p \text{ is a critical point and } df_p = 0.
> \end{aligned}
> $$
>
> ∎

> *Proof (of 1).*
> This is now easier to prove: we are picking an extension of w to a vector field, so we need to show that the definition doesn't depend on that choice.
>
> $$
> \begin{aligned}
> (d^2 f)(_p(v, w) &= v \cdot (\tilde{w} \cdot f)(p) && \text{which doesn't depend on } \tilde{v} \\
> &= (d^2 f)_p(w, v) \\
> &= w \cdot (\tilde{v} \cdot f)(p) && \text{which doesn't depend on } \tilde{w},
> \end{aligned}
> $$
>
> and thus this is independent of both $\tilde{v}$ and $\tilde{w}$.
>
> ∎

Exercise 3.1.6 (?)
Show that the second derivative in local coordinates is given by the matrix H_p above.

Remark 3.1.7: In local coordinates, we can write $v = \sum_{i=1}^{n} a_i \frac{\partial}{\partial x_i}$ and $w = \sum_{i=1}^{n} b_i \frac{\partial}{\partial x_i}$, and thus

$$(d^2 f)_p(v, w) = \mathbf{b}^t H_p \mathbf{a} = \sum_{1 \leq i,j \leq n} a_i b_j \frac{\partial^2 f}{\partial x_i \partial x_j}(p).$$

Definition 3.1.8 (Nondegenerate Critical Points)
A critical point $p \in M$ is called **nondegenerate** if the bilinear form $(d^2 f)_p$ is nondegenerate at p, i.e. for all $v \in T_p M$ there exists a $w \in T_p M \setminus \{\mathbf{0}\}$ such that $(d^2 f)_p(v, w) \neq 0$. This occurs if and only if H_p is invertible.

Definition 3.1.9 (Index of a critical point)
Given a nondegenerate critical point $p \in M$, define the **index** $\operatorname{ind}(p)$ of f at p in the following way: since H_p is symmetric and nondegenerate, its eigenvalues are real and nonzero, so define the index as the number of *negative* eigenvalues of H_p.

Definition 3.1.10 (Morse Function)
A function $f \in C^\infty(M, \mathbb{R})$ is called a **Morse function** if and only if all of its critical points are nondegenerate.

Remark 3.1.11: We'll see that almost every smooth function is Morse, and these are preferable since they have a simple and predictable structure near critical points and don't do anything interesting elsewhere.

Theorem 3.1.12 *(Morse Lemma).*
Let $p \in M$ be a nondegenerate critical point of f with $\operatorname{ind}(p) = \lambda$. Then there exists charts $\varphi : (U, p) \to (\mathbb{R}^n, 0)$ such that writing f in local coordinates yields

$$(f \circ \varphi^{-1})(x) = f(p) - \sum_{i=1}^{\lambda} x_i^2 + \sum_{j=\lambda+1}^{n} x_j^2.$$

Remark 3.1.13 *(Observation 1):* We have

$$H_p = \begin{bmatrix} -2 & & & & & & \\ & \ddots & & & & & \\ & & -2 & & & & \\ & & & 2 & & & \\ & & & & \ddots & & \\ & & & & & 2 & \\ & & & & & & 2 \end{bmatrix} = -2I_\lambda \oplus 2I_{n-\lambda}.$$

Remark 3.1.14 *(Observation 2):* If $\lambda = n$??

Remark 3.1.15 *(Observation 3):* ??

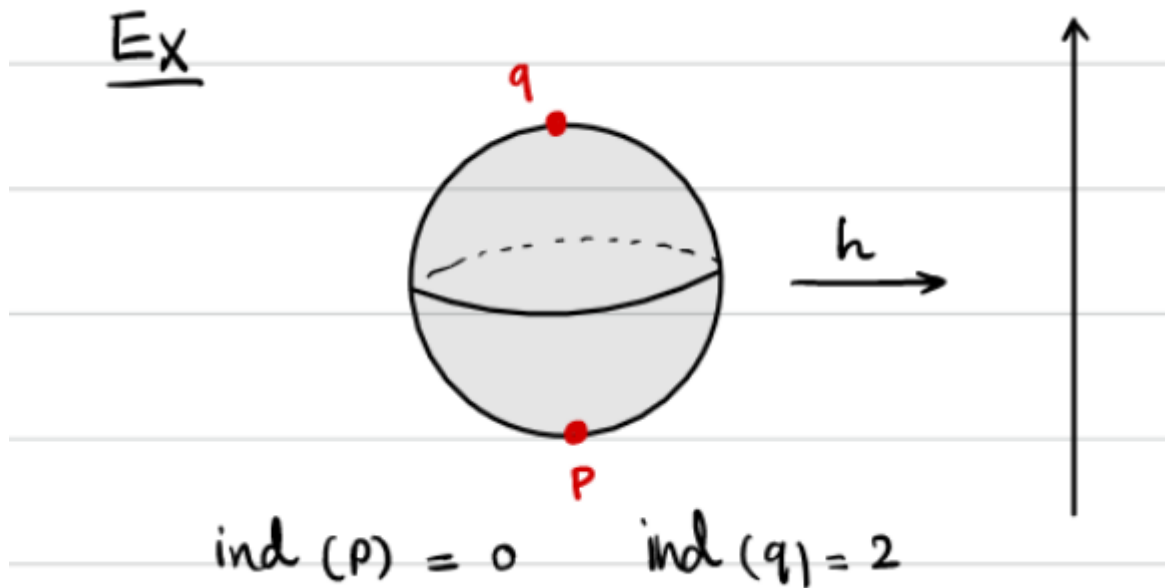**Example 3.1.16** *(Sphere):* Consider S^2 with a height function:

Figure 23: Sphere with a height function

Then we have a local minimum at the South pole p and a local max at the North pole q, where $\mathrm{ind}(p) = 0$ and $\mathrm{ind}(q) = 2$. Note that the critical points essentially occur where the tangent space is horizontal

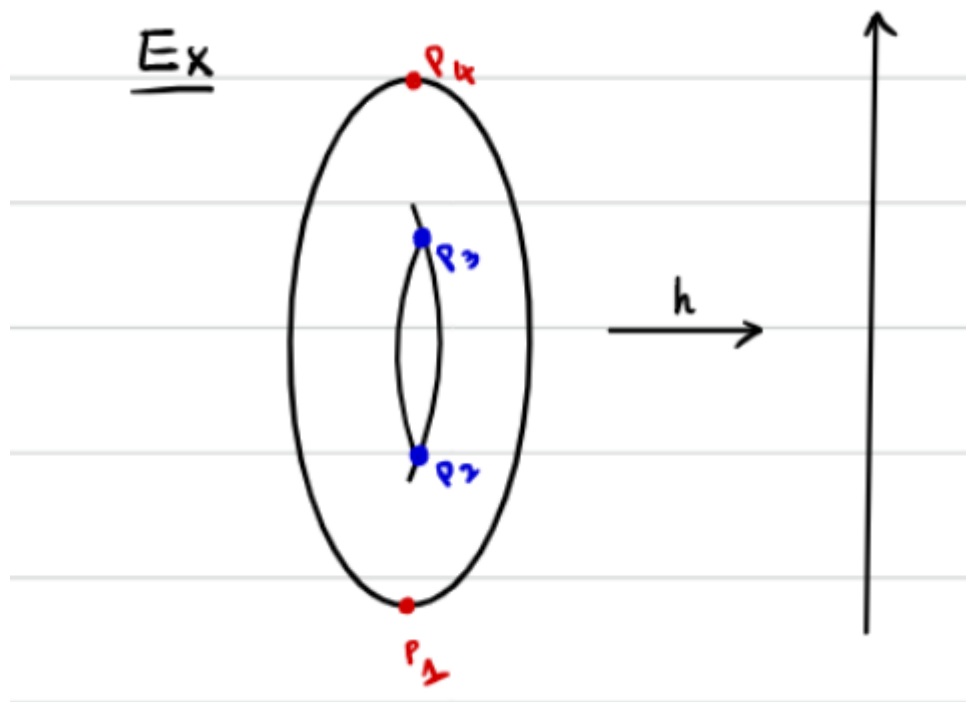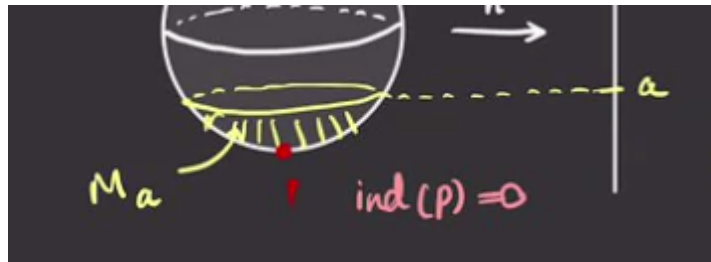**Example 3.1.17** *(Torus):* Consider $\mathbb{T}^2$ with the height function:

Figure 24: Torus with a height function

This has a similar max/min as the sphere, but also has two critical points in the middle that resemble saddles:

Figure 25: Saddle points

Remark 3.1.18: Define $M_a := f^{-1}((-\infty, a])$; we then want to consider how M_a changes as a changes:

Figure 26: M_a on the sphere

Figure 27: M_a on the torus

Lemma 3.1.19 *(?)*.
If $f^{-1}([a,b])$ contains no critical points, then

$$f^{-1}(a) \cong f^{-1}(b)$$
$$M_a \cong M_b.$$

Definition 3.1.20 (Gradients)
Choose a metric g on M, then the **gradient vector** of f is given by

$$g(\nabla f, v) = df(v).$$

Remark 3.1.21: We have

$$df(\nabla f) = g(\nabla f, \nabla f) = \|\nabla f\|^2.$$

Proof (?).
We have the following situation:
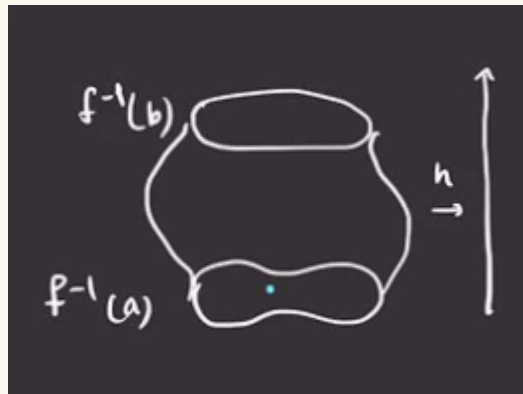
Figure 28: image_2021-01-21-12-11-16

The gradient vector is always tangent to the level sets, so we can consider the curve γ which satisfies $\dot{\gamma}(t) = -\nabla f(\gamma(t))$:
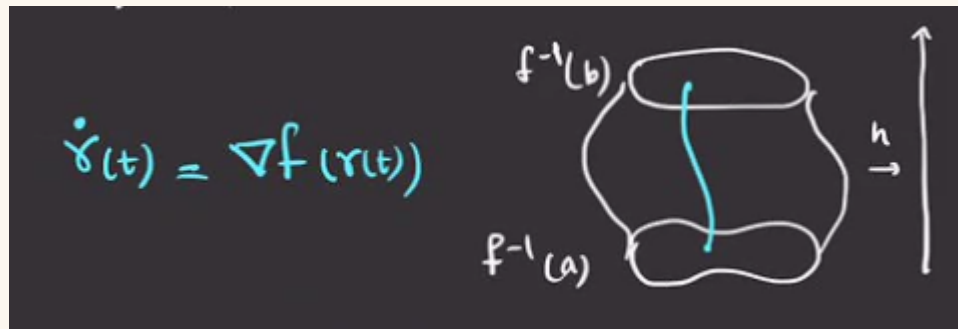
Figure 29: image_2021-01-21-12-12-42

For technical reasons, we want to end up with cohomology instead of homology and will take $-\nabla f$ instead of ∇f everywhere:
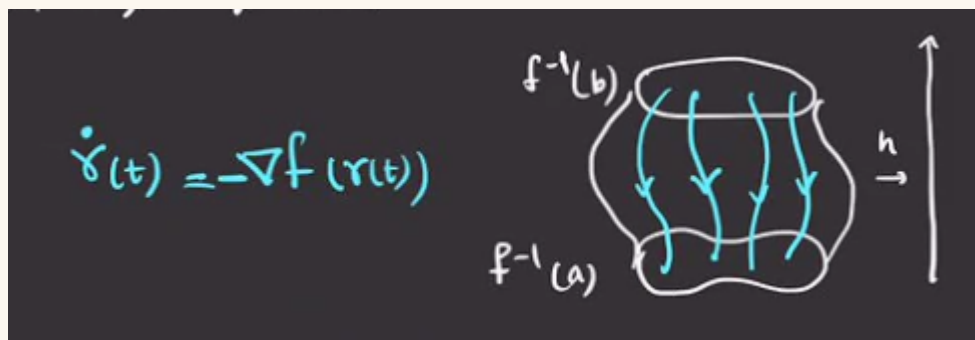
Figure 30: image_2021-01-21-12-13-35

So γ will be a trajectory of $-\nabla f$, and $f^{-1}[a,b] \cong f^{-1}(a) \times [0,1]$. A problem is that following these trajectories may involve arriving at $f^{-1}(a)$ at different times:
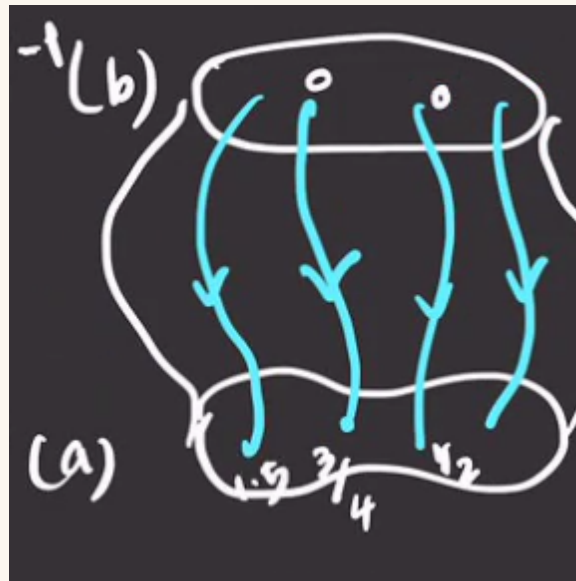
Figure 31: image_2021-01-21-12-15-10

We can fix this by normalizing:

$$V := -\nabla f / \|\nabla f\|^2 \implies (df)(v) = \left\langle \nabla f, \ -\nabla f / \|\nabla f\|^2 \right\rangle = -1.$$

For every $p \in f^{-1}(b)$, if $\gamma(t)$ is the trajectory starting from p, i.e. $\gamma(0) = p$, then $\gamma(b-a) \in f^{-1}(a)$. So define

$$\Phi : f^{-1}(b) \times [0, b-a] \to f^{-1}([a, b])$$
$$(p, t) \mapsto \gamma_p(t),$$

which will be a diffeomorphism.

∎

Theorem 3.1.22 *(?).*
Suppose $f^{-1}([a,b])$ contains exactly one critical point p with $\operatorname{ind}(p) = \lambda$ and $f(p) = c$. Then

$$M_b = M_a \cup_\partial \left(D^\lambda \times D^{n-\lambda} \right)$$

where $n := \dim M$.

Example 3.1.23 *(?):* For $\lambda = 1, n - \lambda = 2$:
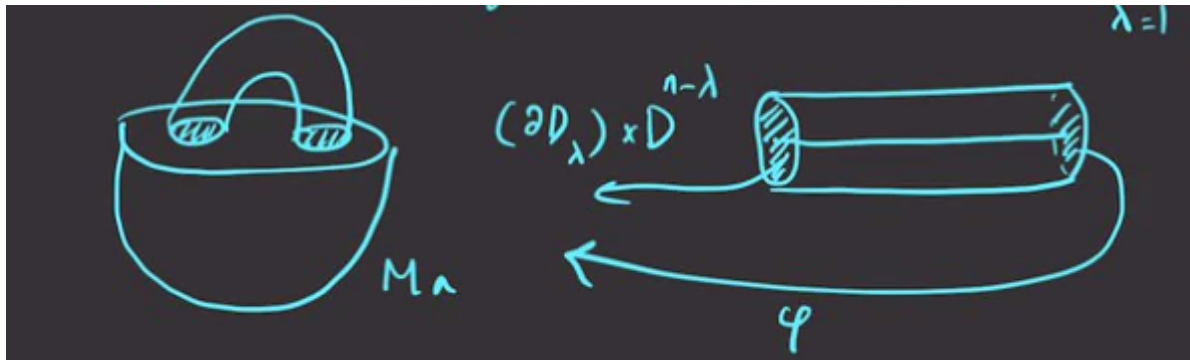
Figure 32: image_2021-01-21-12-32-38
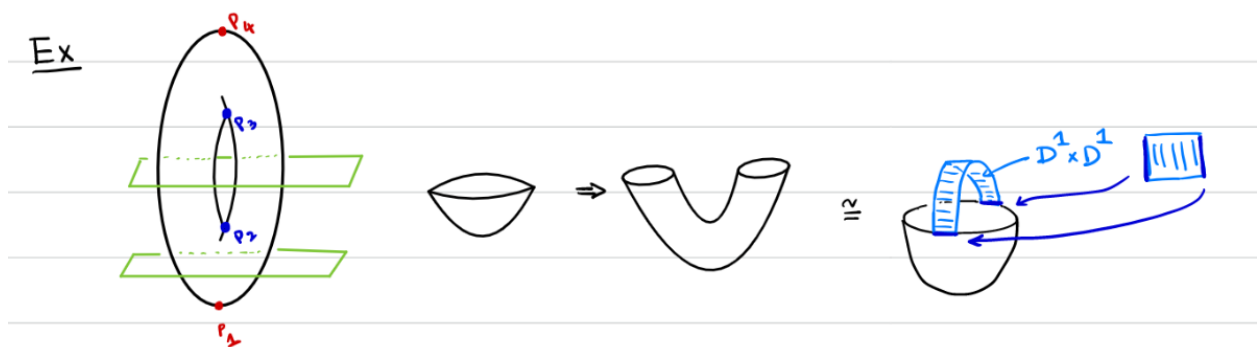
Figure 33: image_2021-01-19-00-53-07

Example 3.1.24*(?)*:

> **Definition 3.1.25** (Unstable Submanifold)
>
> $$W_f^u(p) := \{p\} \cup \left\{ \dot{\gamma}(t) = -\nabla f(\gamma(t)), \lim_{t \to -\infty} \gamma(t) = p, t \in \mathbb{R} \right\}.$$

> **Lemma 3.1.26*(?)*.**
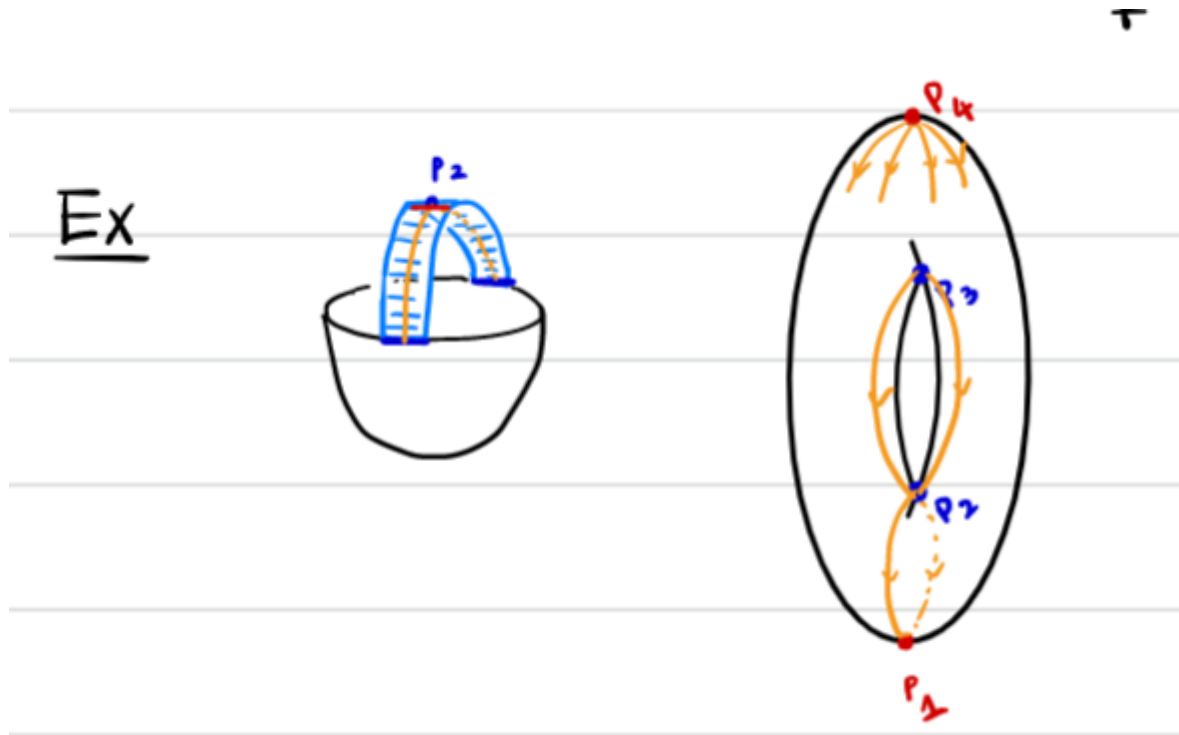> If $\operatorname{ind}(p) = \lambda$ then $W_f^u(p) \cong \mathbb{R}^\lambda$.
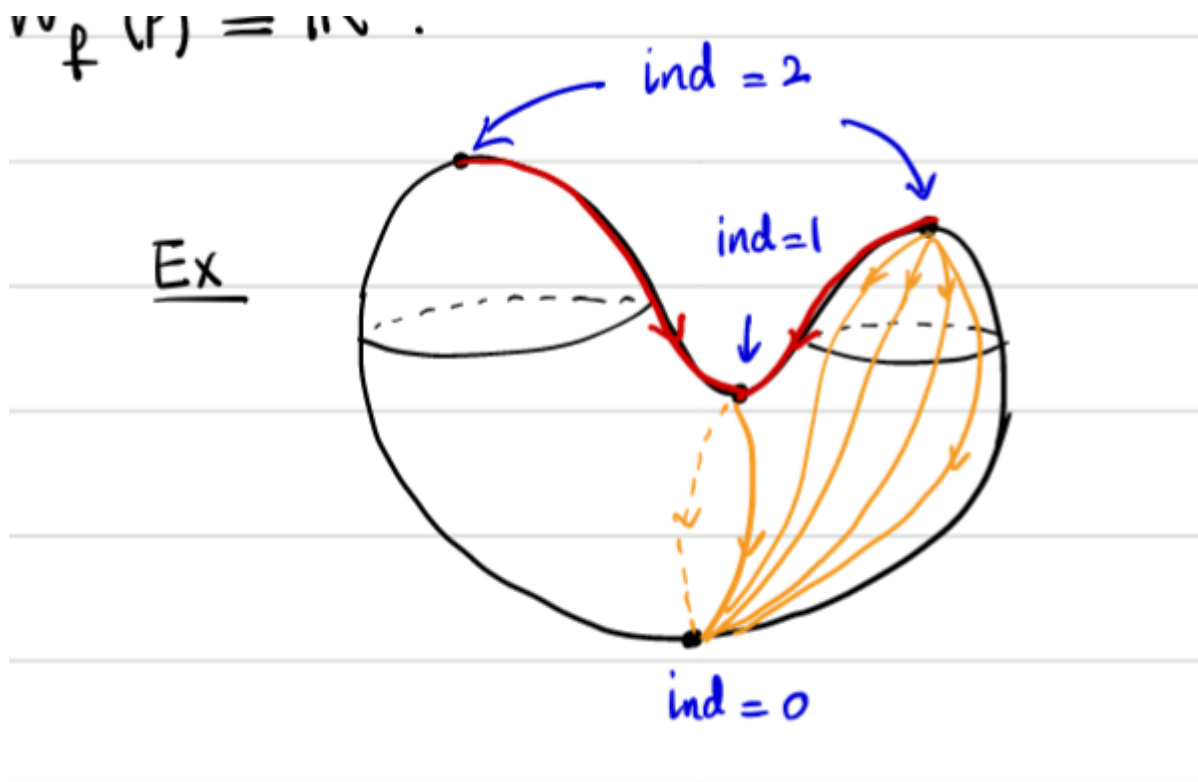
Figure 34: image_2021-01-19-00-55-24

Example 3.1.27*(?):*

Figure 35: image_2021-01-19-00-55-41

Example 3.1.28*(?):*

Definition 3.1.29 (Stable Manifold)

$$W_f^s(p) := \{p\} \cup \left\{ \dot{\gamma}(t) = -\nabla f(\gamma(t)), \lim_{t \to +\infty} \gamma(t) = p, \, t \in \mathbb{R} \right\}.$$

Lemma 3.1.30*(?).*
If $\text{ind}(p) = \lambda$ then $W_f^s(p) \cong \mathbb{R}^{n-\lambda}$.

Definition 3.1.31 (C^∞)
$C^\infty(M; \mathbb{R})$ is defined as smooth function $M \to |RR$, topologized as:

- ?
- ?

And a basis for open neighborhoods around p is given by

$$N_g(f) = \left\{ g : M \to \mathbb{R} \; \Big| \; \left| \frac{\partial^k g}{\partial \partial x_{i_1} \cdots \partial x_{i_k}}(p) - \frac{\partial^k f}{\partial \partial x_{i_1} \cdots \partial x_{i_k}}(p) \right| < \infty \, \forall \alpha, \, \forall p \in h_\alpha(C_\alpha) \right\}.$$

> **Theorem 3.1.32***(?)***.**
> The set of Morse functions on M is open and dense in $C^\infty(M; \mathbb{R})$.

4 | Tuesday, January 26

4.1 Attaching Handles

Remark 4.1.1: Goal: we want to use Morse functions (smooth, nondegenerate critical points) to study the topology of M. Recall that the torus had 4 critical points,
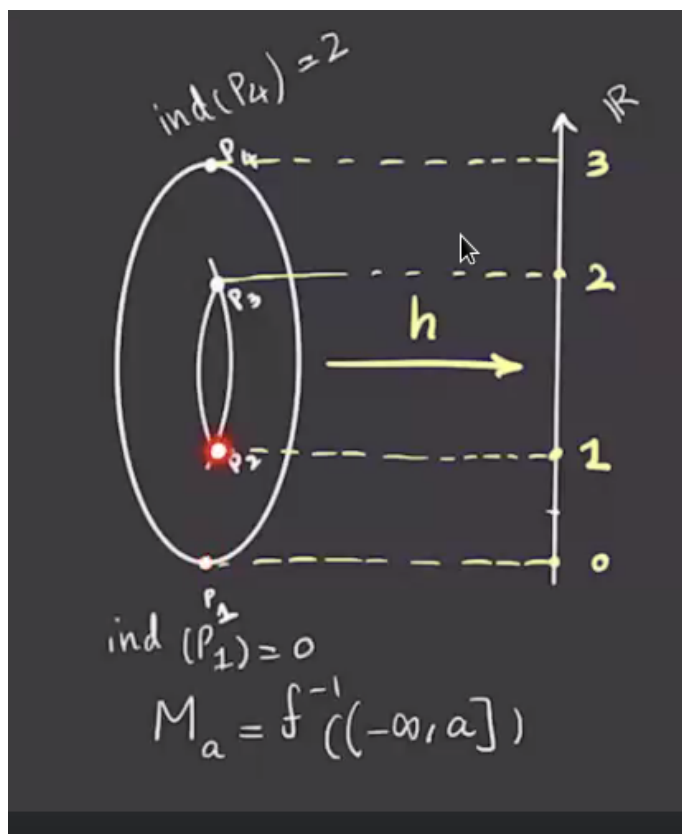

Figure 36: image_2021-01-26-11-14-32

We defined the index as the number of negative eigenvalues of the Hessian matrix. Here the highest index will be the dimension of the manifold, and by the Morse lemma the two intermediate critical points will be index 1.

Remark 4.1.2: We want to use the Morse function to decompose the manifold, so we consider

$M_a := f^{-1}((-\infty, a])$. If $f^{-1}[a, b]$ does not contain a critical point, then $M_a \cong M_b$ and $f^{-1}(a) \cong f^{-1}(b)$. So taking $M_{1/2}$ and $M_{3/4}$ here both yield discs:

Figure 37: image_2021-01-26-11-17-46

Passing through critical points does change the manifold, though:
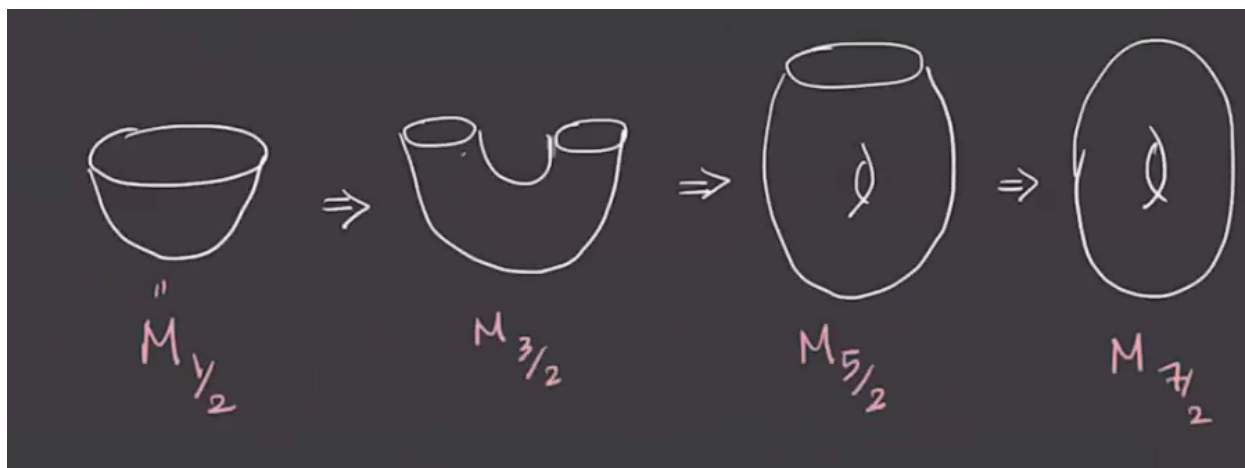
Figure 38: image_2021-01-26-11-19-01

Theorem 4.1.3*(?)*.
Suppose $f^{-1}[a, b]$ contains exactly *one* critical point of index λ then

$$M_b \cong M_a \cup_\varphi (D_\lambda \times D_{n-\lambda}),$$

where $\varphi : (\partial D_\lambda \times D_{n-\lambda}) \hookrightarrow \partial M_a$.

Example 4.1.4*(?):* For the case $\lambda = 1, n = 3$, we have the following situation:
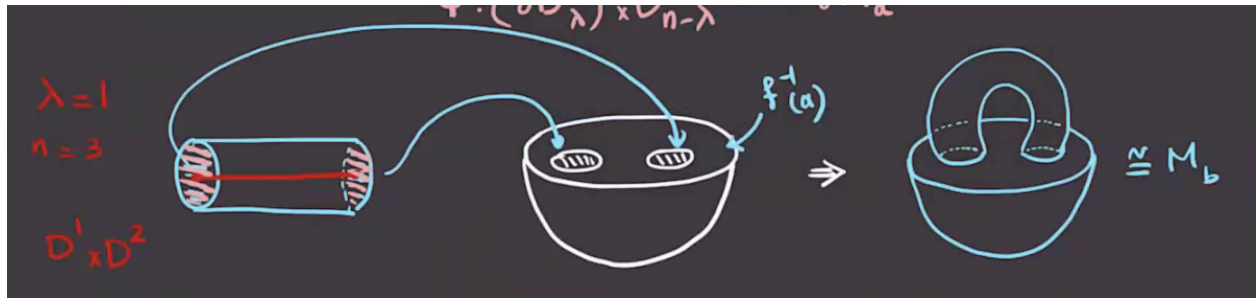
Figure 39: image_2021-01-26-11-24-46

Example 4.1.5*(?):* Taking $\lambda = 1, n = 2$, we attach $D^1 \times D^1$ and get the following situation:
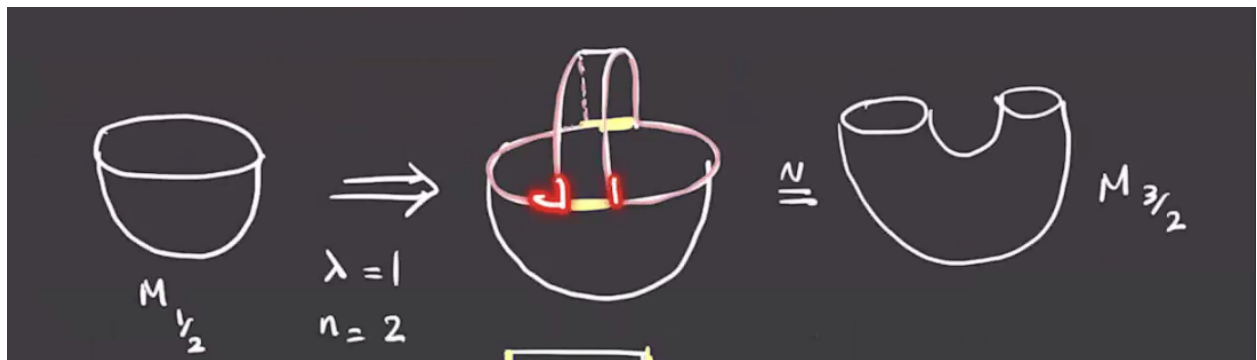
Figure 40: image_2021-01-26-11-27-16

Adding on another piece, the new boundary is given by the highlighted region:

Figure 41: image_2021-01-26-11-32-27

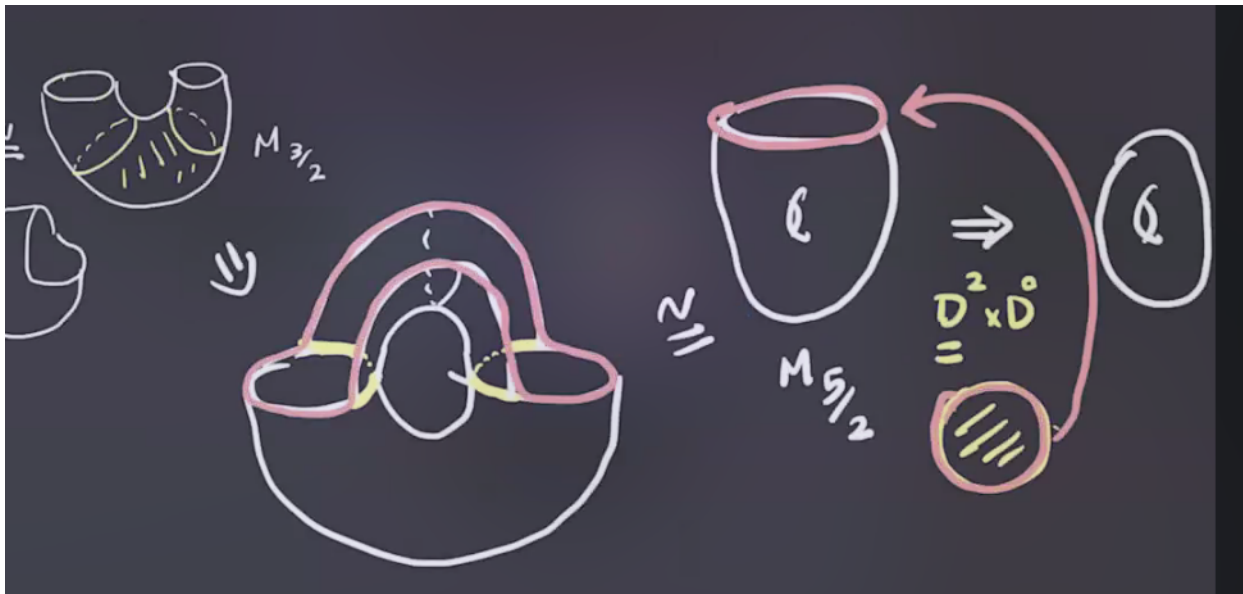And continuing to attach the last pieces yields the following:

Figure 42: image_2021-01-26-11-33-31

Remark 4.1.6: There is a deformation retract $M_b \to M_a \cup C_\lambda$, where C_λ is a λ-cell given by $D_\lambda \times \{0\}$. For example:
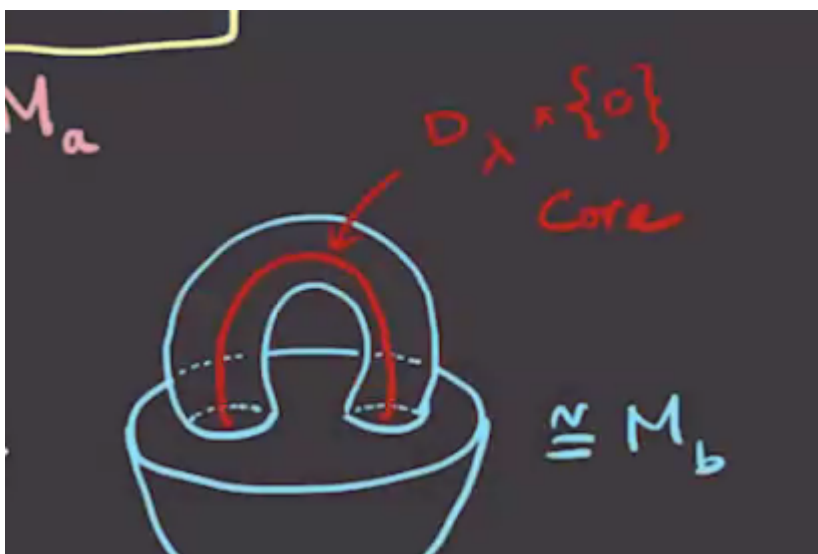
Figure 43: image_2021-01-26-11-36-35

4.2 Stable and Unstable Manifolds

Definition 4.2.1 (Unstable Manifold)
Given $-\nabla f$ for a fixed metric, the **unstable manifold** for a critical point p is defined as

$$W_f^u(p) := \{p\} \cup \left\{ \gamma(t) \;\middle|\; \dot{\gamma}(t) = -\nabla f(\gamma(t)), \; \gamma(t) \overset{t \to -\infty}{\to} p \right\}.$$

Here $\gamma(t)$ is the trajectory of $-\nabla(f)$.

Example 4.2.2*(?):* The unstable manifold is highlighted in blue here:
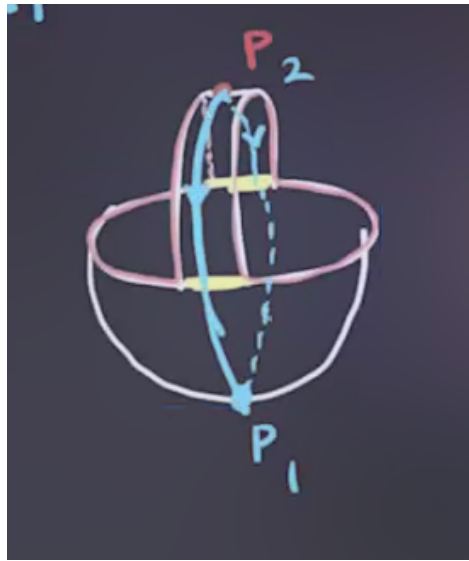
Figure 44: image_2021-01-26-11-42-01

The gradient trajectories for other points are given by the yellow lines in the following:
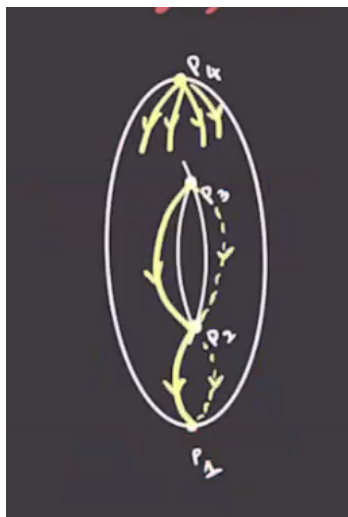
Figure 45: image_2021-01-26-11-44-13

Lemma 4.2.3*(?)*.
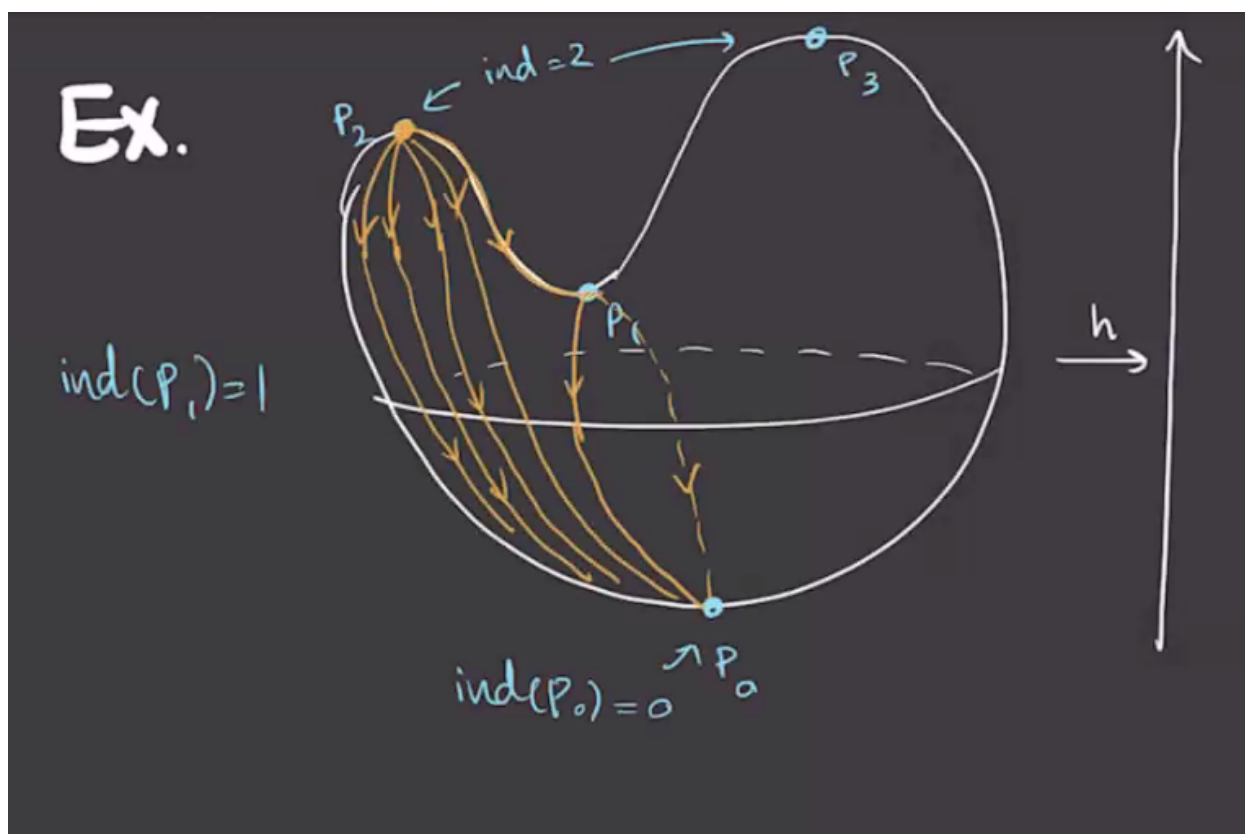If $\text{ind}(p) = \lambda$, then the unstable manifold W_f^u at p is isomorphic to $\mathbb{R}^\lambda$.

Figure 46: image_2021-01-26-11-46-46

Example 4.2.4(?): Here the unstable manifold for p_2 will be 2-dimensional, with one flow line ending at p_1 and the rest ending at p_0.
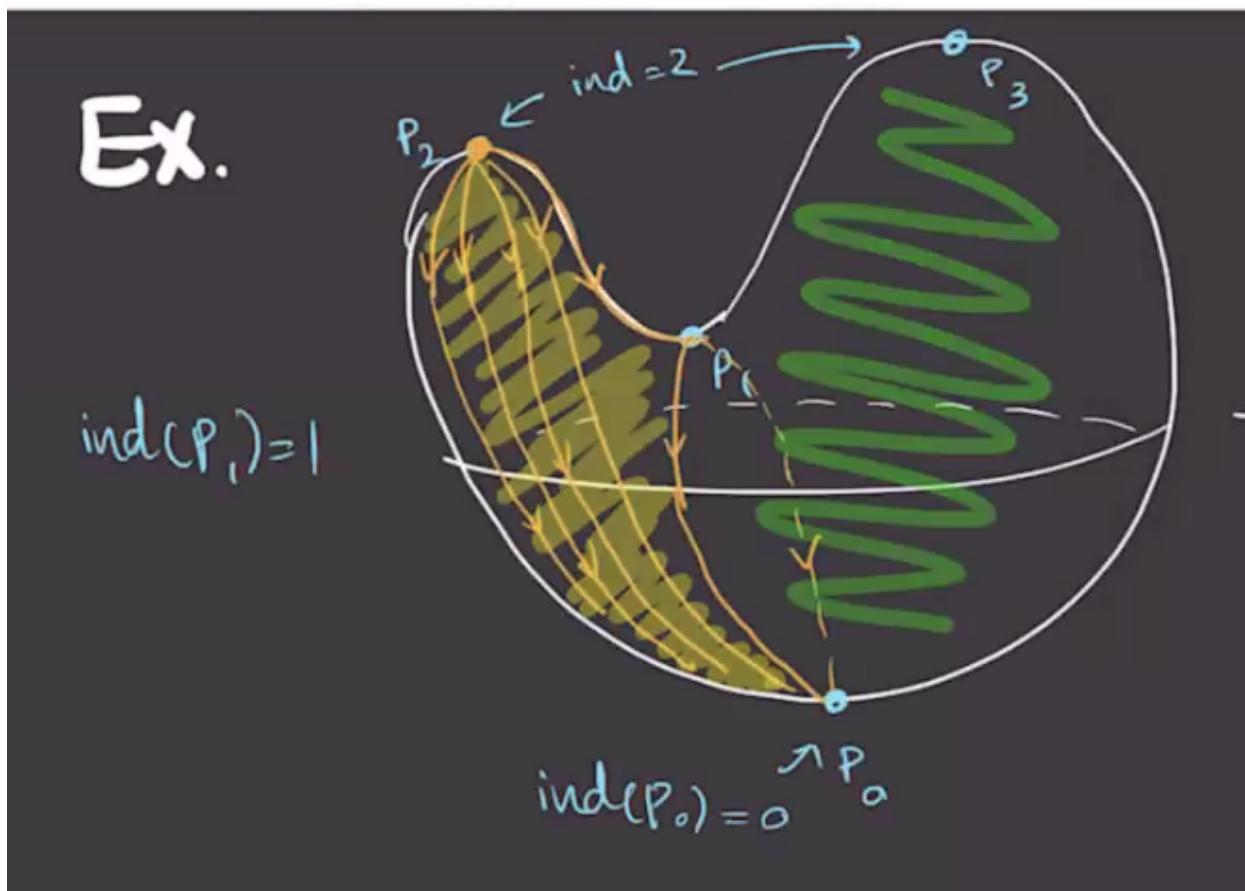

Figure 47: image_2021-01-26-11-47-24

Definition 4.2.5 (Stable Manifold)
The **stable manifold** for a critical point p is defined as

$$W_f^s(p) := \{p\} \cup \left\{ \gamma(t) \mid \dot{\gamma}(t) = -\nabla f(\gamma(t)), \, \gamma(t) \overset{t \to +\infty}{\to} p \right\}.$$

Example 4.2.6(?): The stable manifold for p_0 above is every trajectory ending at p_0. $W^s(p) = S^2 \setminus W^s(p_1) \cup W_s(p_3)$? See video?

Which point p is this for?

4.3 Morse Functions

> **Theorem 4.3.1** *(Existence of Morse Functions).*
> The set of Morse functions is open and dense in $C^\infty(M;\mathbb{R})$ in a certain topology.[a]
>
> ─────────────────────
> [a] See Akram's notes for details.

Remark 4.3.2: We'll use this to define a chain complex $C_*(f,g)$ where g is a chosen metric, define a differential, and use this to define a homology theory. For notation, we'll write $\mathrm{crit}(f)$ as the set of critical points of f, and given $p, q \in \mathrm{crit}(f)$ with γ a trajectory running from p to q, we have

$$W^u(p) \cap W^s(q) = \left\{ \gamma(t) \;\middle|\; \gamma(t) \overset{t \to -\infty}{\to} p,\; \gamma(t) \overset{t \to +\infty}{\to} q \right\}.$$

> **Definition 4.3.3** (Transverse Intersections)
> Two submanifolds $X, Y \subseteq M$ **intersect transversely** if and only if
>
> $$T_p X + T_p Y := \left\{ v + w \;\middle|\; v \in T_p X, w \in T_p Y \right\} = T_p M \qquad \forall p \in X \cap Y.$$
>
> In this case, we write $X \pitchfork Y$.

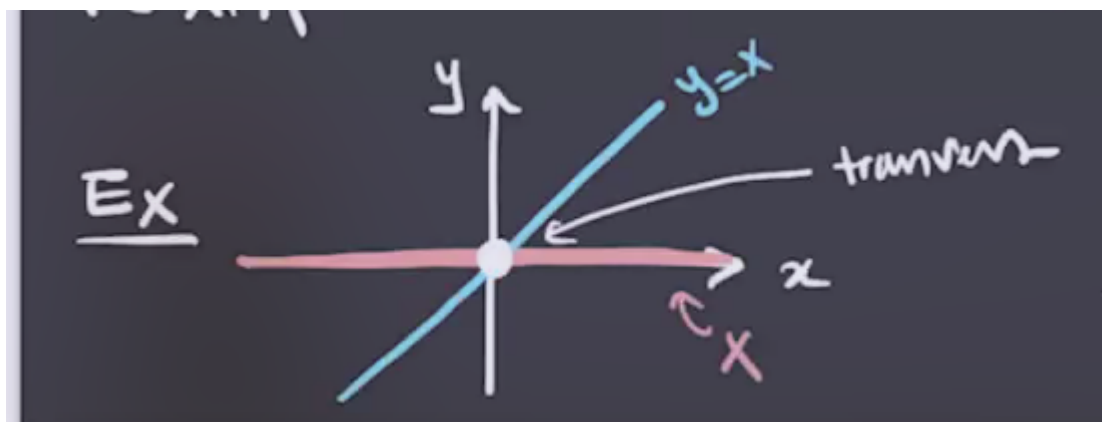**Example 4.3.4***(?):* An example of a transverse intersection:

Figure 48: image_2021-01-26-12-02-29

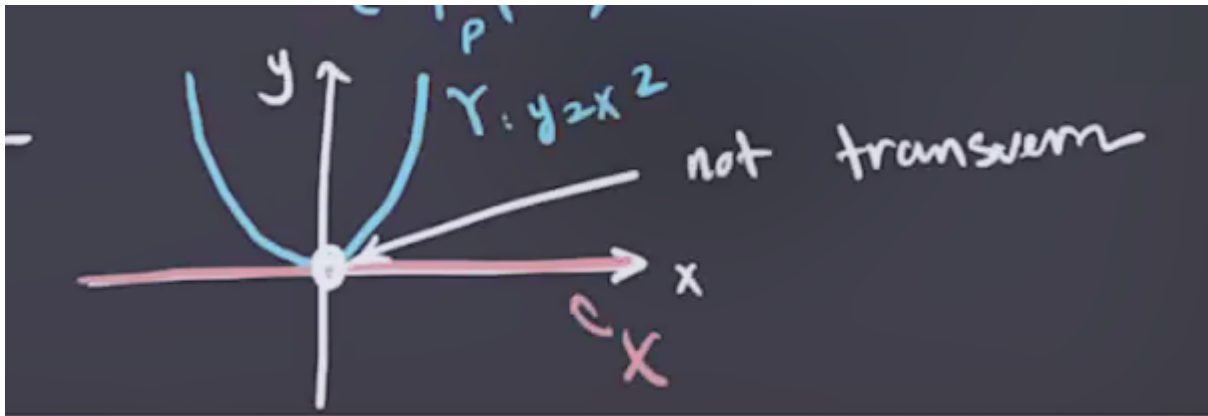**Example 4.3.5***(?):* An example of an intersection that is *not* transverse:

Figure 49: image_2021-01-26-12-03-13

Definition 4.3.6 (Morse-Smale)
A pair (f, g) with f a Morse function and g a metric is **Morse-Smale** if and only if

- f is a Morse function,
- $W^u(p)$ is *transverse* to $W^s(q)$ for all $p, q \in \mathrm{crit}(f)$.

Theorem 4.3.7*(?).*
For a generic metric g, the pair (f, g) is Morse-Smale.

Remark 4.3.8: This means that metrics can be perturbed to become Morse-Smale.

Example 4.3.9*(?):* The following is not Morse-Smale:
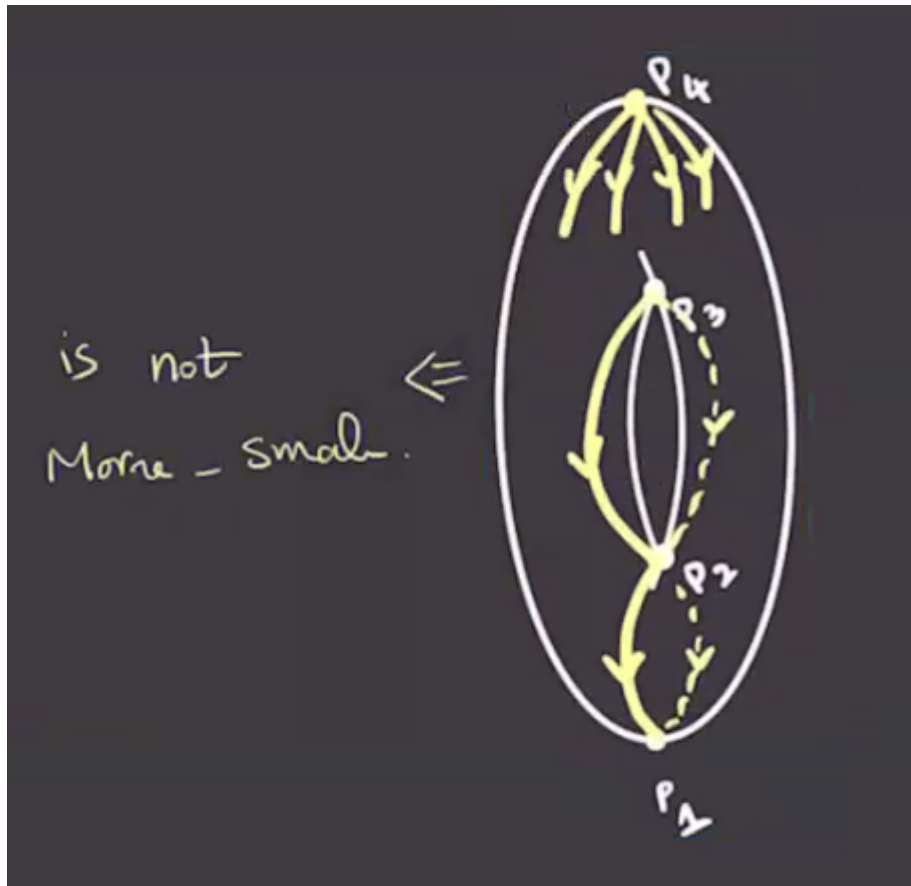
Figure 50: image_2021-01-26-12-06-06

Note that if $X^a \pitchfork Y^b$, then $X \cap Y \subseteq M^n$ is a smooth submanifold of dimension $a+b-n$. In general, we have $M^s(p) \cong \mathbb{R}^{n-\lambda}$ where $\lambda = \mathrm{ind}(p)$.

Observation 4.3.10
If (f,g) is Morse-Smale, then $M^u(p) \pitchfork M^s(q)$. In this case,

$$\dim(M^u(p) \cap M^s(q)) = \mathrm{ind}(p) + n - \mathrm{ind}(q) - n = \mathrm{ind}(p) - \mathrm{ind}(q).$$

Thus if $\mathrm{ind}(p) = \mathrm{ind}(q)$ then $\dim M^s(p) \cap M^s(q) = 0$.

Remark 4.3.11: There is an $\mathbb{R}$-action of $M^s(p) \cap M^s(q)$:

$$(M^s(p) \times M^u(q)) \times \mathbb{R} \to M^s(p) \cap M^u(q)$$
$$(\gamma(t), c) \mapsto \gamma(t+c).$$

If $p \neq q$, this action is free and we can thus quotient by it to obtain

$$\mathcal{M}(p,q) := (M^s(p) \cap M^u(q))/\mathbb{R}.$$

This identifies all points on the same trajectory, yielding one point for every trajectory, and so this is called the **moduli space of trajectories from p to q**.

If $\mathrm{ind}(p) = \mathrm{ind}(q)$, we have $\dim M^u(p) \cap M^s(q) = 0$, making $\dim \mathcal{M}(p,q) = -1$ and thus $\mathcal{M}(p,q) = \emptyset$ and no gradient trajectories connect p to q. Referring back to the example, since $\mathrm{ind}(p_3) = \mathrm{ind}(p_2)$, if (f,g) were Morse-Smale then there would be no trajectory $p_3 \to p_2$, whereas in this case there is at least one.

Remark 4.3.12: If $\mathrm{ind}(p) - \mathrm{ind}(q) = 1$, then $\dim \mathcal{M}(p,q) = \mathrm{ind}(p) - \mathrm{ind}(q) - 1 = 0$, making $\mathcal{M}(p,q)$ a compact 0-dimensional manifold, which is thus finitely many points, meaning there are only finitely many trajectories connecting $p \to q$ and it becomes possible to define a Morse complex.

> **Definition 4.3.13** (Morse Complex)
> Fix (f,g) a Morse-Smale pair, then define
> $$ C_i(f,g) := \mathbb{Z}/2\mathbb{Z}\left[\left\{ p \mid \mathrm{ind}\, p = i \right\}\right] = \bigoplus_{\mathrm{ind}(p)=i} \mathbb{Z}/2\mathbb{Z} \langle p \rangle , $$
> with a differential
> $$ \partial : C_i(f,g) \to C_{i-1}(f,g) $$
> $$ p, \mathrm{ind}(p) = i \mapsto \sum_{\mathrm{ind}(q)=i-1} \#\mathcal{M}(p,q)q, $$
> where we take the count mod 2.

> **Theorem 4.3.14*(?)*.**
> $\partial^2 = 0$, and thus $(C(f,g), \partial)$ is a chain complex.

Remark 4.3.15: Next time we will work on proving this.

5 | Morse Homology and Lagrangian Floer Homology (Thursday, January 28)

5.1 Morse Homology

Remark 5.1.1: Last time: defined the Morse complex. Assumed (f,g) was a Morse-Smale pair, where f is a Morse function and g is a Riemannian metric, and this guarantees that if $p, q \in \mathrm{crit}(f)$ with $\mathrm{ind}(p) - \mathrm{ind}(q) = 1$, then (among other things) there are finitely many gradient trajectories $p \rightsquigarrow q$. We denoted this $\mathcal{M}(p,q)$. The chain complex was defined by $C_i(f,g) := \bigoplus_{\mathrm{ind}(p)=i} \mathbb{Z}_2 \langle p \rangle$ with differential $\partial_i : C_i \to C_{i-1}$ was defined by sending an index i critical point p to $\sum_{\mathrm{ind}(q)=i-1} \#\mathcal{M}(p,q)q$ (mod 2).

Theorem 5.1.2 *(The Morse Complex is a Chain Complex).*
$\partial_i \circ \partial_{i+1} = 0$.

Proof (?).
Idea of the proof: we can directly compute

$$\partial(\partial p) = \partial \left(\sum_{\text{ind}(q)=i-1} \#\mathcal{M}(p,q) q \right)$$

$$= \sum_{\text{ind}(q)=i-1} \#\mathcal{M}(p,q) \partial q$$

$$= \sum_{\text{ind}(q)=i-1} \#\mathcal{M}(p,q) \left(\sum_{\text{ind}(r)=i-2 \#\mathcal{M}(q,r) r} \right)$$

$$= \sum_{\text{ind}(r)=i-2} \left(\sum_{\text{ind}(q)=i-1} \#\mathcal{M}(p,q) \#\mathcal{M}(q,r) \right) r$$

$$= \sum_{\text{ind}(r)=i-2} c_{p,q,r} r$$

$$= 0 \qquad\qquad\qquad\qquad\qquad\qquad \text{(claim).}$$

This happens if and only if $c_{p,q,r} = 0 \pmod 2$ for all r with $\text{ind}(r) = i-2$. This is multiplication of the number of trajectories:

Figure 51: image_2021-01-28-11-23-19

In other words, this is the total number of trajectories $p \rightsquigarrow r$ that pass through q. These trajectories "break" at q, and so we refer to these as **broken trajectories**. ∎

Definition 5.1.3 (Broken Trajectories)
Suppose $\text{ind}(r) = \text{ind}(p) - 2$, then a **broken trajectory** from p to r is a trajectory from p to q followed by a trajectory q to r where $\text{ind}(q) = \text{ind}(p) - 1 = \text{ind}(r) + 1$.

Figure 52: image_2021-01-28-11-26-25

Question 5.1.4
Why is the number of broken trajectories even?

Answer 5.1.5
We can check that $\dim \mathcal{M}(p,r) = \dim \left(W^u(p) \pitchfork W^s(r) \right) / \mathbb{R} = (\operatorname{ind}(p) - \operatorname{ind}(r)) - 1 = 2 - 1 = 1$. We can compactify $\mathcal{M}(p,r)$ by adding in all of the broken trajectories to define

$$\overline{\mathcal{M}(p,r)} \cup \left(\bigcup_{\operatorname{ind}(q) = i-1} \mathcal{M}(p,q) \times \mathcal{M}(q,r) \right).$$

This is useful here because we can appeal to the classification of smooth compact 1-dimensional manifolds, which are unions of copies of S^1 and $D_1 = I$. In particular, the number of boundary points

$$\partial \overline{\mathcal{M}(p,r)} = \bigcup_{\operatorname{ind}(q) = i-1} \mathcal{M}(p,q) \times \mathcal{M}(q,r)$$

is even:

Figure 53: image_2021-01-28-11-32-34

Example 5.1.6*(Morse Homology of the Torus):* Suppose you have two critical points of the same index. The Morse-Smale condition implies that there's no trajectory between them. A counterexample would be $p_3 \rightsquigarrow p_2$ on the torus with the height function:
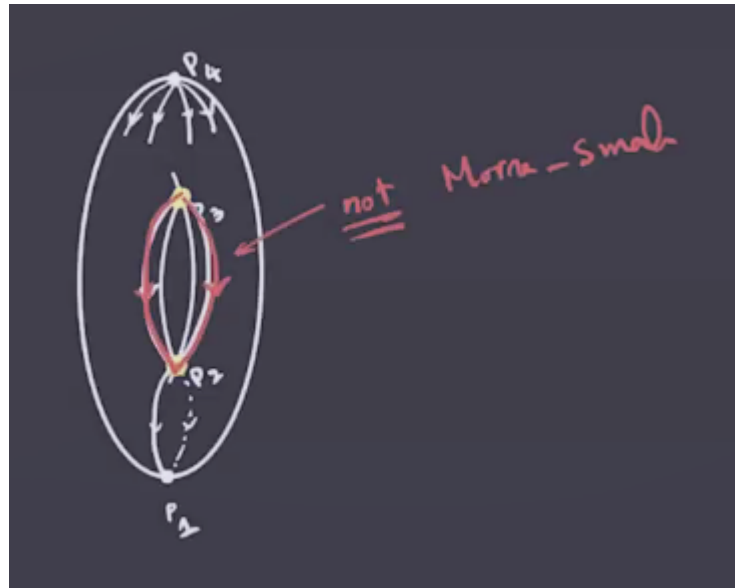
Figure 54: image_2021-01-28-11-45-16

However, if you perturb this slightly, the trajectories can be made to miss p_2 and end at p_1 instead. All of the trajectories are disjoint, so we end up with a situation like the following after perturbing the metric:
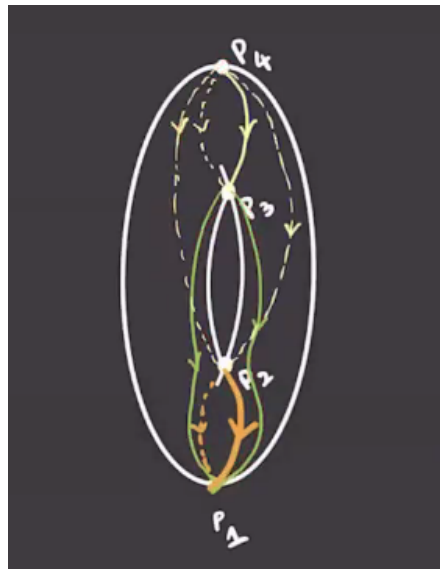
Figure 55: image_2021-01-28-11-48-06

We can cut along a curve on the bottom to better analyze these trajectories:
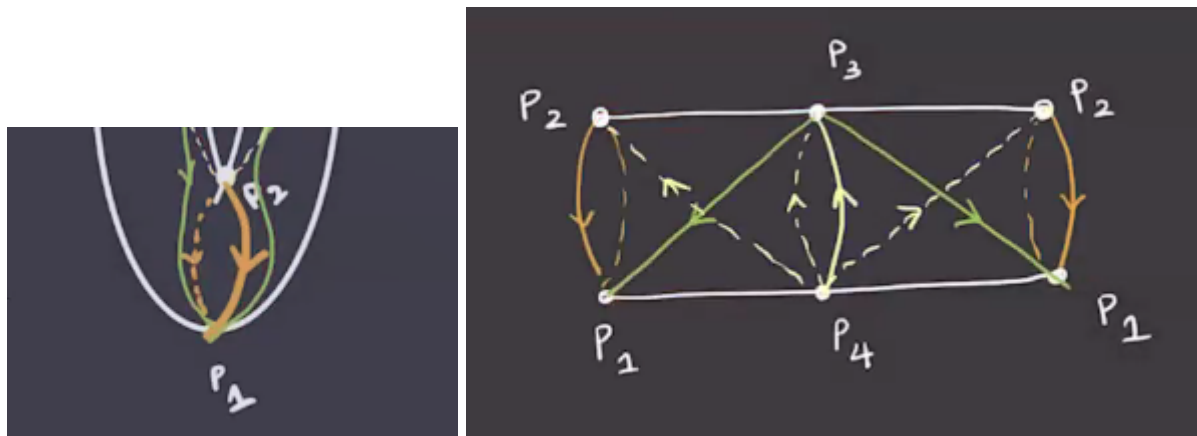
Now cut this cylinder along the trajectories $p_1 \rightsquigarrow p_3 \rightsquigarrow p_1$, i.e. the green trajectories here:
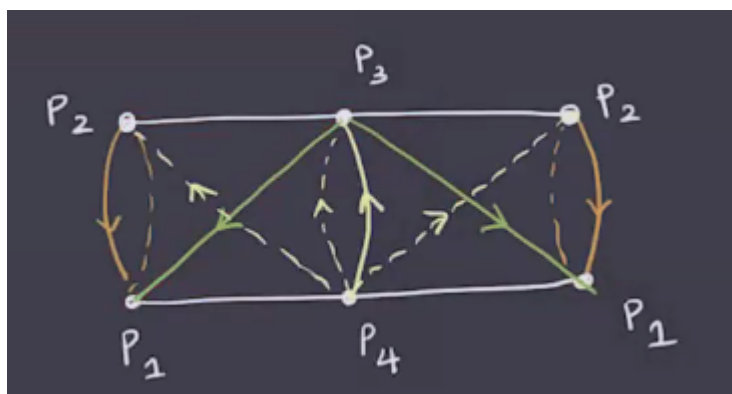
Figure 56: image_2021-01-28-11-51-31
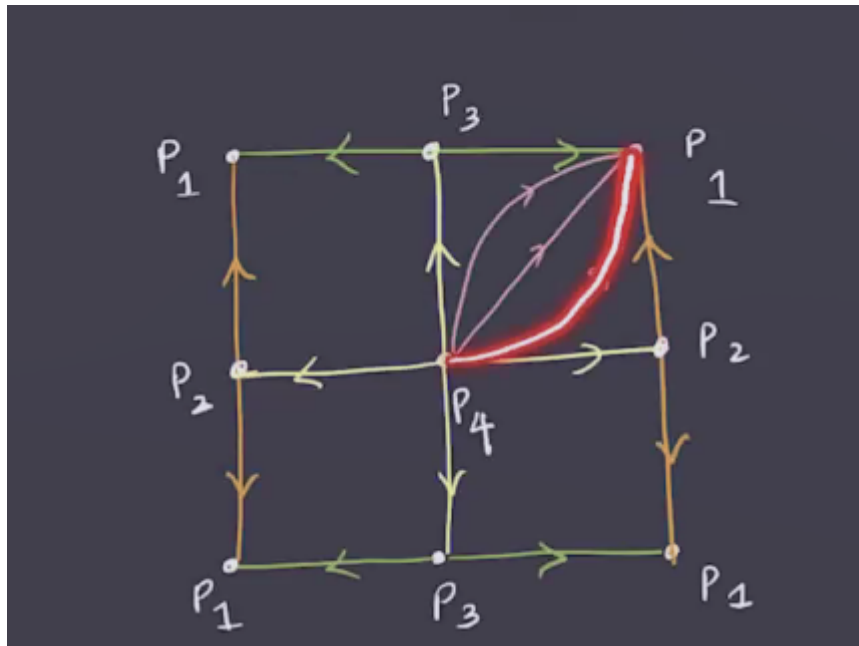
Figure 57: image_2021-01-28-11-53-32

Here we can see that as the trajectories approach the corners, they limit to broken trjacetories:
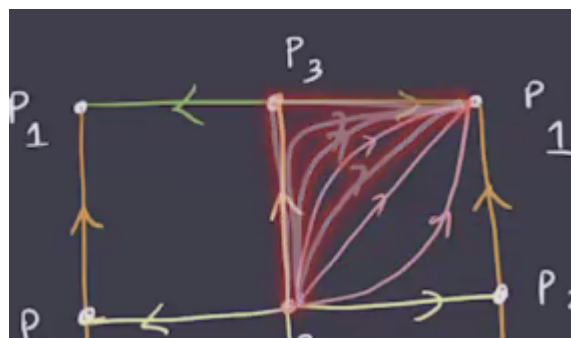
Figure 58: image_2021-01-28-11-54-44

We can compute

- $C_0 = \mathbb{Z}/2\mathbb{Z} \langle p_1 \rangle$
- $C_1 = \mathbb{Z}/2\mathbb{Z} \langle p_2, 3 \rangle$
- $C_2 = \mathbb{Z}/2\mathbb{Z} \langle p_4 \rangle$

Since there are exactly two trajectories p_4 to p_2 or p_3, we get $\partial_2 = 0$. Similarly $\partial_1 = 0$, and we get $HM_i(T) = [\mathbb{Z}/2\mathbb{Z}, \mathbb{Z}/2\mathbb{Z}^2, \mathbb{Z}/2\mathbb{Z}, 0, \cdots]$, which is the same as its singular homology.

> **Theorem 5.1.7***(?)***.**
>
> $$HM_i(f, g) \cong H_i^{\text{Sing}}(M; \mathbb{Z}/2\mathbb{Z}).$$
>
> In particular, it doesn't depend on the choice of Morse-Smale pair (f, g). See proof in references, e.g. Audin.

> *Proof (?).*
> By definition, $\# \operatorname{crit}_i(f) = \operatorname{rank} C_i(f, g) = \operatorname{rank} HM_i(f, g)$, and in any chain complex the rank of the chain groups are always at least the rank of the homology.
> ∎

5.2 Lagrangian Floer Homology

Remark 5.2.1: Suppose $L_0^n, L_1^n \subset M^{2n}$ are compact with $L_0 \pitchfork L_1$, so the intersection is finitely many points.
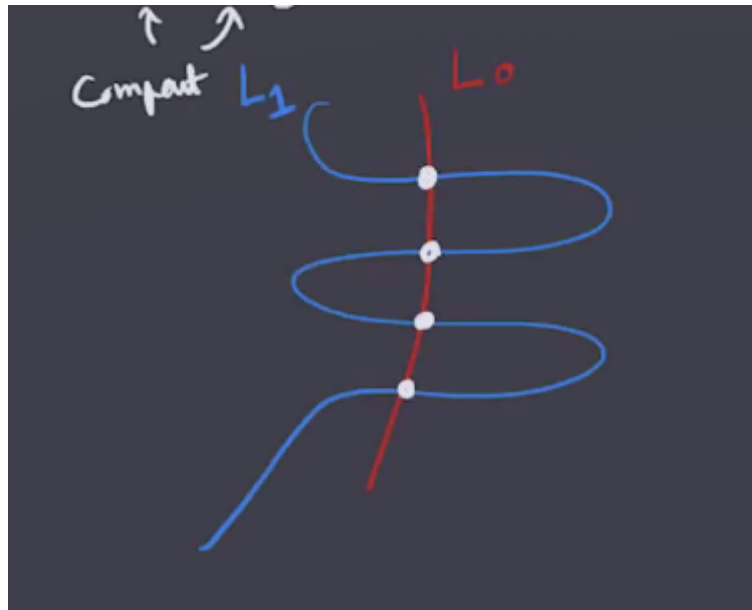
Figure 59: image__2021-01-28-12-16-27

We can do Morse theory on the space of paths between them:

$$\mathcal{P}(L_0, L_1) := \left\{ \gamma : I \to M \mid \gamma(0) \in L_0, \gamma(1) \in L_1 \right\}.$$

We'll find analogs of Morse functions on $P(L_0, L_1)$ such that the critical points are constant paths,

i.e. $L_0 \cap L_1$. The Morse inequalities then gives bounds on the number of intersection points between L_0 and L_1.

> **Definition 5.2.2** (Symplectic Manifolds)
> A **symplectic manifold** is a pair (M^{2n}, ω) with ω a 2-form which is
>
> - Closed, i.e. $d\omega = 0$, and
> - Nondegenerate, i.e. $\bigwedge^n \omega \neq 0$.

> **Definition 5.2.3** (Lagrangian Submanifolds)
> A half-dimensional submanifold $L^n \subset M^{2n}$ is called **Lagrangian** if $\omega|_{L^n} = 0$.

Example 5.2.4*(?):* The pair $(\mathbb{R}^{2n}, \sum_{i=1}^{n} dx_i \wedge dy_i$ is a symplectic manifold (and also a symplectic vector space). Note that this 2-form is also a bilinear form of the following shape:

$$
\begin{bmatrix} 0 & \operatorname{id}_n \\ -\operatorname{id}_n & 0 \end{bmatrix}.
$$

This has a Lagrangian submanifold $\mathbb{R}^n := \{y_1 = \cdots = y_n = 0\}$.

> *Note: See Darboux theorem.*

Remark 5.2.5: The general setup for next time: we'll have (M^{2n}, ω) a symplectic manifold, a pair $L_0, L_1 \subset M$ such that $L_0 \pitchfork L_1$, and we want to do Morse Homology on $\mathcal{P}(L_0, L_1)$.

6 | **Lecture 6 (Tuesday, February 02)**

Remark 6.0.1*(Setup):* We're working with a symplectic manifold, i.e. a pair (M^{2n}, ω) where $\omega \in \Omega^2$ is closed, i.e. $d\omega = 0$, and nondegenerate, i.e. $\bigvee^n \omega \neq 0$. We were also consider $L_0^n, L_1^n \subset M$ Lagrangian submanifolds, i.e. $\omega|_{L_i} = 0$. The goal is to do something like Morse homology on $\mathcal{P}(L_0, L_1)$ where the critical points corresponds to intersection points $L_0 \cap L_1$, where we'll assume $L_0 \pitchfork L_1$.

Question 6.0.2
What is the analog of a Morse function?

Remark 6.0.3: The functional f is defined on the *universal cover* $\overline{\mathcal{P}}(L_0, L_1) \to \mathbb{R}$. We can get around knowing much about f because we only ever need derivatives df and a metric g on the

path space to talk about the gradient $\nabla_g f$. We'll define a 1-form $\alpha : T\mathcal{P}(L_0, L_1) \to \mathbb{R}$, where we can define this tangent space as $T_\gamma \mathcal{P}(L_0, L_1)$ where $\gamma(s) : I \to M$. Set $u(s, t)$ to be a path from γ to γ' where $u(s, 0) = \gamma$ and $u(s, 1) = \gamma'$ and $\left.\dfrac{\partial u}{\partial t}\right|_{t=0}$, which is a tangent vector to γ and thus $\dfrac{\partial u}{\partial t}(s, 0) \in T_{\gamma(s)} M$.
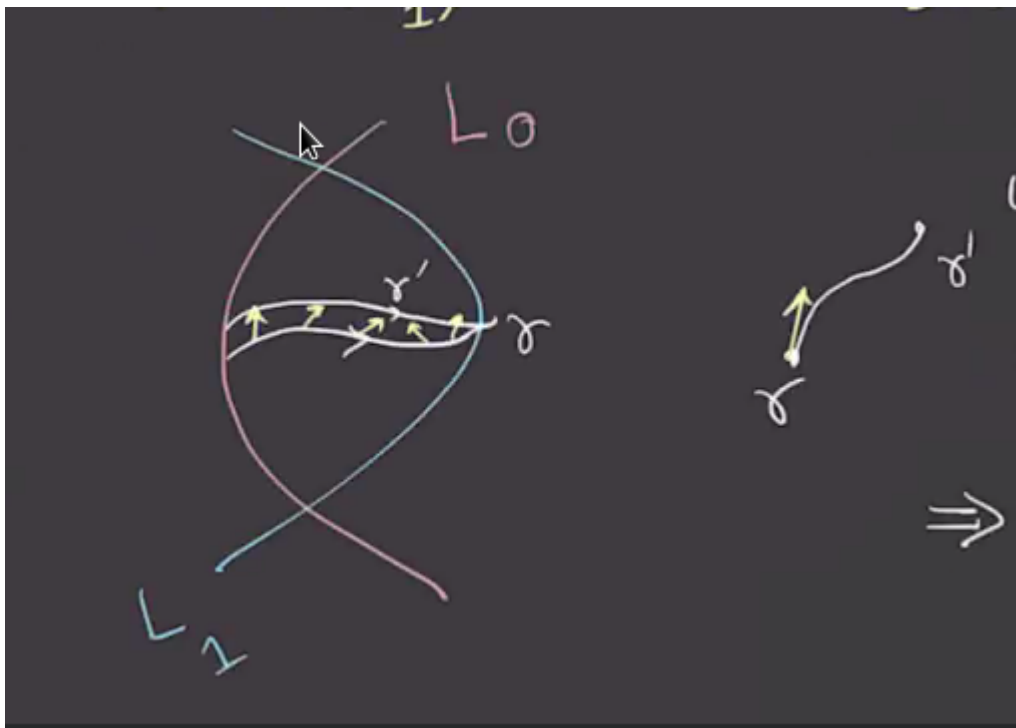

Figure 60: image_2021-02-02-11-29-54

Upshot: tangent vectors in $T_\gamma \mathcal{P}(L_0, L_1)$ are given by $\xi(s) \in T_{\gamma(s)} M$ for every $s \in I$, i.e. a way to push the path off of itself to obtain a new path.

We can thus define

$$\alpha : T\mathcal{P}(L_0, L_1) \to \mathbb{R}$$

$$(\gamma, \xi \in T_\gamma \mathcal{P}) \mapsto \alpha_\gamma \xi := \int_0^1 \omega(\dot\gamma(s), \xi(s)) ds.$$

Does this have the property we want? I.e. is it zero when γ is the constant path?

> **Lemma 6.0.4(?).**
>
> $$\alpha_\gamma \equiv 0 \iff \gamma(s) \text{ is constant} \iff \dot\gamma(s) = 0 \text{ for all } \gamma \iff \gamma(s) \in L_0 \cap L_1.$$

Proof (?).

$$\alpha_\gamma \equiv 0 \iff \int_0^1 \omega(\dot\gamma(s), \xi(s))ds = 0 \text{ for all } \xi \not\equiv 0.$$

Claim: If $\dot\gamma(s) \neq 0$ for some s then this is also true in an open neighborhood by smoothness, so one can find a ξ such that

- $\omega(\dot{\gamma(s)}, \xi(s)) \geq 0$, and
- There is some open subinterval $(a, b) \subseteq [0, 1]$ on which ξ is nonzero, and thus the integral is strictly positive.

We'll need a few tools:

> **Definition *(Almost Complex Structure)***
> An **almost complex structure** is a bundle automorphism $J : TM \to TM$ such that $J \circ J = -\mathbb{1}_{TM}$. It is said to be **compatible** with ω if and only if
>
> - Positivity: For every $v \neq 0$, $\omega(v, Jv) > 0$.
> - "Symplectic Isometry": For all $v, w \in TM$, $\omega(Jv, Jw) = \omega(v, w)$.
>
> In this case, there is a Riemannian metric defined by $g(v, w) = \omega(v, Jw)$. Conversely, given an almost complex structure J and a metric J, there is a symplectic form defined by $\omega(v, w) = \omega(Jv, Jw) := g(Jv, w)$.
>
> This may not be a closed form? Need to check later!

> **Exercise *(?)***
> Check that ω is a symplectic form compatible with J and g is the corresponding metric.

> **Exercise *(?)***
> Given a symplectic form ω and a Riemannian metric g there exists a canonical almost complex structure J compatible with ω such that the previous process sends (ω, J) to g.

> **Corollary 6.0.8*(?).***
> Any symplectic manifold (M, ω) has a compatible almost complex structures J.

> **Theorem 6.0.9*(?).***
> The space of all almost complex structures on M compatible with ω is contractible.

Here we can use that $\xi(s) = J\dot\gamma(s)$ which implies $\omega(\dot\gamma(s), J\dot\gamma(s)) = \omega(\dot{\gamma(s)}, \xi(s)) > 0$, which happens if and only if $\dot\gamma(s) \neq 0$.

So pick an almost complex structure compatible with ω and produce a metric g. We'll define a metric on $\mathcal{P}(L_0, L_1)$ by the following: for $\xi, \eta \in T_\gamma\mathcal{P}$, recalling that $\xi = \xi(s), \eta = \eta(s) \in T_{\gamma(s)}M$, set

$$g_\gamma^{\mathcal{P}}(\xi, \eta) := \int_0^1 g(\xi(s), \eta(s))ds = \int_0^1 \omega(\xi, J\eta)ds.$$

> **Exercise *(?)***
> Check that $g^{\mathcal{P}}$ is a metric on $\mathcal{P}(L_0, L_1)$.

We'll now define a **gradient vector field**:

$$g^{\mathcal{P}}_{\gamma}(-\nabla, -) = \alpha(-).$$

So here α will play the role of $-df$. We can write

$$\int_0^1 \omega(-\nabla, J\xi)ds = \int_0^1 \omega(\cdot\gamma, \xi)ds.$$

Using compatibility, the LHS is equal to

$$\cdots = \int_0^1 \omega(-J\nabla, J^2\xi)ds = \int_0^1 \omega(J\nabla, \xi)ds.$$

So the RHS is equal to this for every ξ, which means that $J\nabla = \dot{\gamma}$. Multiplying both sides by J yields $\nabla = -J\dot{\gamma}$ What are the trajectories of $J \cdot \gamma(s) \in T_{\gamma}\mathcal{P}$? We can compute

$$\frac{\partial u}{\partial t}(s, t) = J\frac{\partial u}{\partial s}(s, t).$$

Here t is the parameter that moves between paths, and s moves along a given path:
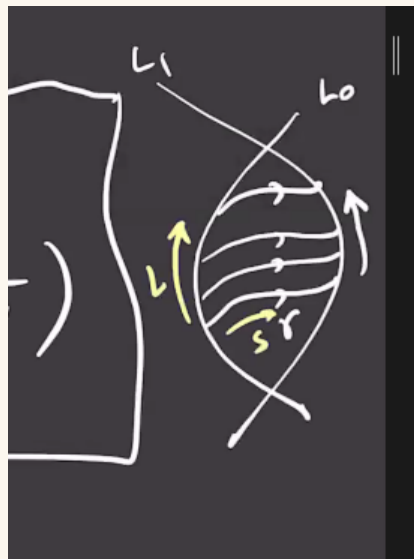
Figure 61: image_2021-02-02-12-34-41

■

7 | Lecture 7 (Thursday February 04)

7.1 Lagrangian Floer Homology

Remark 7.1.1: Recall that we had a symplectic manifold (M^{2n}, ω) with $L_0, L_1 \subset M$ two Lagrangians. We wanted to do something like Morse theory on $\mathcal{P}(L_0, L_1)$.
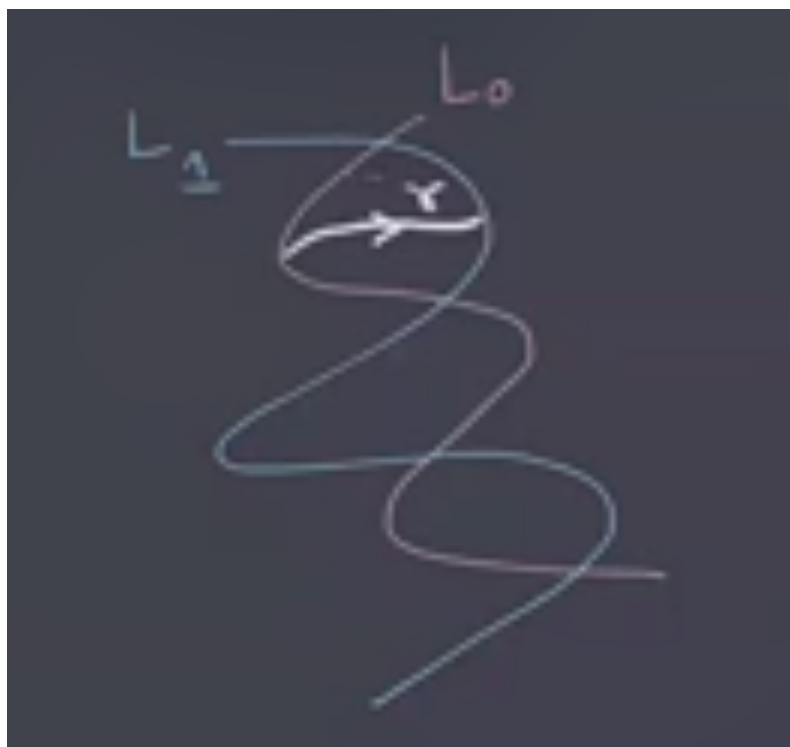
Figure 62: image_2021-02-16-22-21-44

What ingredients do we need?

- Something to replace $-df$: α

- Something to replace the vector field $-\nabla$: we defined a metric $g^{\mathcal{P}}$ using α

To define α we needed to look at

$$T_\gamma \mathcal{P} = \left\{ \xi : I \to TM \;\middle|\; \xi(s) \in T_{\gamma(s)}M \right\},$$

which is like a collection of tangent vectors along γ giving a way to deform the path. Since $\alpha \in \Omega^1(\mathcal{P})$,

for any γ it induces a map

$$T_\gamma M \xrightarrow{\alpha} \mathbb{R}$$

$$\xi \mapsto \alpha_\gamma(\xi) := \int_0^1 \omega(\dot{\gamma}, \xi)\, ds.$$

Observation 7.1.2

$\alpha_\gamma = 0 \iff \gamma$ is constant, which happens if and only if $\gamma \in L_0 \cap L_1$. This corresponds to critical points of the functional yielding intersection points of the Lagrangians.

Remark 7.1.3: We wanted to define the gradient, for which we needed a metric on $\mathcal{P}$. We did this by lifting a metric from M. Pick an almost complex structure J compatible with ω, then this yields a Riemannian metric defined by $g(v, w) = \omega(v, Jw)$. Then we can define

$$g_\gamma^{\mathcal{P}}(\xi, \eta) := \int_0^1 g(\xi(s), \eta(s))\, ds.$$

We used this to compute the vector field $-\operatorname{grad}_\gamma J \cdot \gamma(s)$. What are its trajectories? These are paths of paths $u(s, t) := u_t(s)$ such that $\frac{\partial}{\partial t} u_t(s) = J \frac{\partial}{\partial s} u_t$. We thus get an equation

$$\frac{\partial u}{\partial t}(s, t) = J \frac{\partial u}{\partial s}(s, t).$$

Remark 7.1.4: For $x, y \in L_0 \cap L_1$ trajectories connecting x to y, we'll write this as

$$\mathcal{M}(x, y) := \left\{ u(s, t) : [0, 1] \times \mathbb{R} \to M \begin{array}{c} u(0,t) \in L_0 \\ u(1,t) \in L_1 \\ u(s,t) \xrightarrow{t \to -\infty} x \\ u(s,t) \xrightarrow{t \to \infty} y \\ \frac{\partial u}{\partial t} = J \frac{\partial u}{\partial s} \end{array} \right\}.$$

We can modify this PDE to make things look familiar: multiply both sides with J to obtain

$$J \frac{\partial u}{\partial t} = J^2 \frac{\partial u}{\partial s} \implies J \frac{\partial u}{\partial t} = -\frac{\partial u}{\partial s} \implies \frac{\partial u}{\partial s} + J \frac{\partial u}{\partial t} = 0,$$

which is the Cauchy-Riemann equation.

Exercise 7.1.5 (?)
Check that this equation can be written as $J\, du = du \circ i$ where i is the standard complex structure on $\mathbb{C} \supseteq [0, 1] \times \mathbb{R}$, so du commutes with i and J.

Definition 7.1.6 (*J*-holomorphic or Pseudoholomorphic Discs)
If $J\, du = du \circ i$, then u is called a ***J*-holomorphic disc** or a **pseudoholomorphic disc**.

Remark 7.1.7: Schematically, the situation is the following:
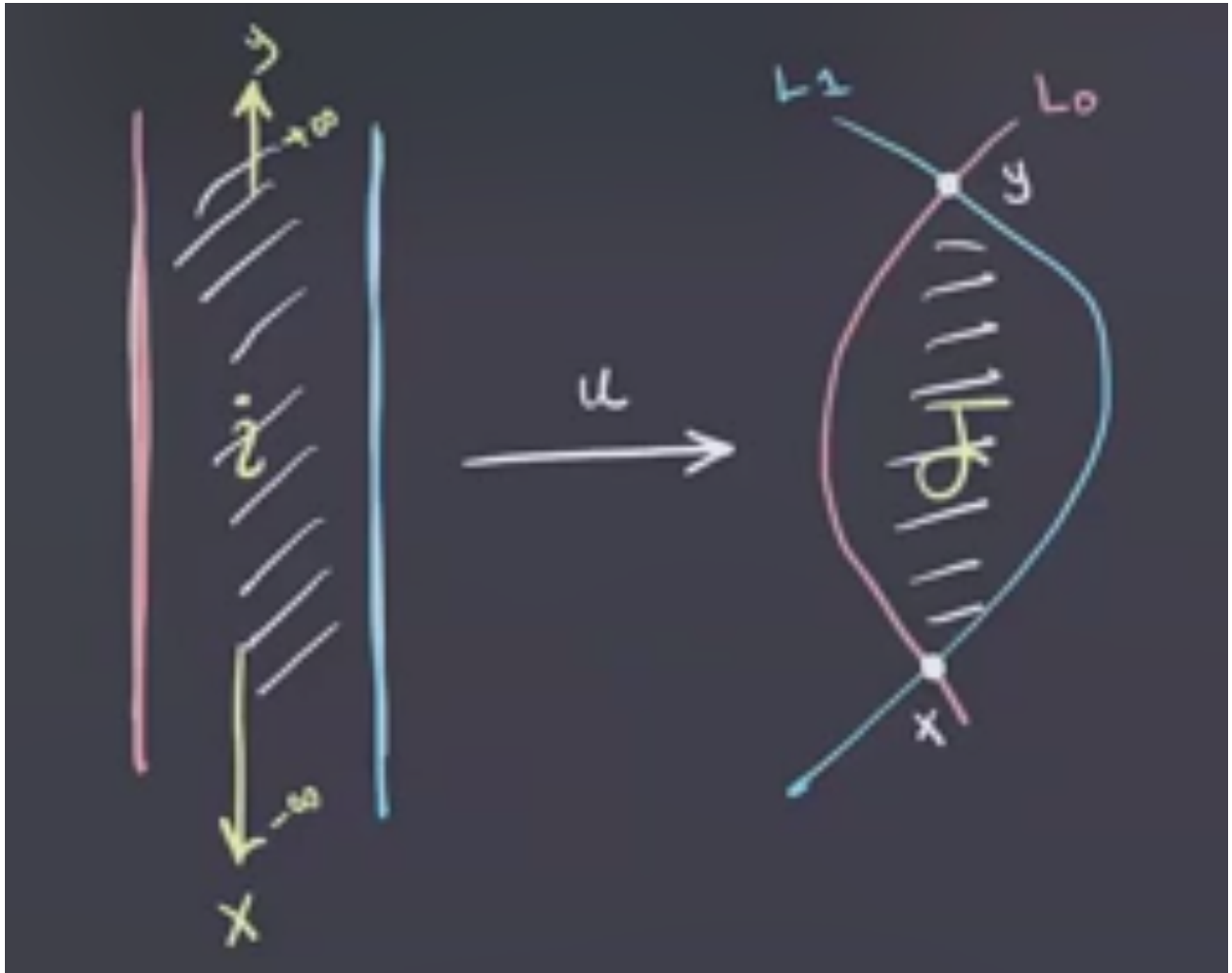
Figure 63: image_2021-02-16-23-22-40

Using the Riemann mapping theorem, the strip on the left-hand side is biholomorphic to $\mathbb{D} \subseteq \mathbb{C}$ with $\pm i$ removed:
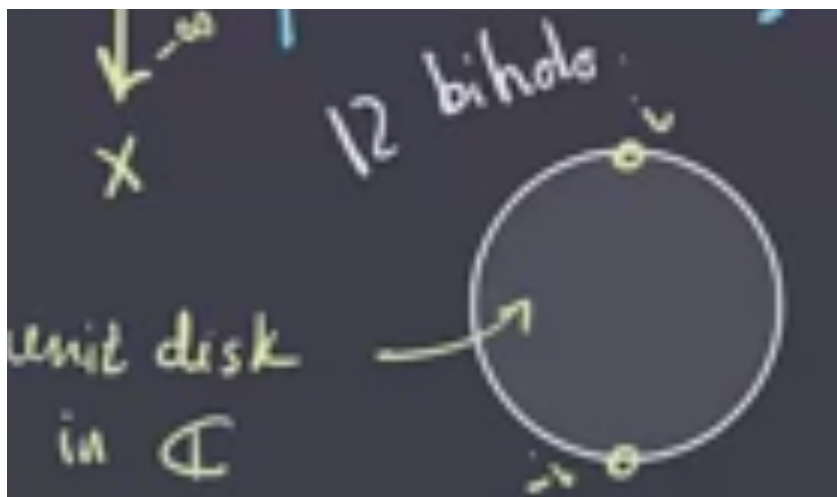
Figure 64: image_2021-02-16-23-23-43

Due to the limit conditions at infinity in the strip, we can extend u to a J-holomorphic map from the entire disc by sending $i \mapsto y$ and $-i \mapsto x$.

Remark 7.1.8: In Morse homology, we have an $\mathbb{R}$ action on the moduli space of trajectories, and that also shows up here. Here $\mathbb{R} \curvearrowright \mathcal{M}(x, y)$ by $u(s, t) \xrightarrow{c} u_c(s, t) := u(s, t + c)$, noting that translating the strip from above still yields a solution.

> **Definition 7.1.9** (?)
> We define
> $$\widehat{\mathcal{M}}(x, y) := \mathcal{M}(x, y)/\mathbb{R}.$$

> **Definition 7.1.10** (?)
> We'll define
> $$CF(L_1, L_2) := \bigoplus_{x \in L_0 \cap L_1} \mathbb{Z}/2\mathbb{Z} \langle x \rangle$$
>
> $$\partial x := \sum_{y \in L_0 \cap L_1} \#\widehat{\mathcal{M}}(x, y) y.$$

Remark 7.1.11: When is the intersection count $\#\widehat{\mathcal{M}}(x, y)$ well-defined? In Morse homology, we have two conditions:

1. (f, g) is Morse-Smale, to ensure that the moduli spaces are smooth manifolds (using Sard's theorem)

2. $\operatorname{ind}(x) - \operatorname{ind}(y) = 1$, ensuring $\mathcal{M}(x, y)$ is 1-dimensional

    3. Compactness of $\widehat{\mathcal{M}}(x, y)$ when 1 and 2 hold.

These were enough to guarantee that $\widehat{\mathcal{M}}(x, y)$ was a smooth compact 0-dimensional manifold, which allowed for point counts. In Lagrangian Floer homology, we have the following replacements:

For 2 (indices): Recall that the index in Morse homology was the dimension of the negative eigenspace of the Hessian, but we're in infinite dimensions here. So we won't have a well-defined index, but we'll have something that can replace the *difference* of indices: the **Maslov index** $\mu(x, y)$, the expected dimension of $\mathcal{M}(x, y)$. To actually have this be the dimension will require some conditions, so it's not always true. This will be the index of some elliptic operator defined using the Cauchy-Riemann equations.

For 1 (transversality): We'll need some version of transversality, which will imply that for a generic J that $\mathcal{M}(x, y)$ is smooth.

For 3 (compactness): We'll use **Gromov compactness** and some extra topological assumptions, which will imply that $\widehat{\mathcal{M}}(x, y), \mathcal{M}(x, y)$ are both compact.

Taken together, these will make the point-count well-defined.

Remark 7.1.12: In order for this to be a chain complex, we'll need $\partial^2 = 0$. We'll look at when $\mu(x, y) = 2$, and we'll compactify $\widehat{\mathcal{M}}(x, y)$ in order to show this holds. Gromov's compactness will give us

$$\partial \overline{\mathcal{M}(x, y)} = \bigcup_{\mu(x,z)=\mu(z,y)=1} \mathcal{M}(x, z) \times \mathcal{M}(z, y),$$

much like the *broken trajectories* from Morse homology. Here we'll need to add in broken J-holomorphic discs:
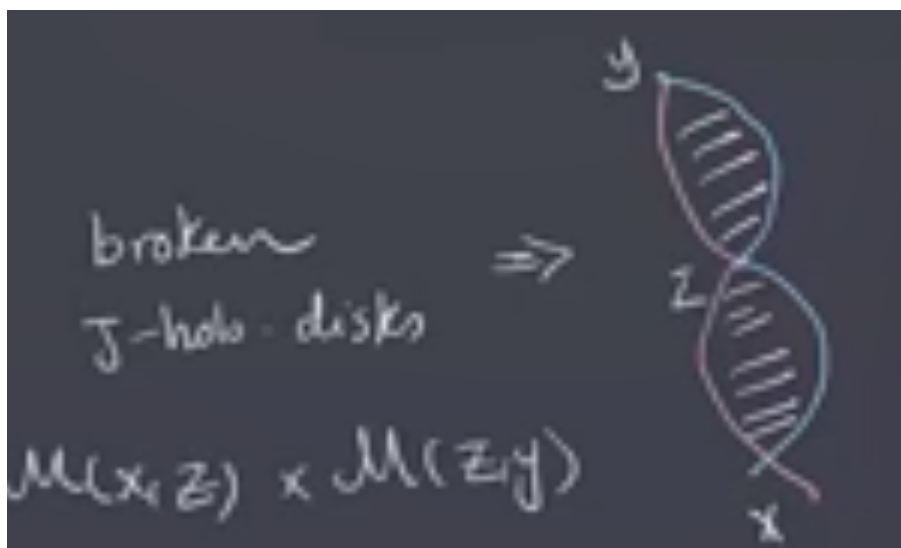
Figure 65: image_2021-02-16-23-45-04

Using the same argument as in Morse homology, we can obtain $\partial^2 = 0$.

Theorem 7.1.13 *(Floer).*
Suppose (M^{2n}, ω) is a compact symplectic manifold with Lagrangians L_0, L_1 such that

1. $L_0 \pitchfork L_1$

2. $\pi_2(M) = \pi_2(M, L_0) = \pi_2(M, L_1) = 0$, which are topological conditions on embedded spheres with boundaries mapped to the L_i.

Under these assumptions, $\partial^2 = 0$ and the homology

$$HF(L_0, L_1) := H_*(CF(L_0, L_1), \partial) := \ker \partial / \operatorname{im} \partial$$

is an invariant of (M, L_0, L_1) up to **Hamiltonian isotopies** of L_0, L_1.

Definition 7.1.14 (Symplectomorphism)
A **symplectomorphism** is a diffeomorphism $\psi : M_1 \to M_2$ such $\psi^* \omega_1 = \omega_2$.

Definition 7.1.15 (Hamiltonian Vector Fields)
A **Hamiltonian vector field** is a vector field V such that

$$\iota_V \omega := \omega(V, -) \in \Omega^1$$

is exact, and thus equal to df for some functional $f \in C^\infty(M, \mathbb{R})$. Note that if one has a functional f, one can find a symplectic form ω such that this holds, so V is sometimes denoted V_f to show this dependence.

Example 7.1.16 *(?):* $\mathbb{R}^{2n}$ with the standard symplectic form $\displaystyle\sum_{i=1}^n dx_i \wedge dy_i$, we have $V_f = \dfrac{\partial f}{\partial y_1}, \cdots, \dfrac{\partial f}{\partial y_n}, -\dfrac{\partial f}{\partial x_1},$
for any $f : \mathbb{R}^{2n} \to \mathbb{R}$. Note that we can have time-dependent vector fields (i.e. one parameter families) as well.

Definition 7.1.17 (Hamiltonian Isotopies)
A **Hamiltonian isotopy** is a family ψ_t of diffeomorphisms of M such that ψ_t is the flow of a 1-parameter family of Hamiltonian vector fields V_t, so taking the derivative of V yields this function.

Exercise 7.1.18 (?)
Show that if ψ_t is a Hamiltonian isotopy, then $\psi_t^* \omega = \omega$ and is thus a symplectomorphism as well.

Remark 7.1.19: Goal: use this as an invariant of closed 3-manifolds in the form of **Lagrangian Floer homology**, defined by Osvath-Szabo. Note that Floer's theorem requires topological assumptions which make the homology well-defined, but we don't have these available in the HF setup. In particular, the assumptions on π_2 won't hold.

8 | Lecture 8 (Thursday, February 04)

8.1 Heegard Splittings

Remark 8.1.1: Goal: we want to use **Lagrangian Floer homology** to defined invariants of *closed* 3-manifolds, where here closed means that $\partial M^3 = \emptyset$. One example of Lagrangian Floer homology is **Heegard Floer homology**. We'll want some symplectic manifold with two Lagrangian submanifolds. Oszvath-Szabo used a 2-dimensional description of closed 3-manifolds called **Heegard diagrams**. We'll need Heegard splittings to define these, and handlebodies to define the splittings.

Definition 8.1.2 (Handlebody of genus g)
A **handlebody** of genus g will mean a compact 3-manifold obtained from $\mathbb{B}^3$ by attaching g solid 1-handles, i.e. $\mathbb{D}^1 \times \mathbb{D}^2$. These are glued in via two copies of $\partial \mathbb{D}^1 \times \mathbb{D}^2$:

Figure 66: image__2021-02-16-19-36-51

Alternatively, these can be defined as a regular neighborhood of $\bigvee\limits_{i=1}^{g} S^1 \subset \mathbb{R}^3$. We'll write H_g for a genus g handlebody, and ∂H_g will be a genus g surface.

Definition 8.1.3 (Heegard Splitting)
A **Heegard splitting** of genus g is a decomposition $M = H_1 \coprod_\varphi H_2$ where $\varphi : \partial H_1 \to \partial H_2$ is a diffeomorphism.

Figure 67: image_2021-02-16-19-41-17

Explicitly, we have

$$H_1 \coprod_\varphi H_2 := \frac{H_1 \coprod H_2}{\left\langle x \sim \varphi(x) \mid \forall x \in \partial H_1 \right\rangle}.$$

Example 8.1.4(?): We can write $S^3 = B_3 \coprod_{\mathbb{1}} B^3$, where both are just genus 0 handlebodies. Note that if you attach a solid 1-handle to B^3, this yields $S^1 \times \mathbb{D}^2$, i.e. a solid torus:

Figure 68: image_2021-02-16-19-42-43

Think of S^3 as the one-point compactification of $\mathbb{R}^3$, we can write (and visualize) a decomposition $S^3 = (S^1 \times \mathbb{D}^2) \coprod_\varphi (S^1 \times \mathbb{D}^2)$. The first copy will be a neighborhood of a circle in the plane:
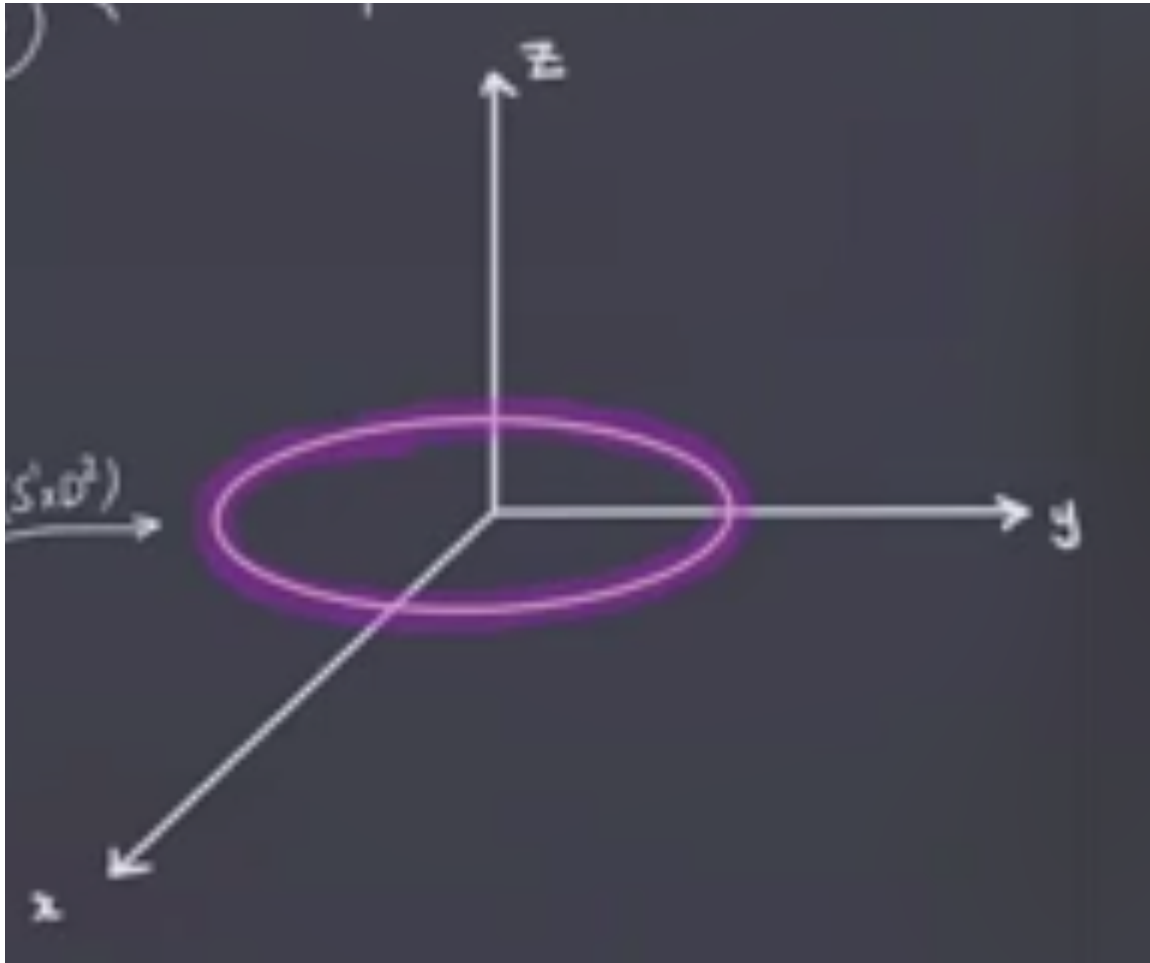
Figure 69: image_2021-02-16-19-44-16

Labeling this circle as $H^1 := \left\{ x^2 + y^2 = 1, z = 0 \right\}$, the complement $H_2 := S^3 \setminus H_1$ will be a regular neighborhood of the z-axis union $\{\infty\}$:
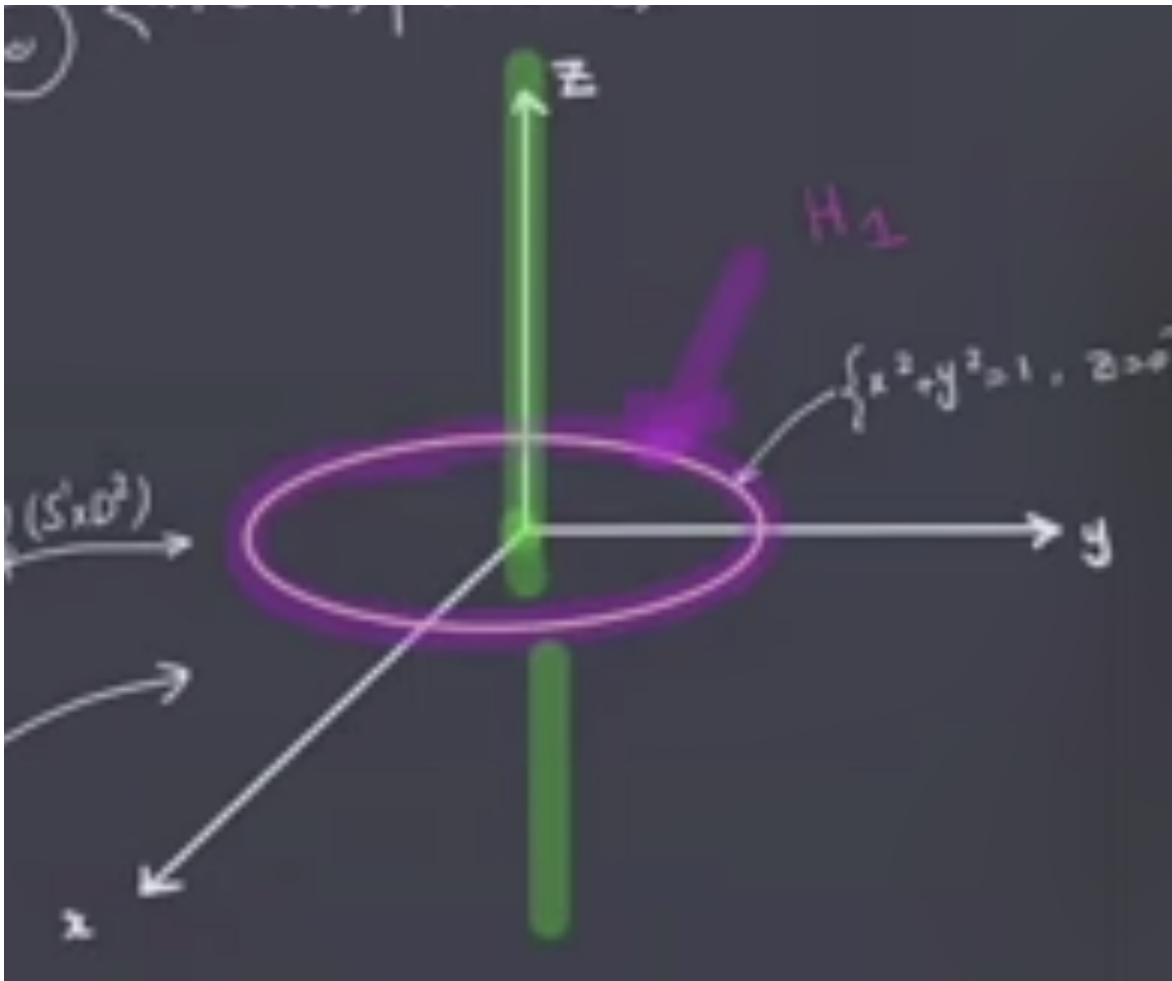
Figure 70: image_2021-02-16-19-45-36

Example 8.1.5*(?):* We can write a Heegard splitting of $S^1 \times S^2$. Note that $S^2 = \mathbb{D}^2 \coprod_{\mathbb{1}} \mathbb{D}^2$, so splitting the product over the union yields $(S^1 \times \mathbb{D}^2) \coprod_{\mathbb{1}} (S^1 \times \mathbb{D}^2)$, where the new map is still the identity since it's just the identity on each factor. This yields two solid torii glued along their boundaries.

> **Theorem 8.1.6*(?).***
> Any closed 3-manifold M^3 admits a Heegard splitting.

> *Proof (?).*
> A fact from Morse theory: there exists a Morse function $f : M^3 \to \mathbb{R}$ such that
>
> 1. $f(p) = i := \mathrm{ind}(p)$ for every $p \in \mathrm{Crit}(f)$ (i.e. f is **self-indexing**), and
>
> 2. f has exactly one index 0 (minimum) and one index 3 (maximum) critical point.
>
> We thus have the following situation:
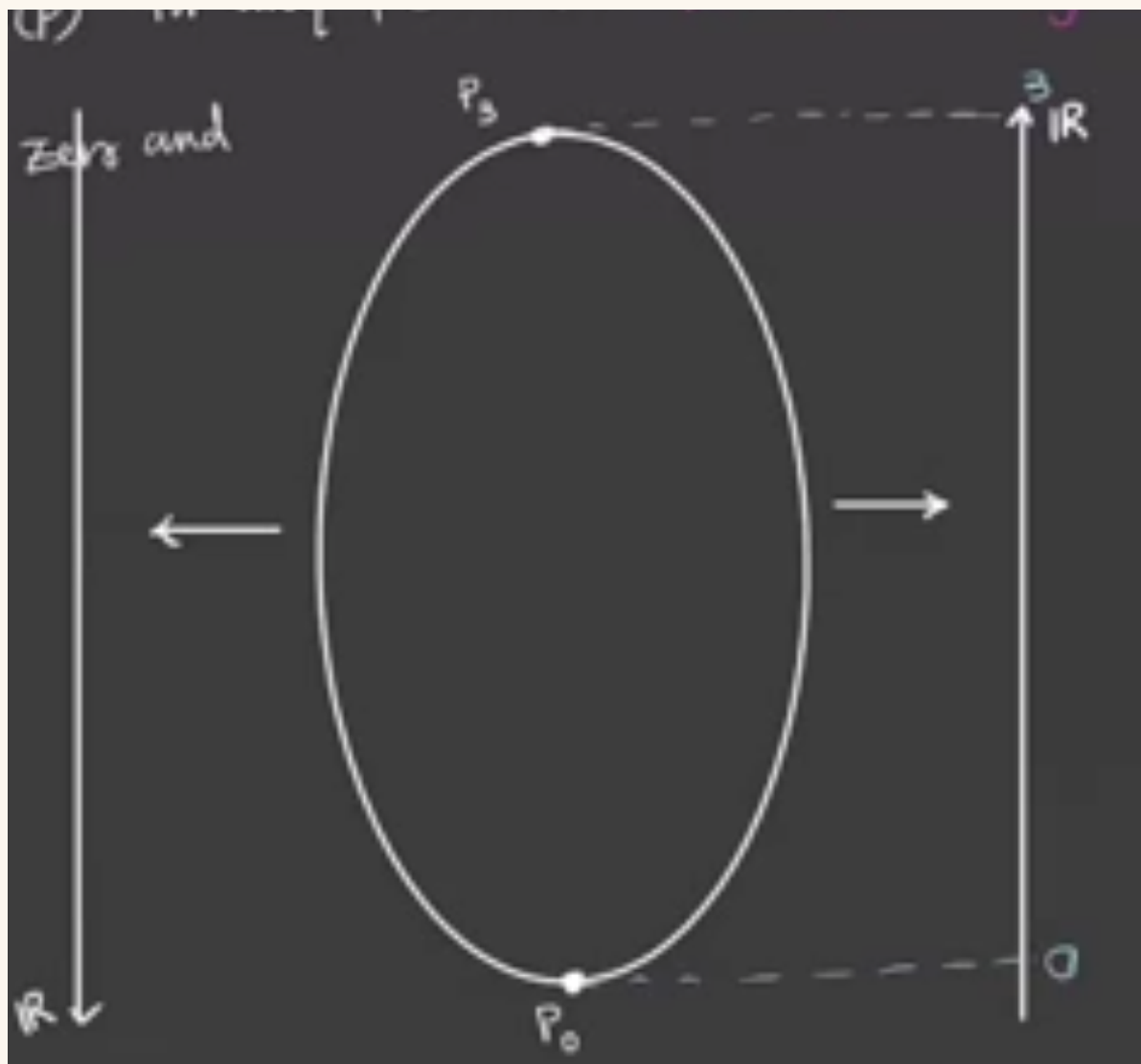
Figure 71: image_2021-02-16-19-51-11

The remaining critical points must occur at 2 and 3:
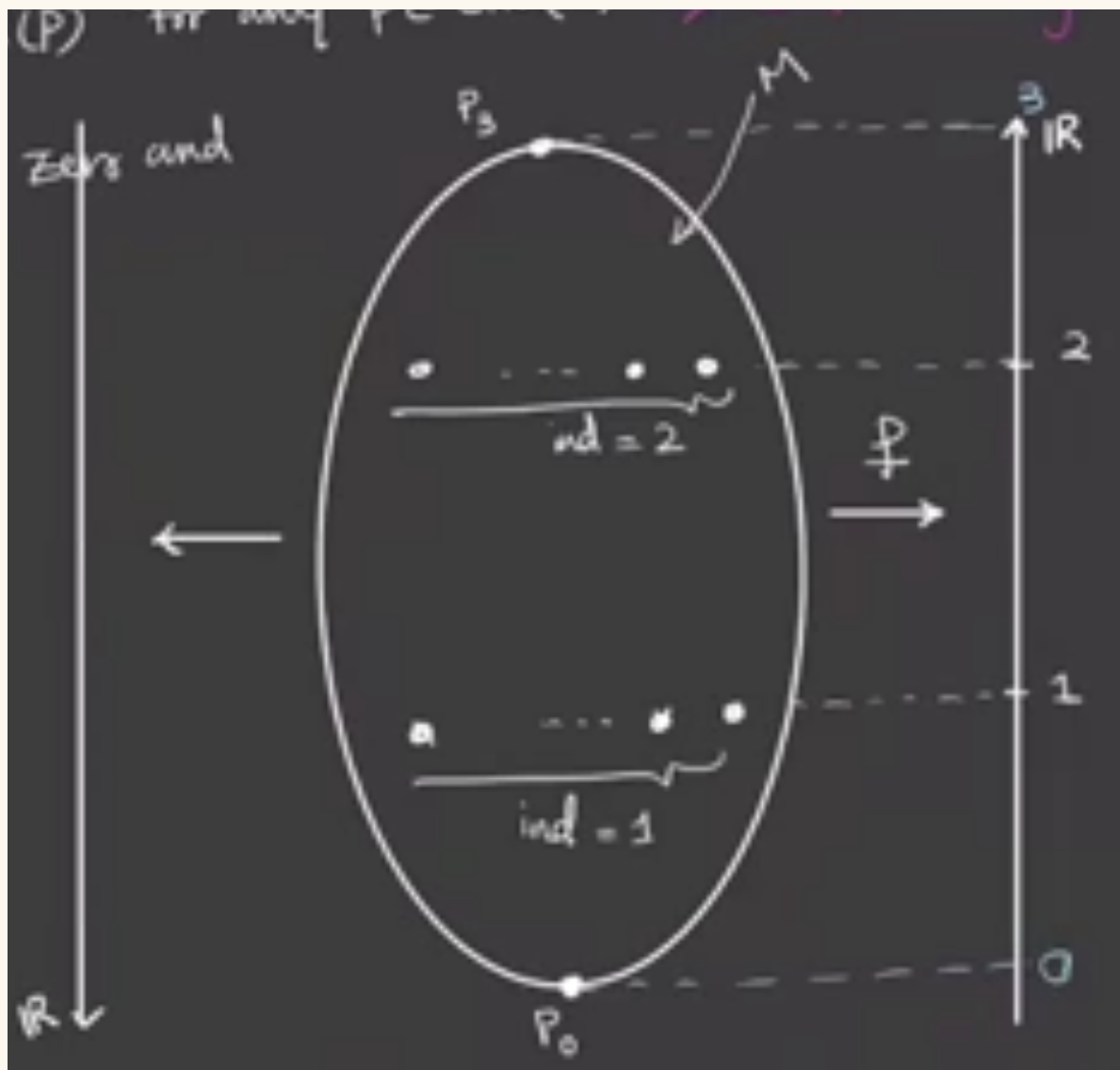
Figure 72: image_2021-02-16-19-52-00

How can we break this into smaller manifolds? Any time we pass a critical point, we attach a one-handle. Note that we can define a new Morse function $h := 3 - f$ Suppose we have g critical points of index 1 for f and g' critical points of index 1 for h.

- We can check that $f^{-1}[0, 1/2] = \mathbb{B}^3$ and $f^{-1}(1/2) = S^2$.

- $f^{-1}[0, 3/2]\Lambda_g$, a genus g handlebody, and thus $f^{-1}(3/2) = \Sigma_g$ will be a genus g surface.
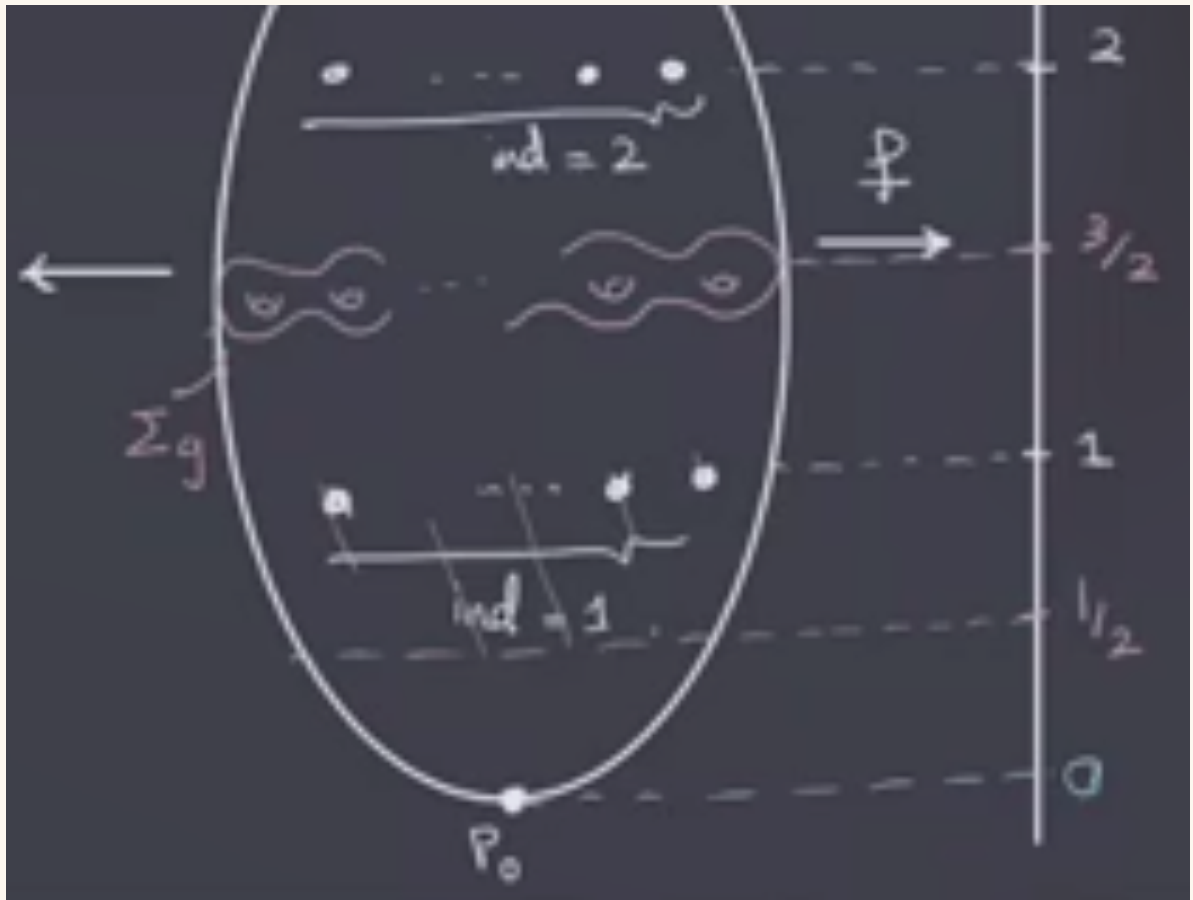
Figure 73: image_2021-02-16-19-54-58

- Repeating the above arguments for h, we get $f^{-1}[0, 3/2] = g^{-1}[3/2, 3] = \Lambda_{g'}$.

> **Exercise *(?)***
> Show that $\operatorname{crit}(f) = \operatorname{crit}(h)$ and if $p \in \operatorname{crit}(f)$ with $\operatorname{ind}_f(p) = i$ then $\operatorname{ind}_h(p) = 3 - i$.

Thus g' is the number of index 2 critical points for f. This means that $\partial h^{-1}[0, 3/2] = h^{-1}(3/2) = f^{-1}(3/2)$ has genus $g = g'$, and thus the $\# \operatorname{crit}(f)_{\operatorname{ind}=1} = \# \operatorname{crit}(h)_{\operatorname{ind}=2} = g$. Even without this, we still have our two handlebodies: $H_1 := f^{-1}[0, 3/2]$ and $H_2 := f^{-1}[3/2, 3]$ glued over $\Sigma_g := f^{-1}(3/2)$, which is a genus g splitting surface. ∎

Definition 8.1.8 (Equivalence of Heegard Splittings)
We'll say that two Heegard splittings $M = H_1 \coprod_\varphi H_2$ and $M = H_1' \coprod_\varphi H_2'$ are **isotopic** if and only if there exists an ambient isotopy $\psi : M \times [0, 1] \to M$ such that $\psi|_{M \times \{1\}}(H_i) = H_i'$ for each i. Recall that *ambient isotopy* means

- $\psi|_{M \times \{0\}} = \mathbb{1}$,

- $\psi|_{M \times \{t\}}$ is a homeomorphism.

Question 8.1.9

Are *any* two Heegard splittings isotopic?

Answer 8.1.10

No! We can distinguish them by the genus of the splitting surface Σ, and we just saw two splittings of S^3, one with genus 0 and one with genus 1.

Remark 8.1.11: There are some moves to relate different Heegard splittings.

Definition 8.1.12 (Stabilization)

Given a genus g Heegard splitting $M = H_1 \coprod_\varphi H_2$, we can produce a genus $g + 1$ splitting $M = H_1' \cup_\varphi H_2'$ where

$H_1' = H_1 \cup \eta(\gamma)$, where the new piece is a closed regular neighborhood of an unknotted arc γ in H_2. Here *unknotted* means that γ is a properly embedded arc in $H_2 \cup \Sigma$ whose boundary is in Σ which bounds a contractible disc:
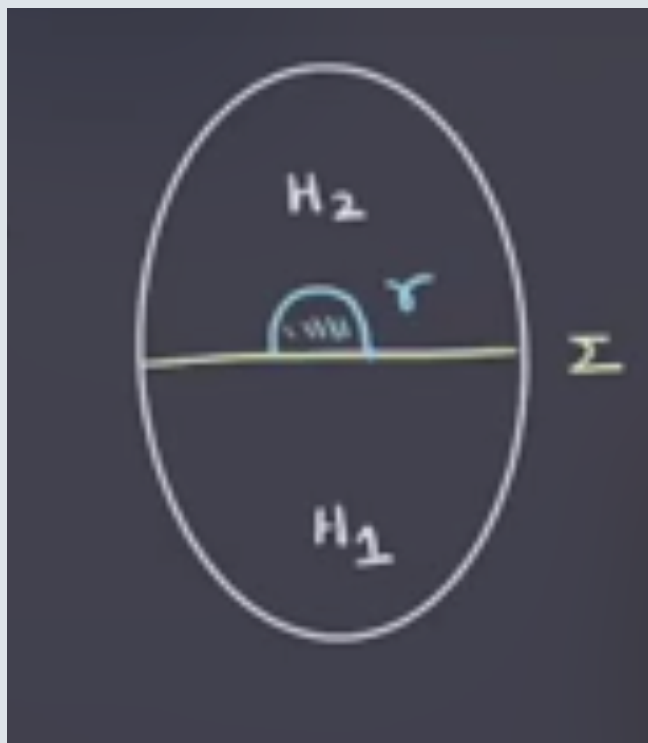
Figure 74: image_2021-02-16-21-00-33

Note that adding a regular neighborhood around γ has the effect of adding a 1-handle to H_1. We can then define $H_2' := H_2 \setminus \eta\gamma$. Why is this still a handlebody? We have this situation:

Figure 75: image_2021-02-16-21-04-24

We have the disc below the 1-handle, and if we thicken it to $\mathbb{D}^2 \times I$, we have $B := \eta(\gamma) \cup (\mathbb{D}^2 \times [0,1]) \cong \mathbb{B}^3$:
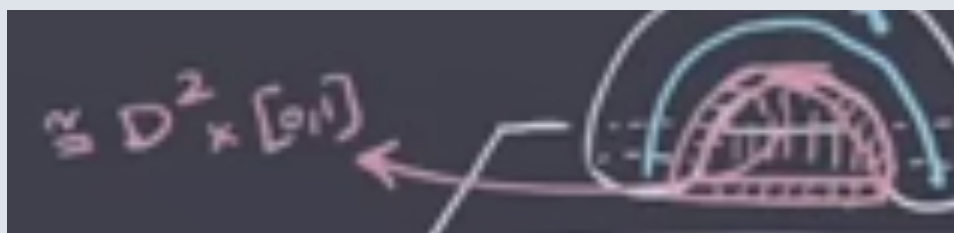
Figure 76: image_2021-02-16-21-07-07

We then have $H_2' := (H_2 \setminus B) \cup (\mathbb{D}^2 \cup [0,1])$, and in fact there is something in the intersection of these two terms. The parts that are attached to H_2 are the front and back discs $\mathbb{D}^2 \times \{0,1\}$:
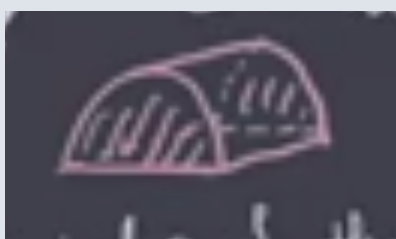
Figure 77: image_2021-02-16-21-07-50

So we can identify this as $H_2' := (H_2 \setminus B) \coprod_{\mathbb{D}^2 \times \{0,1\}} (\mathbb{D}^2 \cup [0,1])$. Note that $H_2 \setminus B \cong_{C^\infty} H_2$ are diffeomorphic, and the right-hand side is a 1-handle. To see why this is, consider attaching the middle red part, and then pushing the center part away in order to see the handle:
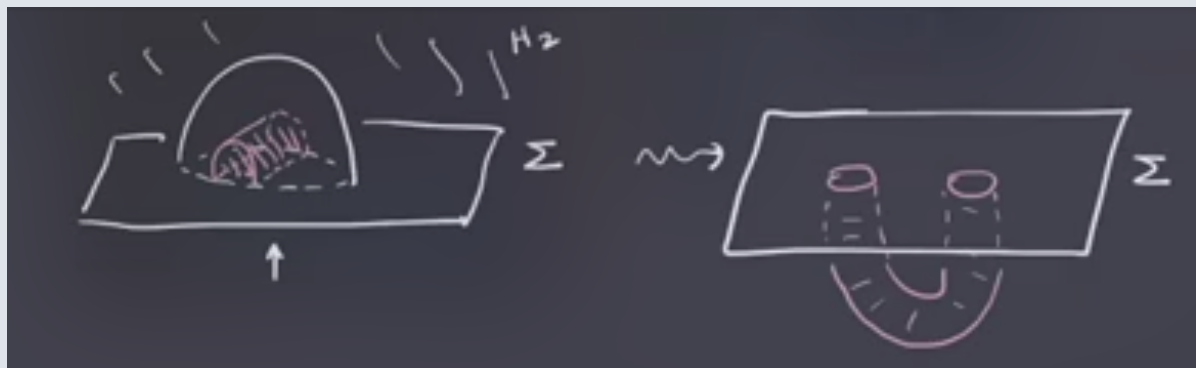
Figure 78: image_2021-02-16-21-21-12

Exercise 8.1.13 (?)
Show that the isotopy type of $H_1' \cup H_2'$ is independent of the choice of γ.

Theorem 8.1.14*(?)*.
Any two Heegard splittings can be made isotopic after sufficiently many stabilizations.

8.2 Heegard Diagrams

2-dimensional pictures of closed 3-manifolds! We have two handlebodies glued along their boundary, so if we can write the handlebodies in terms of 2-dimensional pictures, we can combine them to get a picture of the entire splitting.

Definition 8.2.1 (Attaching Curves)
Let H be a genus g handlebody. A set of **attaching curves** for H is a set $\{\gamma_1, \cdots, \gamma_g\}$ of pairwise disjoint simple closed curves on $\Sigma := \partial H$ such that

1. $\Sigma \setminus \cup \{\gamma_1, \cdots, \gamma_g\}$ is connected,

2. All the γ_i bound a disc in H.

Example 8.2.2*($S^1 \times \mathbb{D}^2$):* For the solid 2-torus, the attaching curves are copies of S^1 that bound discs
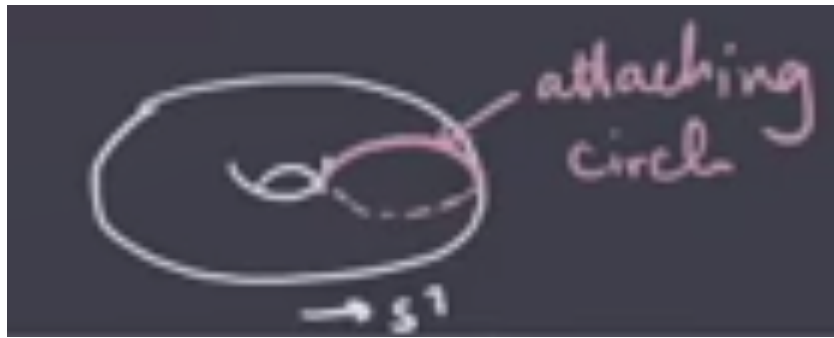
Figure 79: image_2021-02-16-21-27-56

Example 8.2.3*(A genus 2 handlebody):* Consider $\mathbb{B}^3$ with two 1-handles attached, or a solid genus 2 surface:
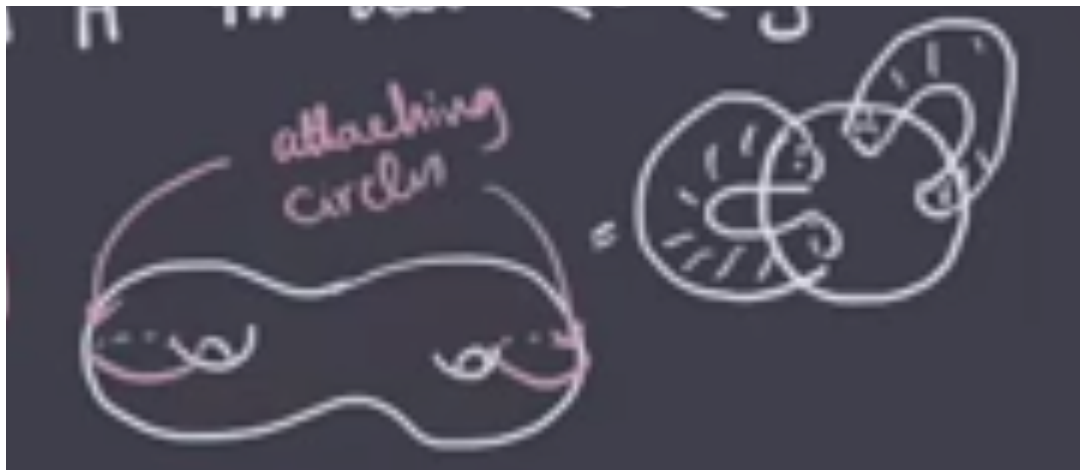
Figure 80: image_2021-02-16-21-29-36

Note that curves running around each of the two handles also work:
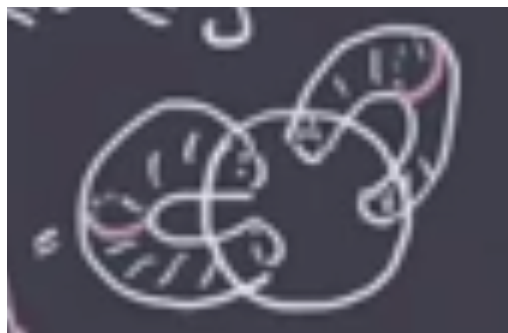
Figure 81: image_2021-02-16-21-30-26

> **Exercise 8.2.4** (?)
> Show that $\Sigma \backslash \cup \{\gamma_1, \cdots, \gamma_g\}$ is connected $\iff$ the classes $[\gamma_1], \cdots, [\gamma_g]$ are linearly independent in $H_1(\Sigma; \mathbb{Z})$.

> **Proposition 8.2.5** *(Handlebody from a Heegard Diagram).*
> Given a surface and a set of attaching curves, so the data of $(\Sigma, \{\gamma_1, \cdots, \gamma_g\})$, we can build a handlebody H. Note that we can go the other way: given a genus g handlebody H, we can take $\Sigma = \partial H$ and find g attaching circles.
> **The recipe:**
>
> 1. Thicken Σ to $\Sigma \times [0, 1]$ to get a 3-manifold with 2 boundary components, $\Sigma \times \{1\}$ and $\Sigma \times \{2\}$.
>
> 2. Attach thickened discs $\gamma_i \times \{0\}$ for each i, yielding some S^2 boundary components.
>
> 3. Fill the S^2 boundary component with a $\mathbb{B}^3$.
>
> This yields a genus g handlebody H such that $\partial H = \Sigma_g \times \{1\}$, where the curves $\{\gamma_1 \times \{1\}, \cdots, \gamma_g \times \{1\}\}$.

Example 8.2.6*(?):* Note that after attaching the disc on one end of this new cylinder, we have the following:
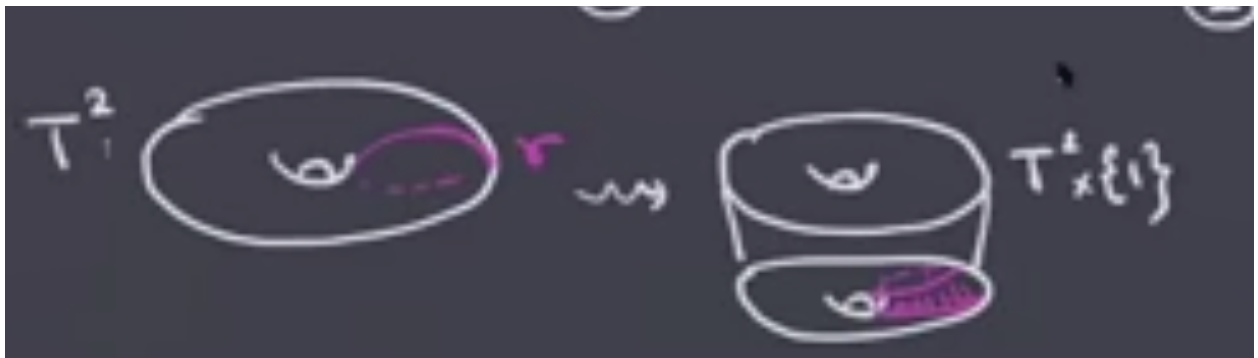
Figure 82: image_2021-02-16-21-37-08

What's left on the boundary is the following:
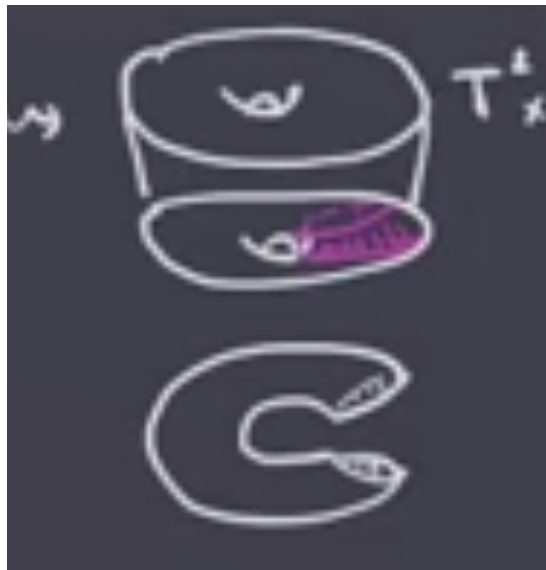
Figure 83: image_2021-02-16-21-37-43

This is a copy of S^2.

> **Exercise 8.2.7** (?)
> Show that for any g we get a 3-manifold with boundary $\Sigma \times \{1\} \coprod S^2$ after step (2) above.

9 | Lecture 9 (Thursday, February 11)

9.1 Heegard Diagrams

Remark 9.1.1: Last time we saw that $M_3 = H_1 \coprod_\varphi H_2$ as two handlebodies glued along their boundary by a diffeomorphism $\varphi : \partial H_1 \to \partial H_2$. This is referred to as a **Heegard splitting** for M. We can specify a genus g handlebody as $(\Sigma, \{\gamma_1, \cdots \gamma_g\}$ where $\Sigma \setminus \{\gamma_1, \cdots, \gamma_g\}$ is connected and each γ_i bounds a disc in H.

Figure 84: image_2021-02-11-11-15-56

Moreover, we can go backwards: given such data, we can build a handlebody H by

1. Thickening Σ to obtain $\Sigma \times [0,1]$ This yields $\partial(\Sigma \times [0,1]) = (\Sigma \times \{0\})\coprod(\Sigma \times \{1\})$.

2. Attach thickened discs to $\gamma_i \times \{0\}$. This makes the boundary $(\Sigma \times \{1\})\coprod S_2$

3. Fill in the S^2 boundary with a B^3.
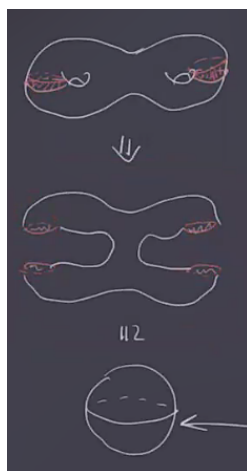
Figure 85: image_2021-02-11-11-22-43

> **Definition 9.1.2** (Heegard Diagrams)
> A **Heegard diagram** for M^3 compatible with a splitting $M = H_1 \coprod_\varphi H_2$ is a triple $(\Sigma, \alpha, \beta$
> where α and β are attaching circles for H_1 and H_2 respectively.

Example 9.1.3*(Heegard diagram for S^3):* The following two curves on a torus determine a Heegard splitting for S^3:

Figure 86: image_2021-02-11-11-28-43

Example 9.1.4*(Heegard diagram for $S^1 \times S^2$):* Writing $S^1 \times S^2 = D_2 \coprod_{\mathbb{1}_{\partial D^2}} D^2$, or also $(S^1 \times D^2) \coprod_{\mathbb{1}} (S^1 \times D^2)$.

Figure 87: image_2021-02-11-11-30-50

Exercise 9.1.5 (?)
Show that the following diagram is a Heegard diagram for $\mathbb{RP}^3$:
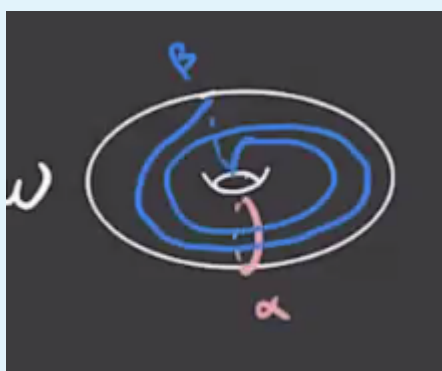
Figure 88: image_2021-02-11-11-31-45

Hint: use that $\mathbb{RP}^3 \cong L(2,1)$ and find a Heegard diagram for $L(p,q)$.

Example 9.1.6*(?):* Given a self-indexing Morse function $f : M \to \mathbb{R}$ with exactly one index 0 and

one index 3 critical point, pick a generic metric g so that (f, g) is a Morse-Smale pair (so the stable and unstable submanifolds intersect transversally). Taking $-\nabla f$, we can obtain a Heegard diagram The stable submanifolds are codimension of their indices, so e.g. for each index critical point there is a 2-dimensional stable submanifold that intersects the next submanifold in a curve:
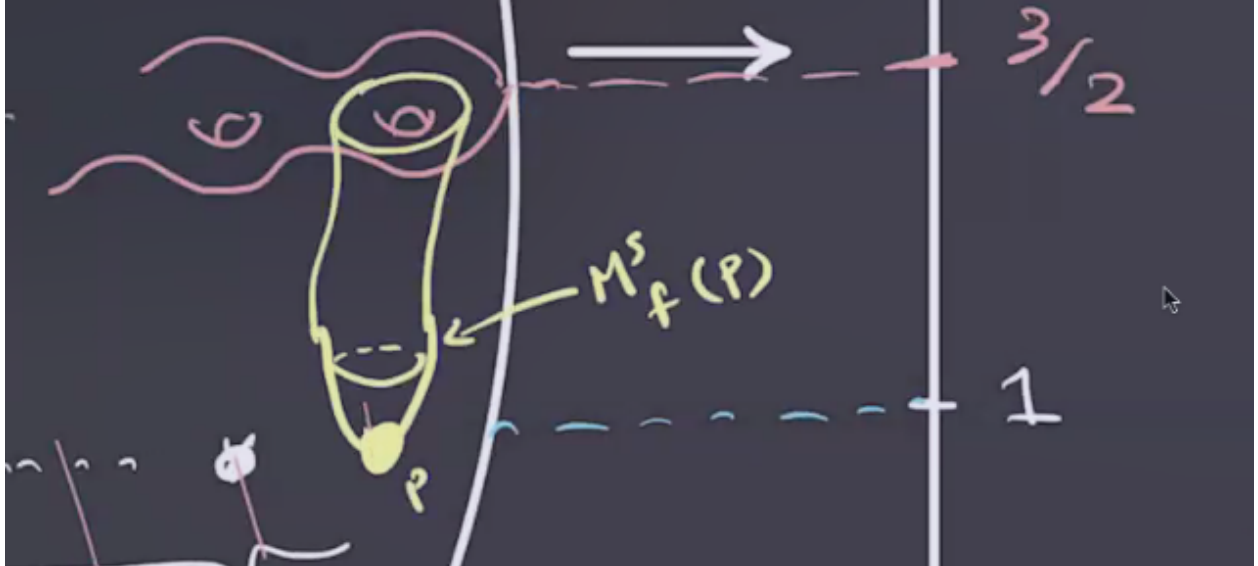
Figure 89: Stable submanifold

This occurs for (say) the g critical points of index 1 here, and since they are distinct critical points the stable submanifolds are disjoint. So we can obtain a set of attaching circles for the bottom handlebody $f^{-1}([0, 3/2])$:

$$\left\{ M^s(p) \cap f^{-1}(3/2) \mid p \in \mathrm{crit}(f), \ \mathrm{ind}(p) = 1 \right\}.$$

So setting these to be the α curves, repeating with index 2 to get β curves, and setting $\Sigma := f^{-1}(3, 2)$ we get a Heegard diagram for M.

Remark 9.1.7: Note that given $(\Sigma, \alpha, \beta$ we can construct M in the following way:

- $(\Sigma, \alpha$ builds H_α with $\partial H_\alpha = \Sigma$.
- $(\Sigma, \beta$ builds H_β with $\partial H_\beta = \Sigma$.

> **Exercise 9.1.8** (?)
> Show that Heegard splittings can be used to compute homology, and
>
> $$H_1(M; \mathbb{Z}) \cong H_1(\Sigma; \mathbb{Z}) / \langle [\alpha_1], \cdots, [\alpha_g], [\beta_1], \cdots, [\beta_g] \rangle.$$

9.2 Heegard Moves

Proposition 9.2.1*(?)***.**
Given $M = H_1 \cup H_2 = H_1' \cup H_2'$, we can *stabilize* to obtain $M = \tilde{H}_1 \cup \tilde{H}_2$. Is there a way to relate the two corresponding Heegard diagrams?

1. Isotopy. Exchange $\alpha = \{\alpha_1, \cdots, \alpha_g\}$ with an ambient isotopy of Σ, and similarly β, keeping curves of the same type disjoint during the isotopy (where e.g. it's fine if an α curve intersects a β curve).
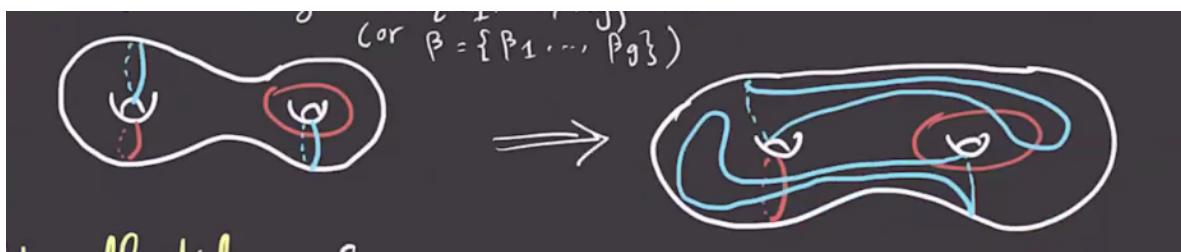
Figure 90: image_2021-02-11-11-49-46

2. Handleslides (of α or β curves).
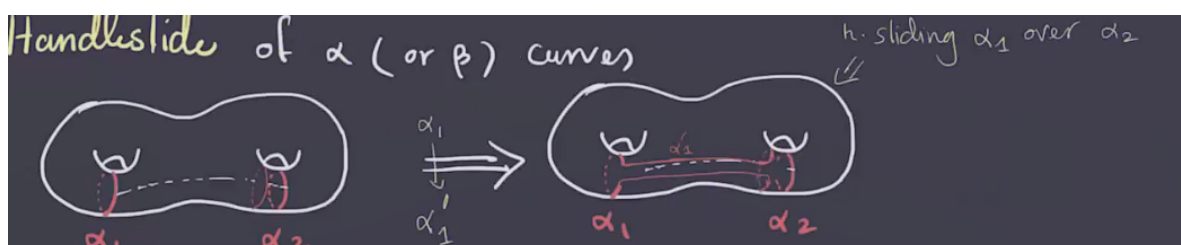
Figure 91: image_2021-02-11-11-51-54

Equivalently, handle sliding α_1 over α_2 replaces α_1 with α_1' such that the triple $\alpha_1, \alpha_1', \alpha_2$ bound a pair of pants.
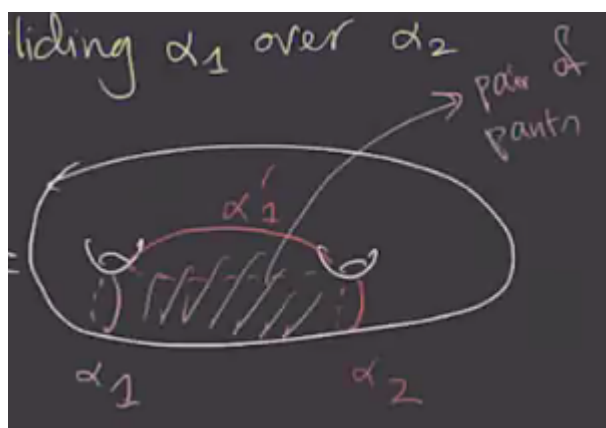
Figure 92: image_2021-02-11-11-53-22

3. Stabilization. This changes $(\Sigma, \alpha, \beta) \mapsto (\Sigma \# T^2, \alpha \cup \{\alpha_{g+1}, \beta\} \cup \{\beta_{g+1}\}$, where $\alpha_{g+1}, \beta_{g+1} \subseteq T^2$ and intersect in exactly on point.
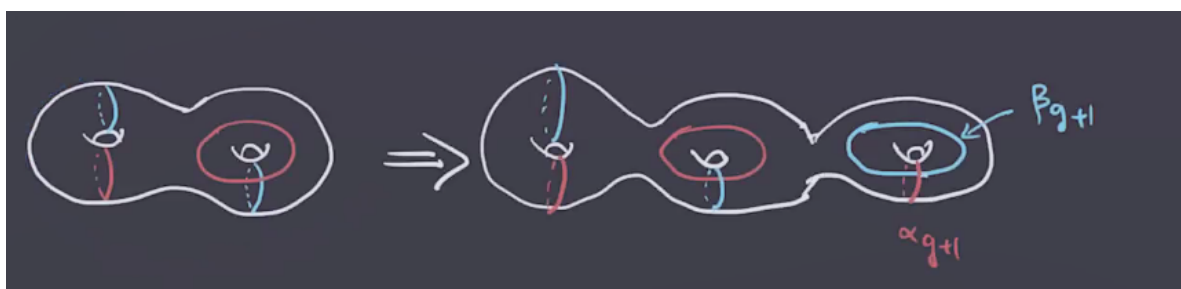
Figure 93: image_2021-02-11-12-10-06

3'. Destabilization. Reversing the stabilization operation.

Exercise 9.2.2 (?)
Show that any two sets of attaching curves for a handlebody H can be related by a finite sequence of (1) and (2).

Exercise 9.2.3 (?)
Show that stabilization yields a Heegard diagram for the same manifold.
Hint: the new summand is a Heegard diagram for S^3, and connect sums in the diagrams correspond to connect sums of the corresponding manifolds. Moreover, $M \cong M \# S^3$.

Theorem 9.2.4(?).
Any two Heegard diagrams for M can be connected by a finite sequence of the above moves.

10 | Tuesday, February 16

Remark 10.0.1: Note that critical points can be used to compute the Euler characteristic, using the fact the $\chi(C) = \chi(H_*(C))$, i.e. it can be computed on dimensions of chains or ranks of homology, along with the fact that Morse homology is isomorphic to singular homology. So e.g. for a 3-manifold M^3, we can show

$$
\begin{aligned}
\chi(M^3) &= \sum_{i=0}^{3} \operatorname{rank} H_i \\
&= \sum_{i=0}^{3} \operatorname{rank} CM_i \\
&= 1 - \#\operatorname{crit}_1(f) + \#\operatorname{crit}_2(f) - 1 \\
&= 0,
\end{aligned}
$$

since the number of index 2 and index 3 critical points will be the same.

10.1 Symmetric Product Spaces

Remark 10.1.1: Let M^3 be a closed 3-manifold, then there is a Heegard splitting

$$
(\Sigma_g, \alpha = \{\alpha_1, \cdots, \alpha_g\}, \beta = \{\beta_1, \cdots, \beta_g\} = (\Sigma_g, H_\alpha, H_\beta) \qquad \partial(H_\alpha) = \partial(H_\beta) = \Sigma,
$$

where $M^3 = H_\alpha \coprod_{\Sigma} H_\beta$ and g is the genus of HD. We refer to Σ as a **Heegard surface**, and this set of data as a **Heegard diagram**.

We'll define $\operatorname{Sym}^g(\Sigma)$ by letting $S_g \curvearrowright \Sigma^{\times g}$ where if $\varphi \in S_g$ we set $\varphi(x_1, \cdots, x_g) = x_{\varphi(1)}, \cdots, x_{\varphi(g)}$. Then set $\Sigma^{\times g} := \Sigma^{\times g}/S_g$. Why does this yield a smooth manifold? Is this action free? The diagonal $D \subseteq \Sigma^{\times g}$ consists of the points with at least 2 equal coordinates, and it's easy to see that $S_g \curvearrowright D$ can not be free. However, this still yields a smooth submanifold!

> **Lemma 10.1.2(?).**
> $\operatorname{Sym}^g(\Sigma)$ is smooth, and any complex structure j on Σ will induce a complex structure on the quotient, denoted $\operatorname{Sym}^g(j)$, which is unique in the sense that the quotient map $\Sigma^{\times g} \xrightarrow{\pi} \operatorname{Sym}^g(\Sigma)$ is holomorphic.

> *Proof (?).*
> We'll check this locally, and then leave it as an exercise to check that it extends globally – this is easy by just considering what happens under transition functions and checking that π is

holomorphic. Locally we want to produce a map

$$\mathrm{Sym}^g(\mathbb{C}) \xrightarrow{f} \mathbb{C}^g$$

$$\{z_1, \cdots, z_g\} \mapsto \left(\prod_{i=1}^{g} (z - z_i) = z^g + a_1 z^{g-1} + \cdots + a_g \mapsto [a_1, \cdots, a_g] \right).$$

This is a bijection, and by the fundamental theorem of algebra, there is an inverse. Equip $\mathrm{Sym}^g(\mathbb{C})$ with a complex structure that makes f biholomorphic, then $\mathrm{Sym}^g(j)$ is the complex structure locally equal to this one. This structure is obtained by just pulling back the standard complex structure $i \times i \times \cdots i$ on $\mathbb{C}^g$.

■

Remark 10.1.3: $\mathrm{Sym}^g(\Sigma)$ is a complex manifold of complex dimension g (or real dimension $2g$). We want to find half-dimensional submanifolds to do Lagrangian-Floer homology. Using the Heegard splitting, write $\mathbb{T}_\alpha := \prod_{i=1}^{g} \alpha_i \subset \Sigma^{\times g}$, which is a g-dimensional torus such that $\mathbb{T}_\alpha \cap D = \emptyset$ since the α_i are pairwise disjoint. Composing the inclusion above with π, we can note that the action of S^g is free away from the diagonal D, so this composition is an embedding $\mathbb{T}_\alpha \hookrightarrow \mathrm{Sym}^g(\Sigma)$. Similarly, $\mathbb{T}_\beta := \prod_{i=1}^{g} \beta_i \hookrightarrow \mathrm{Sym}^g(\Sigma)$.

Note that we're only working with complex structures now, and haven't upgraded it to a symplectic structure yet. But we don't really need this to count holomorphic discs. Lagrangians L were defined as submanifolds where $\omega|_L = 0$, how do we do this without a symplectic form?

> **Definition 10.1.4** (?)
> Given a complex manifold (X, J), a submanifold $L \subseteq X$ is **totally real** if none of its tangent spaces contains a complex line, i.e. $T_p L \cap J(T_p L) = \{p, \mathbf{0}\}$ for all $p \in L$.

Example 10.1.5*(?):* Take a genus g surface Σ:
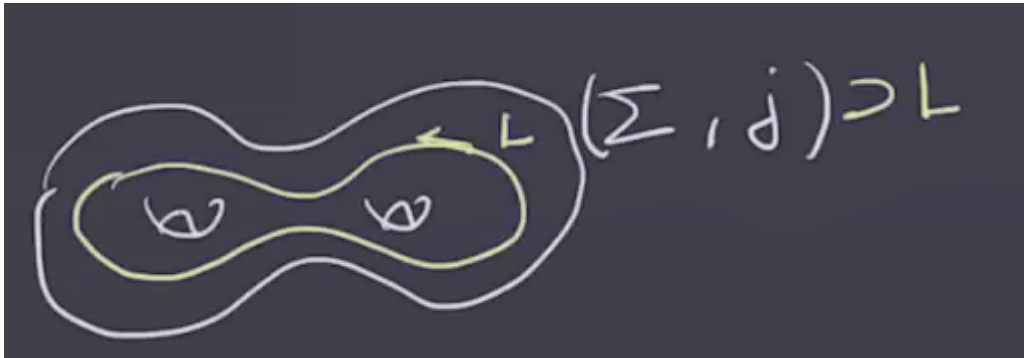
Figure 94: image_2021-02-16-11-49-52

Here any tangent vector has to get rotated out of the tangent space: if it were an eigenvector for

J, then the rank of J would be too low, contradicting its definition. Note that any 1-dimensional submanifold of (Σ, j) is totally real, and so $\mathbb{T}_\alpha, \mathbb{T}_\beta$ are also totally real submanifolds of $\Sigma^{\times g}$. If you restrict π to $\Sigma^{\times g} \setminus D \xrightarrow{\pi} \mathrm{Sym}^g(\Sigma) \setminus \pi(D)$, this yields a biholomorphic map.

Remark 10.1.6: We'll write $\Delta := \pi(D) \subseteq \mathrm{Sym}^g(\Sigma)$. Note that if $\alpha \pitchfork \beta$, then $\mathbb{T}_\alpha \pitchfork \mathbb{T}_\beta$. Any intersection point $x \in \mathbb{T}_\alpha \cap \mathbb{T}_\beta$ is of the form $x = \{x_1, \cdots, x_g\} \subseteq \Sigma$ such that each α_i, β_j contain exactly one of the coordinates of x.

Example 10.1.7*(?):* The following is a diagram for $\mathbb{RP}^3$:
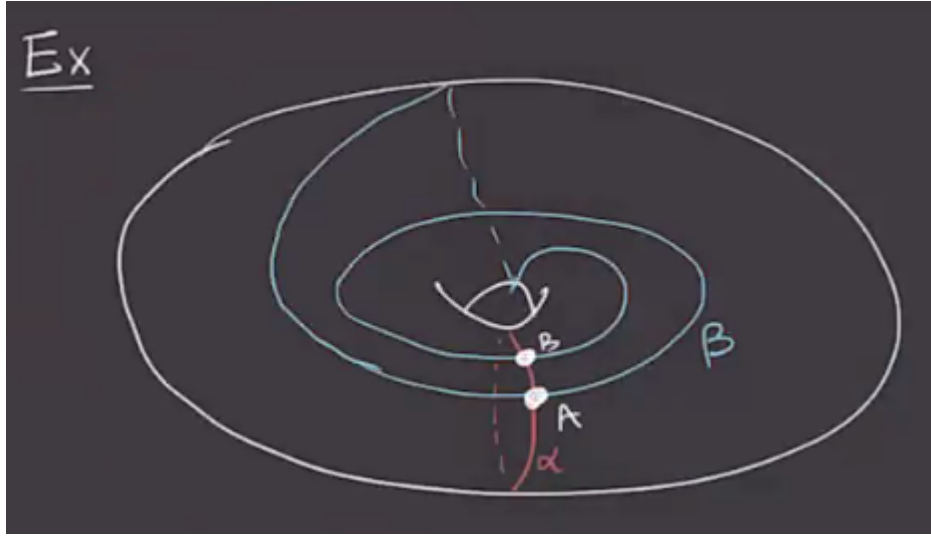
Figure 95: Heegard diagram for $\mathbb{RP}^3$

Here $g = 1$ and so $\mathrm{Sym}^1(T^2) = T^2$. We also have $\mathbb{T}_\alpha = \alpha, \mathbb{T}_\beta = \beta$, and their intersection is $\mathbb{T}_\alpha \cap \mathbb{T}_\beta = \alpha \cap \beta = \{A, B\}$

Example 10.1.8*(Heegard diagram for the Poincaré homology sphere):* Here we have a Poincaré homology sphere P^3, i.e. a 3-manifold with the same homology as S^3, i.e. $H_*(P^3) = [\mathbb{Z}, 0, 0, \mathbb{Z}]$ (??)
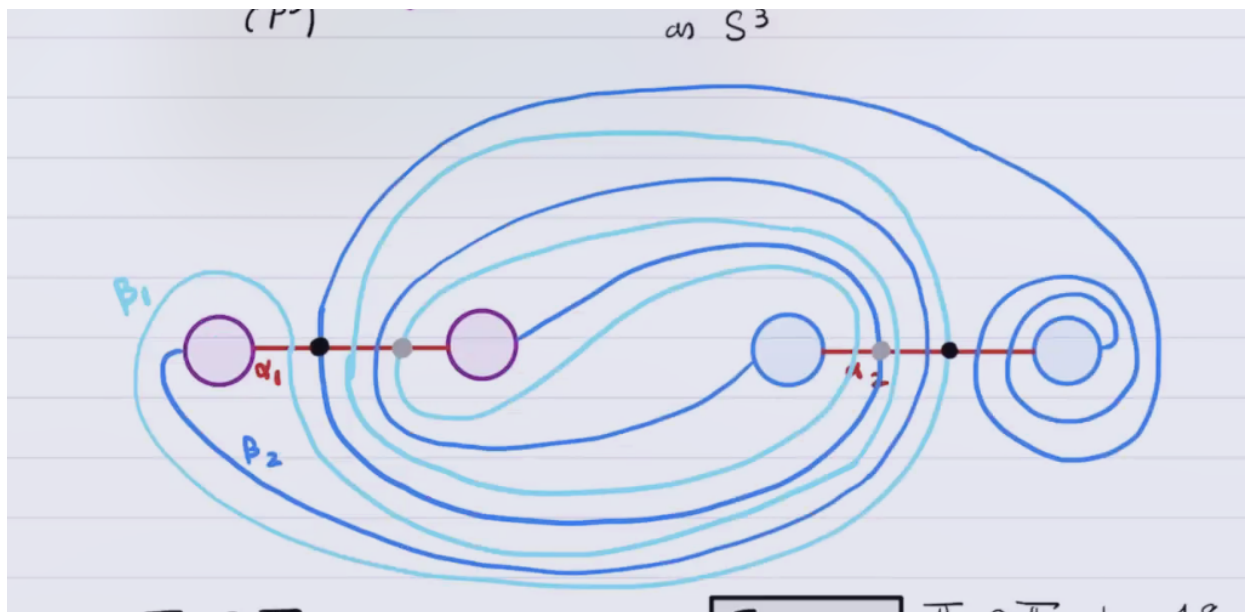
Figure 96: image_2021-02-16-12-01-57

> **Exercise 10.1.9*(?)***
> Compute $H_*(P^3)$ using this diagram, particularly H_1. Using Poincaré duality here is fine!

The circles with the same color are the "feet" of a handle attachment, or equivalently removing the two circles and identifying their boundary with reversed orientation. The two different colors for circles indicate that this will be genus 2 The arcs between same-colored circles indicate loops that continue through the handle which aren't shown. Tracing through the lines on the diagram, there are two α curves and two β curves. Since $g = 2$, we can identify $\mathrm{Sym}^2(\Sigma) \supseteq \alpha_1 \times \alpha_2 = \mathbb{T}_\alpha, \beta_1 \times \beta_2 = \mathbb{T}_\beta$. The two black circles indicate intersection points in $\mathbb{T}_\alpha \cap \mathbb{T}_\beta$. However, there are more than just those two!

> **Exercise 10.1.10*(?)***
> Show that $|\mathbb{T}_\alpha \cap \mathbb{T}_\beta| = 18$.

Computing the intersections:
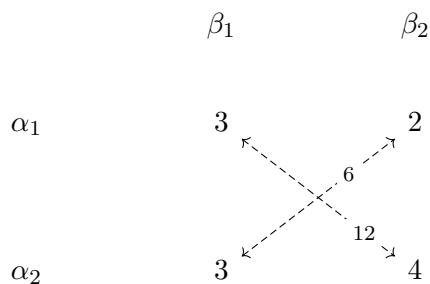
> How to read this from the diagram?

We're really working in $\mathrm{Sym}^g(\Sigma)$, but for computations, we'll work directly with the Heegard diagram.

Remark 10.1.11: For Lagrangian Floer homology, we'll have a triple $(\mathrm{Sym}^g(\Sigma), \mathbb{T}_\alpha, \mathbb{T}_\beta)$. We'll define

$$CF(\Sigma, \alpha, \beta) := \bigoplus_{x \in \mathbb{T}_\alpha \cap \mathbb{T}_\beta} \mathbb{Z}/2\mathbb{Z} \langle x \rangle$$

$$\partial(x) := \sum_{y \in \mathbb{T}_\alpha \cap \mathbb{T}_\beta, \mu=1} \# \widehat{\mathcal{M}} y.$$

We'll first figure out how to count continuous discs up to homotopy classes, since holomorphic discs are much more restrictive. We'll see that π_2 plays a role, and define the topology of Sym^g.

11 | **Thursday, February 18**

Remark 11.0.1: Today: topology of symmetric product spaces Sym^g. We had an assignment

$$(\Sigma_g, \alpha, \beta) \mapsto (\mathrm{Sym}^g(\Sigma), \mathbb{T}_\alpha, \mathbb{T}_\beta),$$

where if α, β are all transverse then so far $\mathbb{T}_\alpha, \mathbb{T}_\beta$, since e.g. $\mathbb{T}_\alpha = \prod_{i=1}^{g} \alpha_i$. We wanted to define a chain complex

$$CF(\sigma, \alpha, \beta) := \bigoplus_{x \in \mathbb{T}_\alpha \cap \mathbb{T}_\beta} \mathbb{Z}/2\mathbb{Z} \langle x \rangle$$

$$\partial x := \sum_{\substack{y \in \mathbb{T}_\alpha \cap \mathbb{T}_\beta \\ \mu(x,y)=1}} \# \mathcal{M}(x,y) y,$$

where μ is the *Maslov index* and we want to count holomorphic discs. We'll first talk about continuous (topological) discs.

> **Lemma 11.0.2***(?).*
>
> $$\pi_1(\mathrm{Sym}^g(\Sigma)) \cong H_1(\mathrm{Sym}^g(\Sigma)) \cong H_1(\Sigma),$$
>
> so the fundamental group is abelian.

Remark 11.0.3: For a proof of the first isomorphism, see Lemma 2.6 in [**OSZ04a**]. Idea of proof for the second isomorphism: we'll define a map

$$\iota : H_1(\Sigma) \to H_1(\mathrm{Sym}^g(\Sigma))$$
$$x \mapsto \{x, z, \cdots, z\},$$

for some fixed $z \in \Sigma$, along with its inverse. Note that we're identifying an embedding $\iota(\Sigma) = \Sigma \times \{z\}^{\times g-1} \subseteq \mathrm{Sym}^g(\Sigma)$. Now define $j := \iota_*$ the induced map on homology.

$$j : H_1(\mathrm{Sym}^g(\Sigma)) \to H_1(\Sigma)$$

.

Picking a loop $\gamma : S^1 \to \mathrm{Sym}^g(\Sigma)$, note that $\Delta \subset \mathrm{Sym}^g(\Sigma)$ has codimension 2, and so we can perturb γ to be disjoint from Δ. We can arrange so that γ is the union of g paths $\gamma_1, \cdots, \gamma_g$ such that each γ_i connects $x_i \in \gamma(0)$ to $x_{\sigma(i)} \in \gamma(0)$ where $\gamma_0 = \{x_1, \cdots, x_g\}$ and $\sigma \in S_g$ is a permutation.

Example 11.0.4*(?):* For example, for $g = 3$:
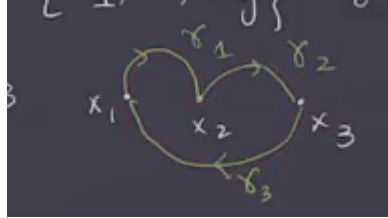
Figure 97: image_2021-02-18-11-30-51

Then $\{\gamma_1(t), \gamma_2(t), \gamma_3(t)\}$ is a loop from $\gamma(0) \to \gamma(0) \in \mathrm{Sym}^3(\Sigma)$.

This means that $\bigcup_{i=1}^{g} \gamma_i$ is a 1-cycle in Σ, and thus $[\cup g_i] \in H_1(\Sigma)$. So we'll define this as $j([\gamma]) = [\cup \gamma_i]$.

Let $M := \left\{ (\mathbf{x}, y) \mid \mathbf{x} \in \mathrm{Sym}^g(\Sigma), y \in \mathbf{x} \right\}$, then we'll define a $g : 1$ branched cover away from $\pi^{-1}\Delta$ that yields a fiber bundle:

$$
\begin{array}{ccc}
S^1 & \xrightarrow{\exists \tilde{\gamma}} & M \\
{\scriptstyle \exists g:1} \downarrow & & \downarrow {\scriptstyle \pi, \, g:1} \qquad \searrow^{\pi_2} \\
S^1 & \xrightarrow{\gamma} & \mathrm{Sym}^g(\Sigma) \qquad \Sigma
\end{array}
$$
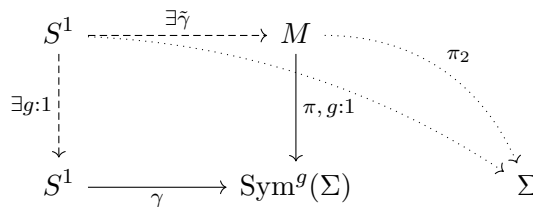
Link to Diagram

This can be restricted to $M \setminus \pi^{-1}(\Delta) \xrightarrow{g:1} \mathrm{Sym}^g(\Sigma) \setminus \Delta$. Here $j([\gamma]) = [\pi_2 \circ \gamma]$ and $j \circ \iota_* = \mathbb{1}$.

Example 11.0.5*(?):* We can use a Heegard diagram and Mayer Vietoris to compute the homology:

$$H_1(M;\mathbb{Z}) = \frac{H_1(\Sigma;\mathbb{Z})}{\langle[\alpha_1],\cdots,[\alpha_g],[\beta_1],\cdots,[\beta_g]\rangle} \cong \frac{H_1(\mathrm{Sym}^g(\Sigma))}{\langle H_1(\mathbb{T}_\alpha), H_1(\mathbb{T}_\beta)\rangle}.$$

> **Proposition 11.0.6*(?).***
>
> $$\pi_2(\mathrm{Sym}^g(\Sigma)) \cong \mathbb{Z}.$$

Remark 11.0.7: The generator comes from hyperelliptic involution:
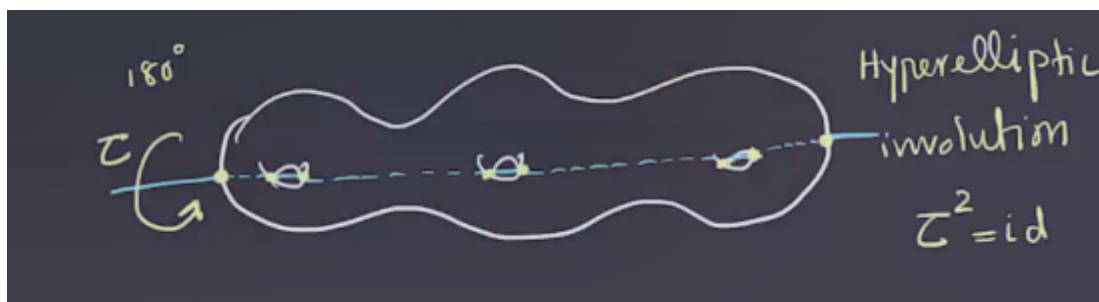
Figure 98: image_2021-02-18-11-58-40

Then consider the quotient Σ/τ. To identify this quotient, since the top half is identified with the bottom half, we can first forget about the bottom half, and then forget about half of the arcs along the axis of rotation:
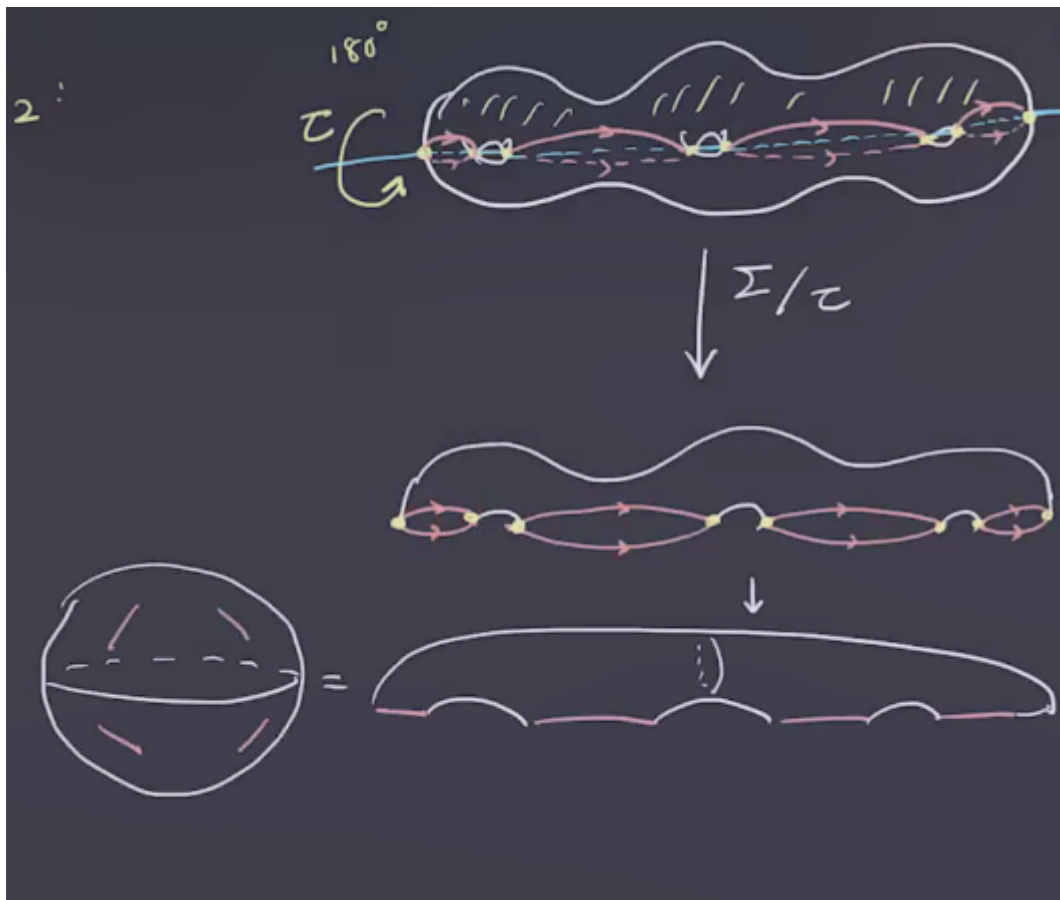
Figure 99: image_2021-02-18-12-01-41

Note that this results in a copy of S^2. We can define a map

$$\Sigma \to \Sigma^{\times g}$$
$$x \mapsto (x, \tau(x), z, \cdots, z).$$

This extends to a map to $\mathrm{Sym}^g(\Sigma)$, since $\tau(x) \mapsto (\tau(x), x, z, \cdots, z)$ and these will be equal in Sym^g. So we can factor this through the quotient from above:

$$
\begin{array}{ccc}
\Sigma & \xrightarrow{\;\;f\;\;} & \Sigma^{\times g} \\
{\scriptstyle q}\downarrow & & \vdots \\
S^2 & \dashrightarrow & \mathrm{Sym}^g(\Sigma)
\end{array}
$$

Definition 11.0.8 (Whitney Disc)

Given $x, y \in \mathbb{T}_\alpha \cap \mathbb{T}_\beta$, a **Whitney disc** from x to y is a map

$$\varphi : \mathbb{D}^2 \to \mathrm{Sym}^g(\Sigma)$$

such that

$$\varphi(-i) = x$$
$$\varphi(i) = y$$
$$\varphi(e_1) \subseteq \mathbb{T}_\alpha$$
$$\varphi(e_2) \subseteq \mathbb{T}_\beta.$$

Figure 100: image_2021-02-18-12-22-03

We say $\varphi_1 \sim \varphi_2$ if and only if they are homotopic relative to $\mathbb{T}_\alpha, \mathbb{T}_\beta$. We'll write $\pi_2(x, y)$ for the homotopy class of Whitney discs from x to y. There is a concatenation operation:

$$* : \pi_2(x, y) \times \pi_2(y, z) \to \pi_2(x, z).$$
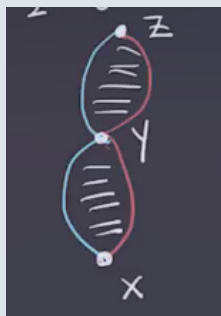
Figure 101: image_2021-02-18-12-24-03

Note that this is precisely concatenation of paths in the path space $\mathcal{P}$.

> **Exercise 11.0.9** (?)
> If $x = y = z$, then this yields an operation on $(\pi_2(x, x), *)$ which defines a group.

Remark 11.0.10: We can find obstructions to holomorphic discs by just looking at the topology. For $x, y \in \mathbb{T}_\alpha \cap \mathbb{T}_\beta$, choose two paths connecting them:

$$a : I \to \mathbb{T}_\alpha$$
$$b : I \to \mathbb{T}_\beta.$$
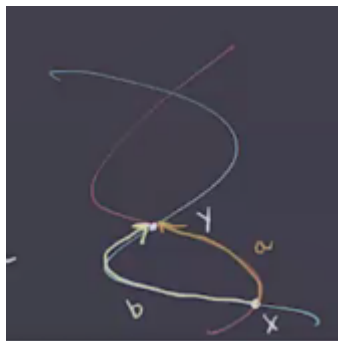
Figure 102: image_2021-02-18-12-27-15

We can consider the homology class $[a - b]$ to investigate π_1. This is well-defined as a loop

$$\varepsilon(x, y) := [a - b] \in \frac{H_1(\mathrm{Sym}^g(\Sigma))}{\langle H_1(\mathbb{T}_\alpha) \oplus H_1(\mathbb{T}_\beta) \rangle} \cong H_1(M).$$

This turns out to be independent of the choice of a, b, and thus

$$\varepsilon(x, y) \neq 0 \implies \pi_2(x, y) = \emptyset,$$

and there are no continuous discs.

12 | Tuesday, February 23

12.1 Whitney Discs

Remark 12.1.1: For $x, y \in \mathbb{T}_\alpha \cap \mathbb{T}_\beta$, recall that we had the following situation:
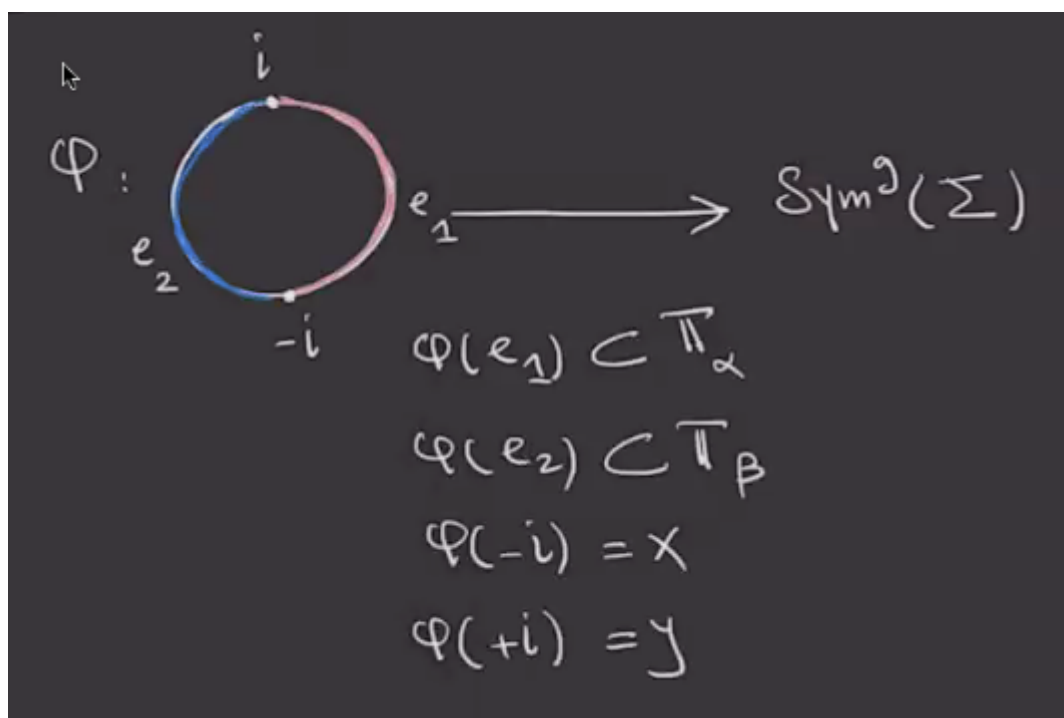
Figure 103: Whiteney Disc

Then $\pi_2(x, y)$ was defined to be the homotopy classes of discs connecting x to y. The obstruction to the existence of such discs was denoted $\varepsilon(x, y) \in H_1(M)$ for $M \in \mathsf{Mfd}^3$. We're checking if there exist two paths connecting x to y,

$$a : I \to \mathbb{T}_\alpha$$
$$b : I \to \mathbb{T}_\beta$$

such that $a - b$ is nullhomotopic. In this case, $\pi_2(x, y) \neq \emptyset$.
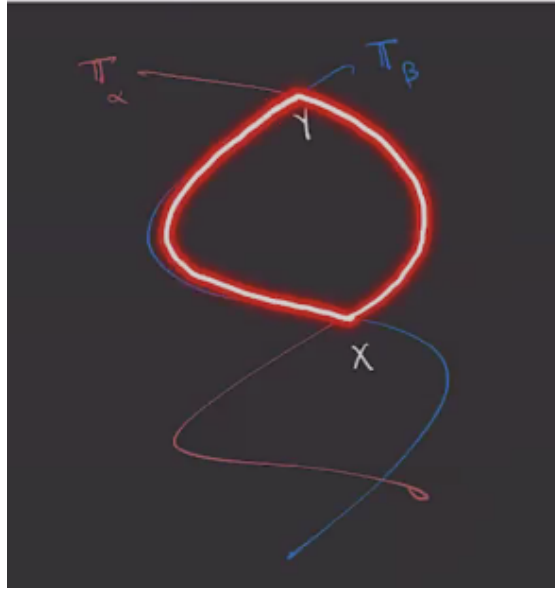
Figure 104: image_2021-02-23-11-17-30

We had a theorem that $\pi_1(\mathrm{Sym}^g \Sigma) \cong H_1(\mathrm{Sym}^g \Sigma)$, so we can replace nullhomotopic with nullhomologous above. We can also use the fact that $H_1(\mathrm{Sym}^g \Sigma) \cong H_1\Sigma$. Note that $[a - b]$ isn't well-defined, since we can append any loop to a for example, but the following is well-defined:

$$\varepsilon(x, y) := [a - b] \in \frac{H_1 \mathrm{Sym}^g \Sigma}{H_1 \mathbb{T}_\alpha \oplus H_1 \mathbb{T}_\beta} \cong \frac{H_1\Sigma}{\langle [\alpha_1], \cdots, [\beta_1], \cdots \rangle} \cong H_1 M.$$

How can we compute ε using the Heegard diagrams? Recall that a path in $\mathrm{Sym}^g \Sigma$ was a union of g paths in Σ. So choose arcs $a_1 \cup \cdots \cup a_g$ on Σ such that $a_i \subseteq \alpha_i$ is sub-arc and $\partial(a_1 \cup \cdots \cup a_g) = y_1 + \cdots + y_g - x_1 - \cdots - x_g$, and similarly choose $b_1 \cup \cdots \cup b_g$. Note that if $\varepsilon(x, y) \neq 0$ then $\pi_2(x, y) = \emptyset$.

Example 12.1.2*(L(2, 3))***:** The following is a Heegard diagram for $L(2, 3)$ of minimal genus, where we take α to be the horizontal line and β will be a line of slope 2/3:
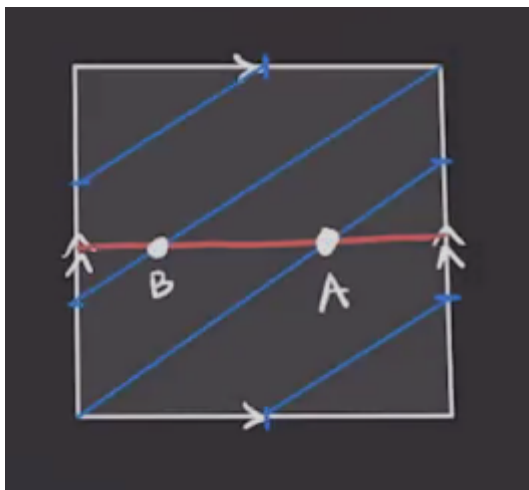
Figure 105: image_2021-02-23-11-28-10

Then $\mathbb{T}_\alpha \cap \mathbb{T}_\beta = \{A, B\}$. Now draw arcs connecting A and B, e.g. the ones in orange and green here:
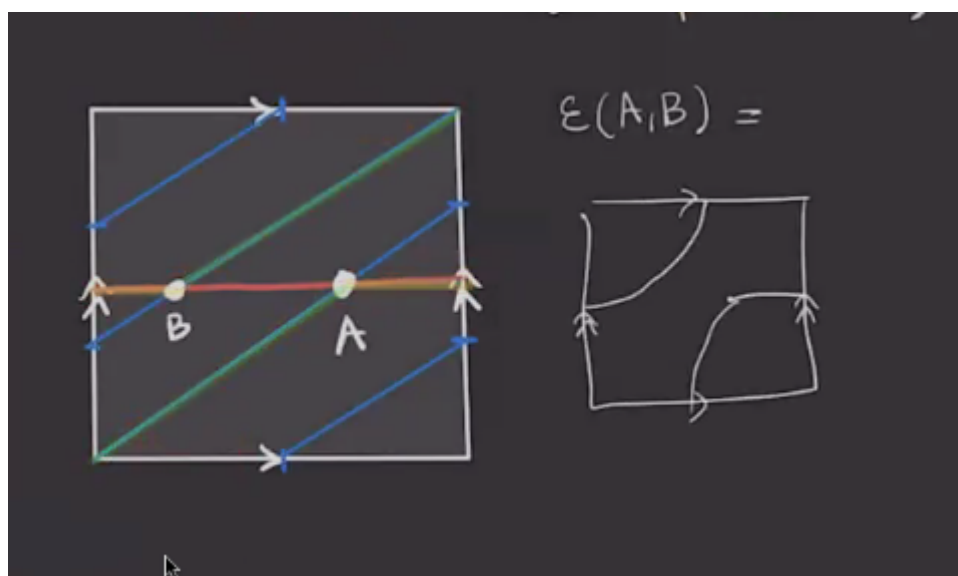
Figure 106: image_2021-02-23-11-29-54

Note that we have two generators of homology for the torus, say x, y, and we can write
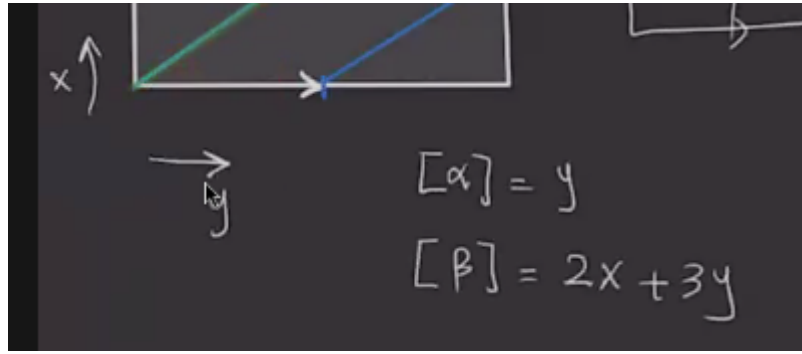
Figure 107: image_2021-02-23-11-30-37

Then the union of the two arcs is exactly $x + y$, so we can write

$$H_1(L(2,3)) = \frac{\mathbb{Z}\langle x, y\rangle}{\langle y, 2x + 3y\rangle}.$$

Moreover, $\varepsilon(A, B) = x + y \neq 0$ in this quotient, so there is not Whitney disc connecting A to B and $\pi_2(A, B) = \emptyset$.

Remark 12.1.3: We'll define $x \sim y \iff \varepsilon(x, y) = 0$, and this turns out to be an equivalence relation which partitions the set of paths.

- $\varepsilon(x, y) = 0 \implies \varepsilon(y, x) = 0$, which follows from $\varepsilon(x, y) = [a - b] = [b - a] = \varepsilon(y, x)$

- $\varepsilon(x, x) = 0$ by picking a, b constant.

> **Exercise 12.1.4** (?)
> Show that $\varepsilon(x, y) + \varepsilon(y, z) = \varepsilon(x, z)$.

> **Corollary 12.1.5(?).**
> If $x \sim y$ and $y \sim z$, so $\varepsilon(x, y) = \varepsilon(y, z) = 0$, we have $\varepsilon(x, z) = 0 \implies x \sim z$.

> **Exercise 12.1.6** (?)
> Find the equivalence classes under $\sim$ for the Poincaré homology sphere using the genus 2 Heegard diagram.

Remark 12.1.7: For $\varphi \in \pi_2(x, y)$, the **shadow** is the 2-chain $D(\varphi)$ on Σ defined in the following way: remove the α, β arcs to obtain

$$\Sigma \setminus (\alpha \cup \sigma) = \coprod_{i=1}^{m} D_i,$$

where ^{o} denotes that the set is open. Then $D(\varphi) = \sum_{i=1}^{m} a_i D_i$.

> **Definition 12.1.8** (?)
> Given $z \in \Sigma \setminus (\alpha \cup \beta)$, define a hyperplane
>
> $$L_z = \left\{ \mathbf{w} \in \mathrm{Sym}^g(\Sigma) \mid z \in \mathbf{w} \right\}.$$
>
> Note that this will be codimension 2. Then for a disc $\varphi \in \pi_2(x, y)$, define
>
> $$n_z(\varphi) = \# \left(\mathrm{im}(\varphi) \cap L_z \right).$$
>
> which is an algebraic (signed) count of how many entries in a tuple contain the point z. We can then define $a_i := n_{z_i}(\varphi)$ and define
>
> $$D(\varphi) = \sum_{i=1}^{m} a_i D_i, \qquad\qquad z_i \in {}^{o}D_i.$$

Remark 12.1.9: The following comes from "Introduction to Heegard Floer Homology" (Osvath-Szabo), which we've been following relatively closely so far.

> **Exercise 12.1.10** (?)
> Let D be a domain of a disc connecting $\{x_1, x_2\}$ to $\{y_1, y_2\}$ in the following way:
>
>
>
> Figure 108: image_2021-02-23-11-54-09
>
> Attach 1-handles in the following way to obtain β curves:
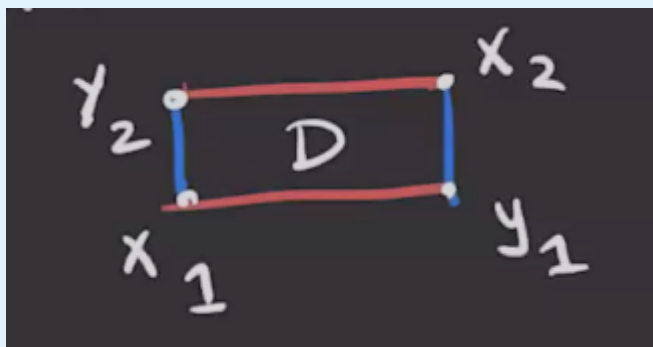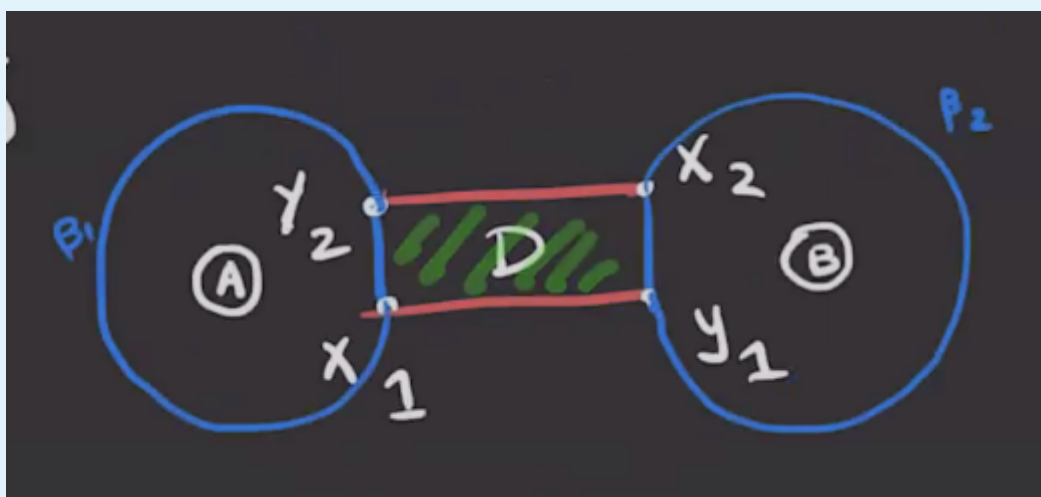
Figure 109: image_2021-02-23-11-55-13

Use these handles to add curves running through the handles:
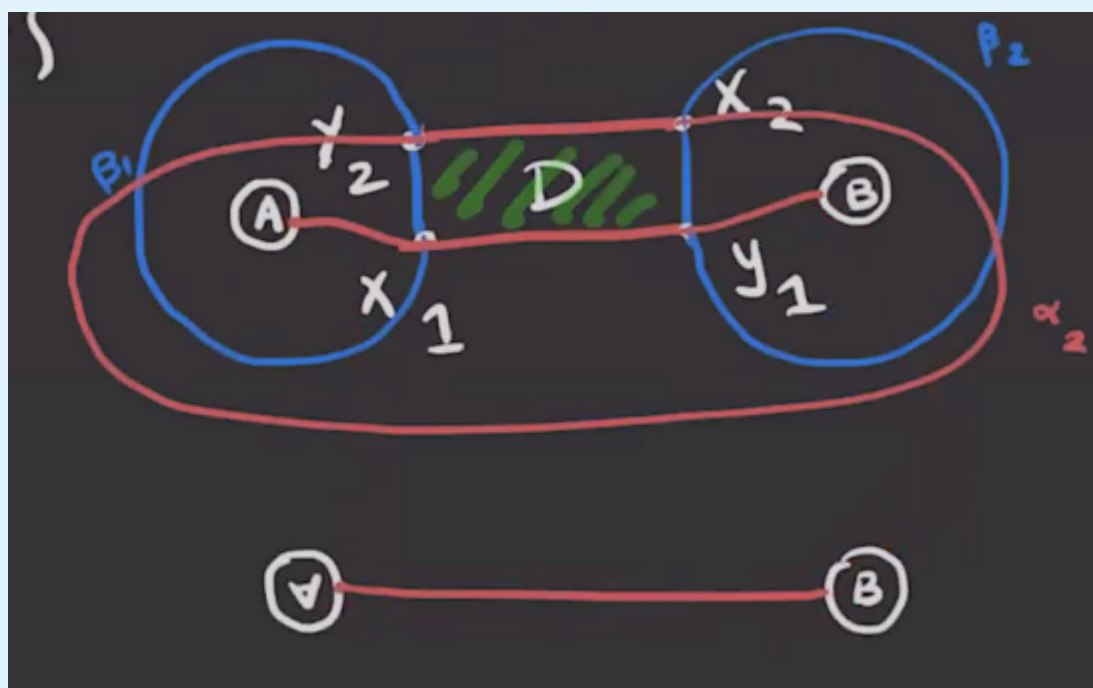
Figure 110: image_2021-02-23-11-56-26

Exercise 12.1.11 (?)
What is a Heegard diagram for?

Pick a point in the center of the rectangle and connect it to the 4 vertices, noting that it includes in Σ :
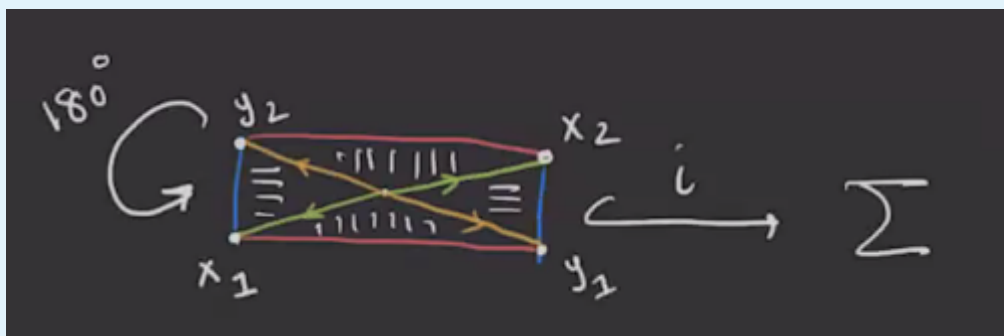
Figure 111: image_2021-02-23-11-58-15

Applying a rotation by π and taking the quotient, we get a 2-fold branched cover of S^1:
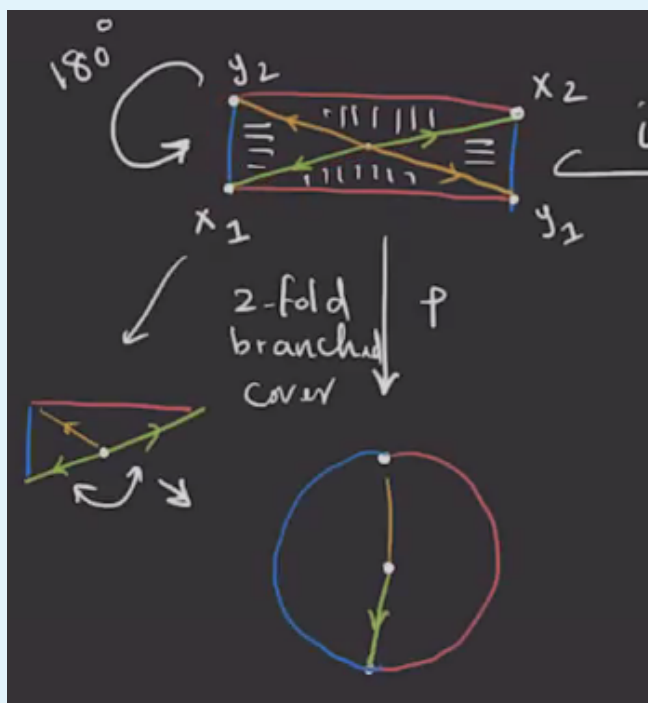
Figure 112: image_2021-02-23-11-59-29

Here $x_1, x_2 \mapsto -i$ and $y_1, y_2 \mapsto +i$. We can now get a map φ to $\mathrm{Sym}^2(\Sigma)$:
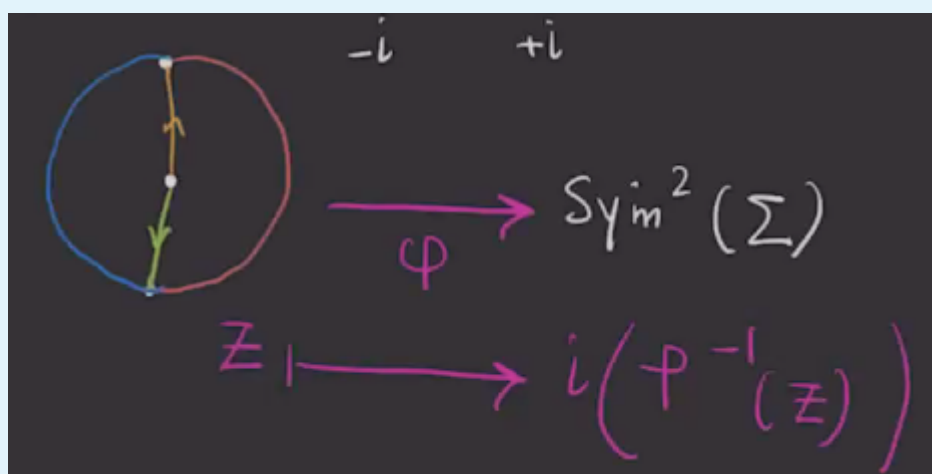
Figure 113: image_2021-02-23-12-01-02

In the image we get 2 points with multiplicity on Σ, and thus an element of $\mathrm{Sym}^2 \Sigma$. We know $\varphi(-i) = \{x_1, x_2\}$ and $\varphi(+i) = \{y_1, y_2\}$.

Example 12.1.12(?): Show that D' is the domain of a disc from $\{x_1, x_2\} \to \{y_1, y_2\}$:
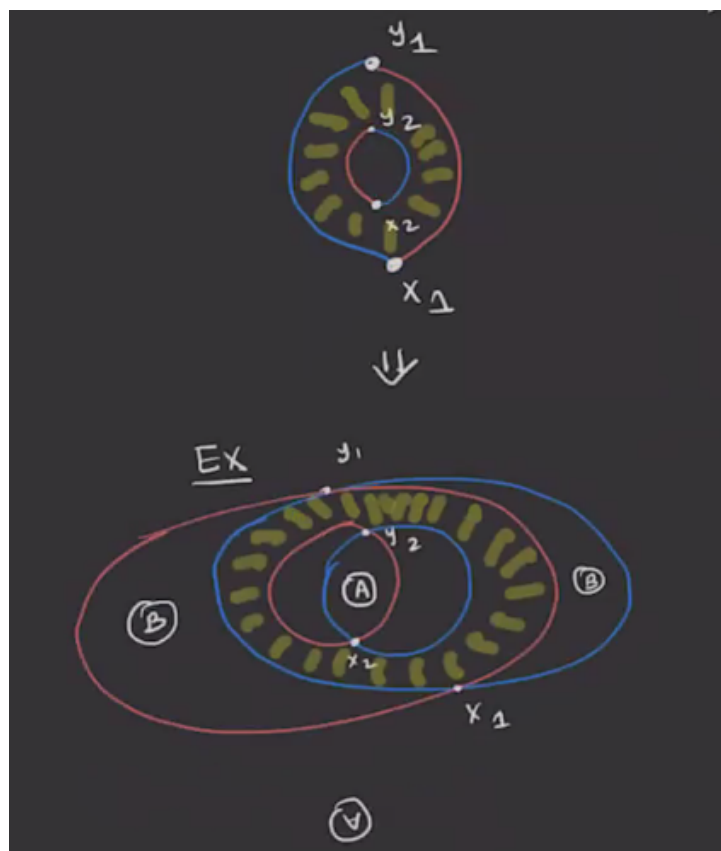
Figure 114: image_2021-02-23-12-18-15

We want to make a similar 2-fold cover like in the previous example, so we'll take the two rectangles bounding the arcs, then taking the rotation by π yields the cover:
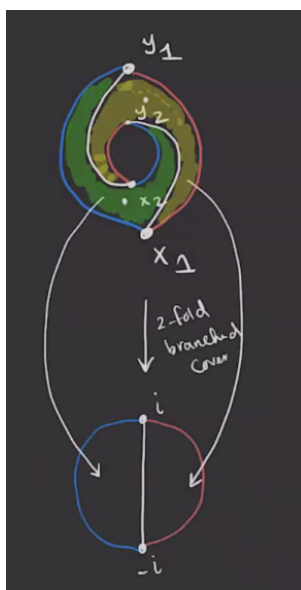
Figure 115: image_2021-02-23-12-20-27

As before, we get a map to $\operatorname{Sym}^2 \Sigma$:
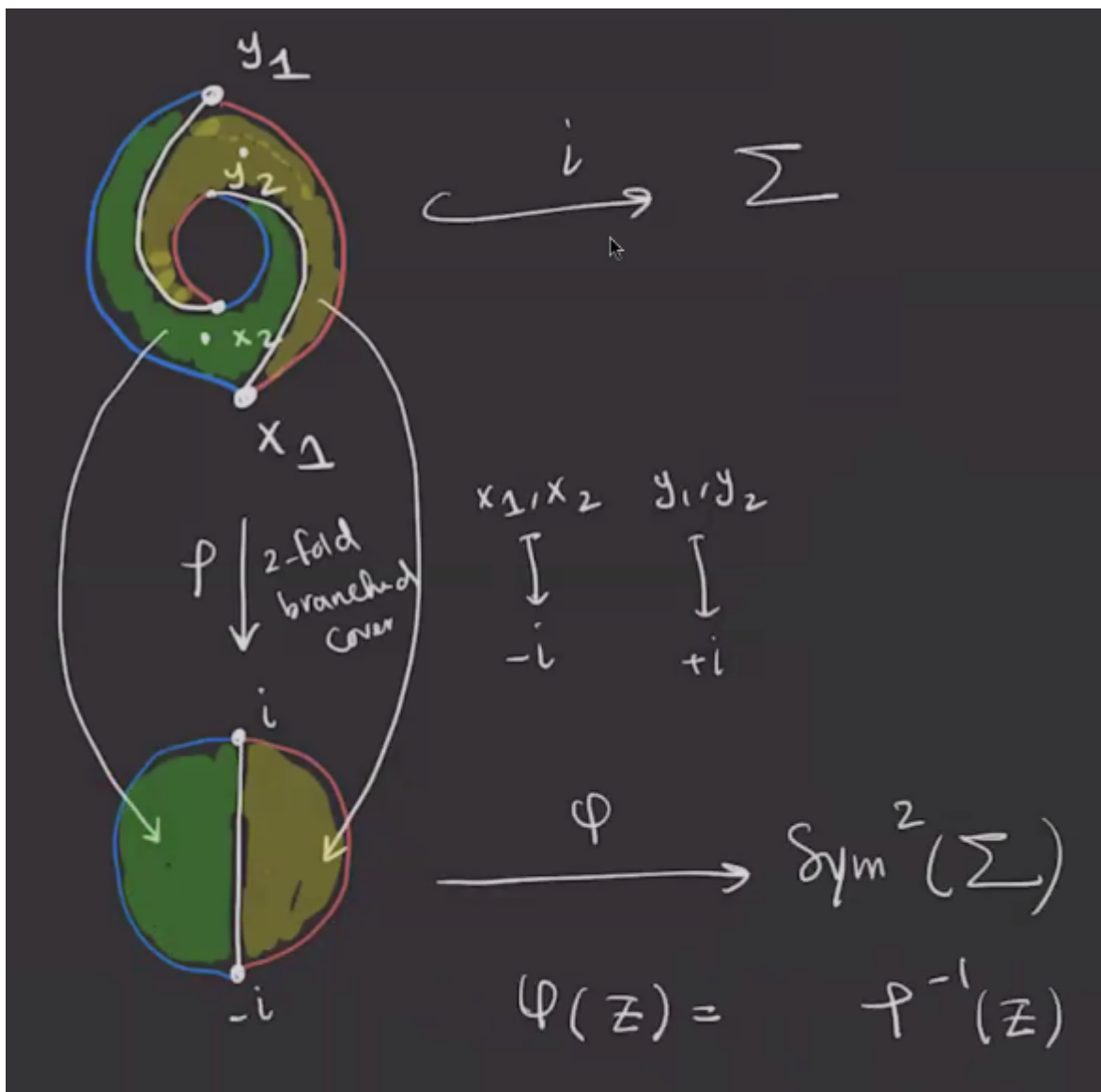
Figure 116: image_2021-02-23-12-22-36

As a result, we again get $\varphi(-i) = \{x_1, x_2\}$ and $\varphi(+i) = \{y_1, y_2\}$.

> **Exercise 12.1.13** (?)
> . Suppose $x = \{x_1, \cdots, x_g\}$ and $y = \{y_1, \cdots, y_g\}$ such that $x_i \in \alpha_i \cap \beta_i$ and $y_i \in \alpha_i \cap \beta_{\sigma^{-1}(i)}$ for some permutation $\sigma \in S_g$. Then for any $\varphi \in \pi_2(x, y)$, show that
>
> $$\partial\left(\partial D(\varphi) \cap \alpha_i\right) = y_i - x_i,$$
>
> where the inner term is a 1-chain in α_i, and
>
> $$\partial\left(\partial D(\varphi) \cap \beta_i\right) = x_i - y_{\sigma(i)}.$$

13 | **Thursday, February 25**

13.1 Whitney Discs

Remark 13.1.1: Recall that we discussed the domains of discs: for $\varphi \in \varphi_2(x, y)$ we defined the 2-chain $D(\varphi) = \sum_{i=1}^{n} a_i D_i$ where we've written

$$\Phi \setminus \alpha \cup \beta = \coprod_{i=1}^{m} \mathring{D}_i$$

and a_i is the number of points in $\operatorname{im}(\varphi) \cap L_{z_i}$ for $z_i \in D_i$.

> **Exercise 13.1.2** (?)
> For $\varphi \in \pi_2(x, y)$, $\partial D(\varphi)$ is a 1-chain in $\alpha \cup \beta$. Then
>
> $$\partial D(\varphi)|_{\alpha} = \sum_{i=1}^{g} y_i - \sum_{i=1}^{g} x_i \qquad \partial D(\varphi)|_{\beta} = \sum_{i=1}^{g} x_i - \sum_{i=1}^{g} y_i$$
>
> where $x_i, y_i \in \alpha_i$.

> **Corollary 13.1.3(?).**
> For $\varphi \in \pi_2(x, y)$, consider an intersection point w which labels 4 nearby regions with coefficients a, b, c, d:
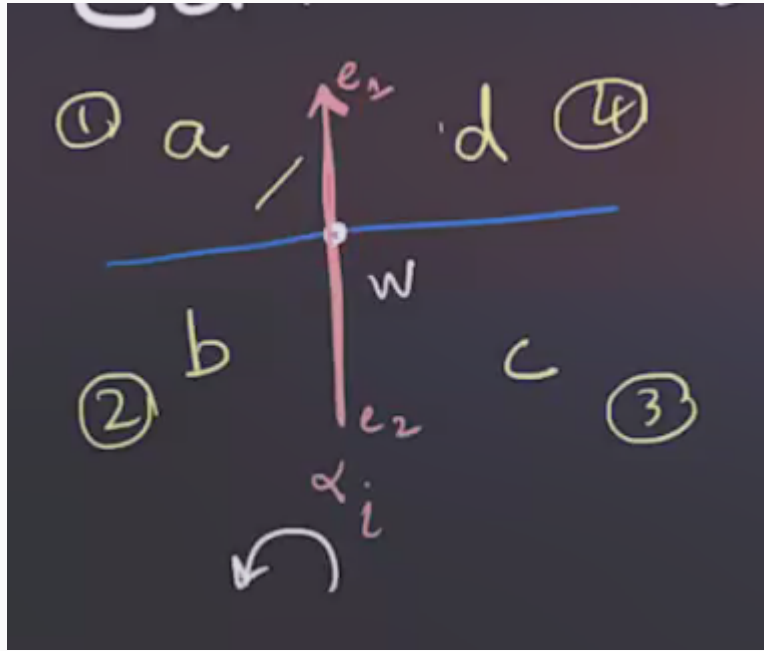
Figure 117: image_2021-02-25-11-28-01

Consider several cases:

1. $w \notin x$ and $w \notin y$: Then $\partial\left(\partial D(\varphi)|_\alpha\right) \not\ni w$. We can expand this out as

$$D(\varphi) = aD_1 + bD_2 + cD_3 + dD_4$$
$$\partial^2 D(\varphi) = \partial\left(a\partial D_1\right) + \cdots.$$

   Now restrict this to α_i to yield

$$\partial^2 D(\varphi) = ae_1 + be_2 - ce_2 - de_1.$$

   Checking coefficients of w contributes $-aw + bw - cw - d(-w)$, and these should sum to zero. This yields $a + c = b + d$, and similarly if $w \cap x \cap y$, this also yields $a + c = b + d$.

2. $w \in x$ and $w \notin y$ implies that $a + c = b + d + 1$.

3. $w \notin x$ and $w \in y$ implies $a + c + 1 = b + d$.

Remark 13.1.4: So if you want to check to see if some 2-chain could be the domain of a Whitney disc, this local condition can be checked, i.e. this is an obstruction to existence. It turns out that this is an if and only if condition.

> **Definition 13.1.5** (?)
> A 2-chain $A := \sum_{i=1}^{m} a_i D_i$ **connects** x to y if and only if the following local linear conditions are

satisfied:

$$\partial^2 A|_\alpha = y - x$$
$$\partial^2 A|_\beta = x - y$$

.

Proposition 13.1.6*(?)*.
Suppose $g > 1$. If a 2-chain A connects x to y then there exists a Whitney disc $\varphi \in \pi_2(x, y)$ such that $D(\varphi) = A$. If $g > 2$, φ is uniquely determined by A.

Remark 13.1.7: See proof in Osvath-Szabo paper.

Example 13.1.8*(?):* Think of the screen as a plane, and circled letters are handles attached out of the page according to their orientations. Consider the following diagram along with the indicated intersection points:
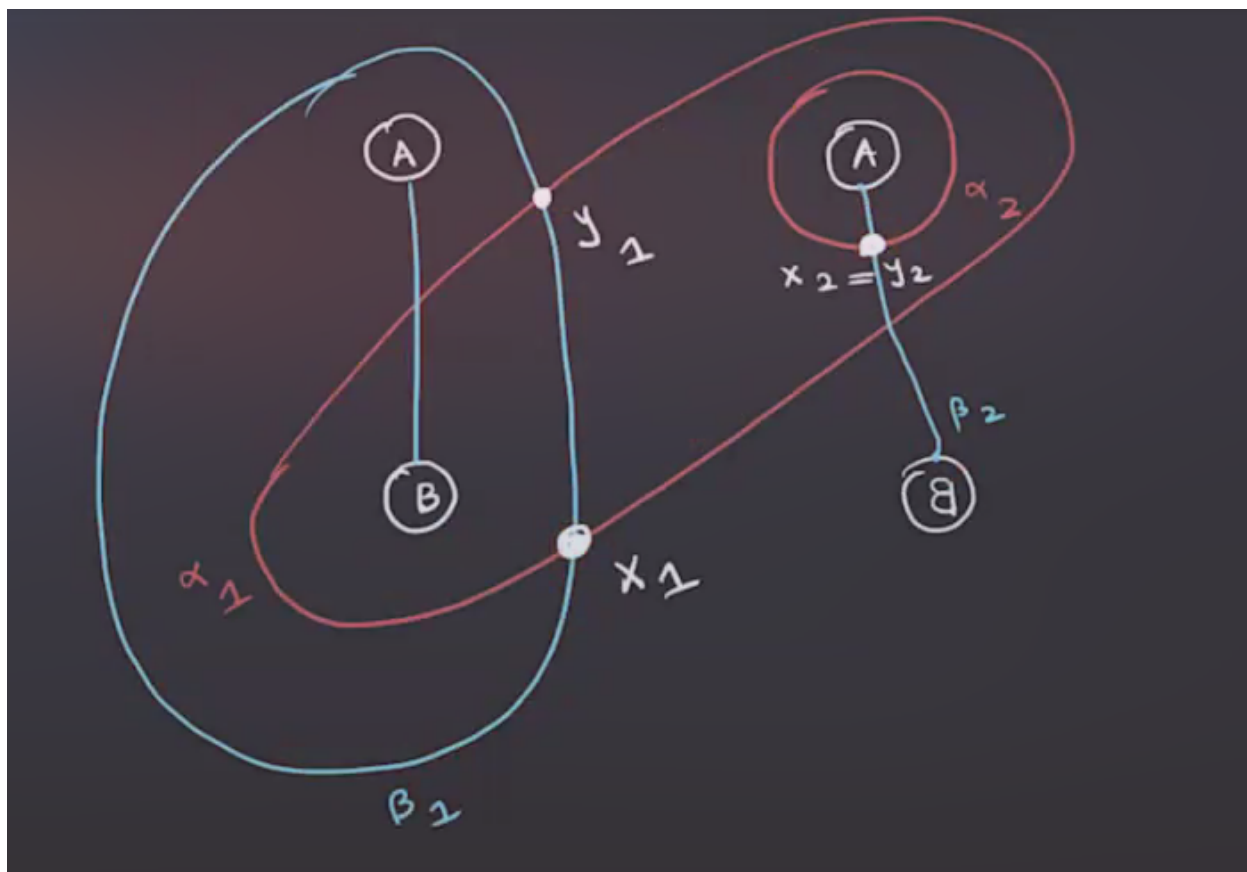
Figure 118: image_2021-02-25-11-45-11

Set the coefficients of the unlabeled regions to zero, and let $x := \{x_1, x_2\}$ and $y := \{y_1, y_2\}$. We can

check that if the following yellow region has coefficient 1, it can be the domain of a Whitney disc:
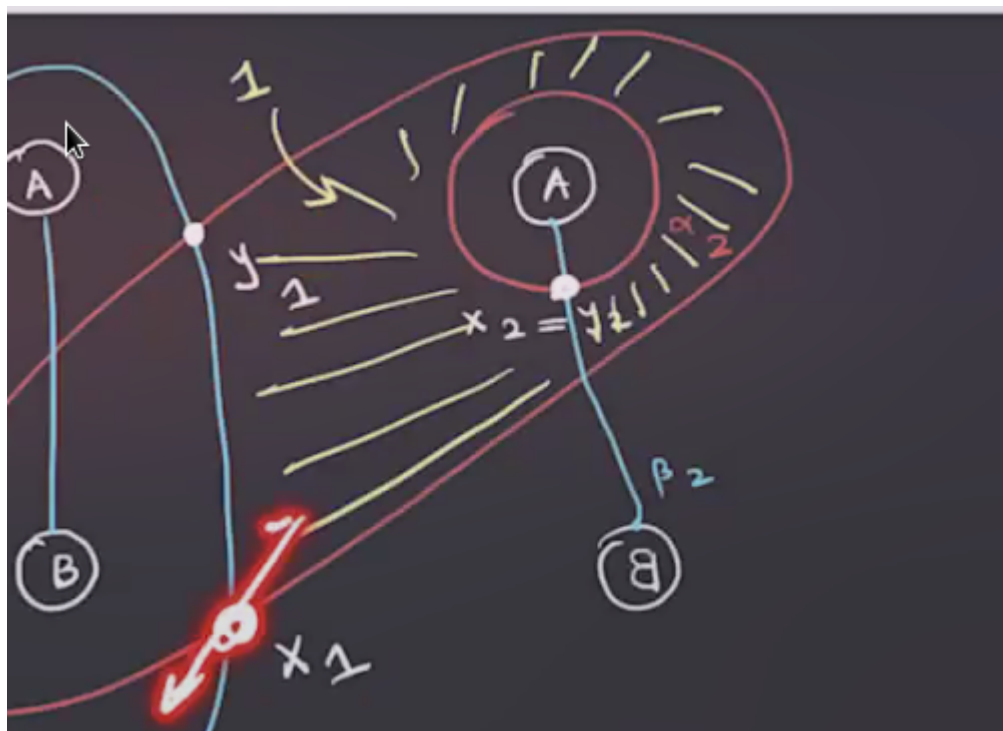
Figure 119: image_2021-02-25-11-47-15

This follows from checking the local conditions (there is a mnemonic involving the diagonal sums for the various cases).

Example 13.1.9*(?):* Consider a new diagram, changed by an isotopy (here: a "finger move"):
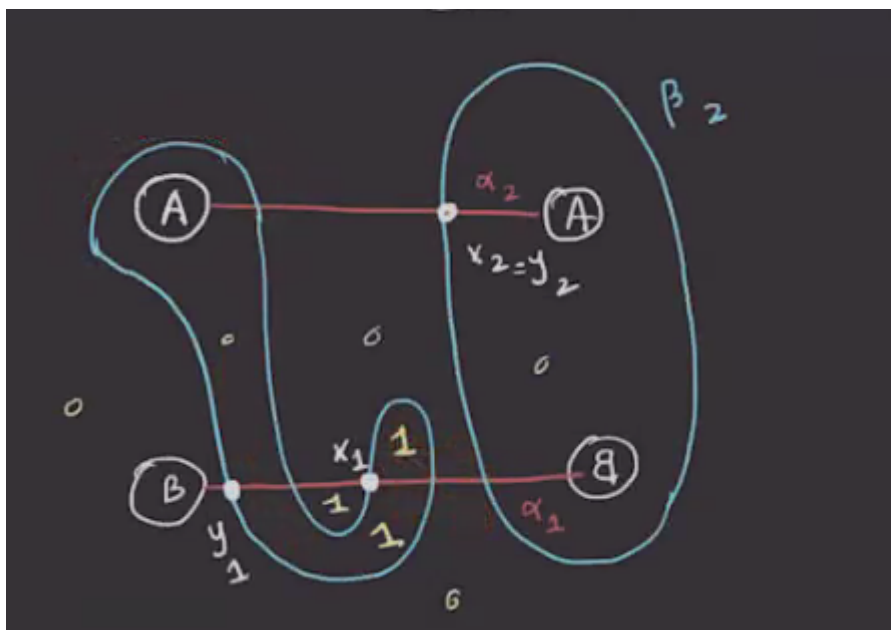
Figure 120: image_2021-02-25-11-52-12

Is there a Whitney disc connecting $x := \{x_1, x_2\} \xrightarrow{\varphi} y := \{y_1, y_2\}$? Checking the diagonals, all of the local conditions hold, so yes.

> **Exercise 13.1.10** (?)
> Find the 3-manifold that these two diagrams represent.

13.2 Holomorphic Discs

Remark 13.2.1: Ultimately these are what we want to define the differential in the chain complex.

Figure 121: image_2021-02-25-12-08-55

We'll set up a correspondence:

$$
\left\{
\begin{array}{c}
\text{(Riemann surfaces } F, \partial_\alpha F, \partial_\beta F) \overset{\pi_\Sigma}{\longrightarrow} (\Sigma, \alpha, \beta) \\
\Downarrow \qquad g\text{-fold branched cover } \pi_D \\
(D, e_1, e_2) \\
\partial F = (\partial_\alpha F) \coprod_\partial (\partial_\beta F) \\
\pi_D(\partial_\alpha) = e_1 \qquad \pi_D(\partial_\beta) = e_2
\end{array}
\right\}
\rightleftharpoons \left\{ \text{holomorphic } u : (D^2, e_1, e_2) \to (\mathrm{Sym}^g(\Sigma), \mathbb{T}_\alpha, \mathbb{T}_\beta) \right\}
$$

To do this, we define $u(z) = \pi_\Sigma(\pi_D^{-1}(z)) \in \mathrm{Sym}^g(\Sigma)$. Check that if π_D, π_Σ are holomorphic, then u is holomorphic.

Then if u is holomorphic, it can be shown that π_D, π_Σ are also holomorphic. Given $\varphi \in \pi_2(x, y)$, define $\mathcal{M}(\varphi)$ to be the moduli space of holomorphic discs connecting x to y in the same homotopy class as φ (i.e. such discs *represent* φ). After perturbing the complex structure $\mathrm{Sym}^g(j)$ to make it generic, $\mathcal{M}(\varphi)$ will be smooth. We'll have a notion of dimension, the *Maslov index* $\mu(\varphi)$, which is the expected dimension of $\mathcal{M}(\varphi)$. There will be an $\mathbb{R}$-action on $\mathcal{M}(\varphi)$, where we remember the biholomorphism between the disc and the vertical strip:
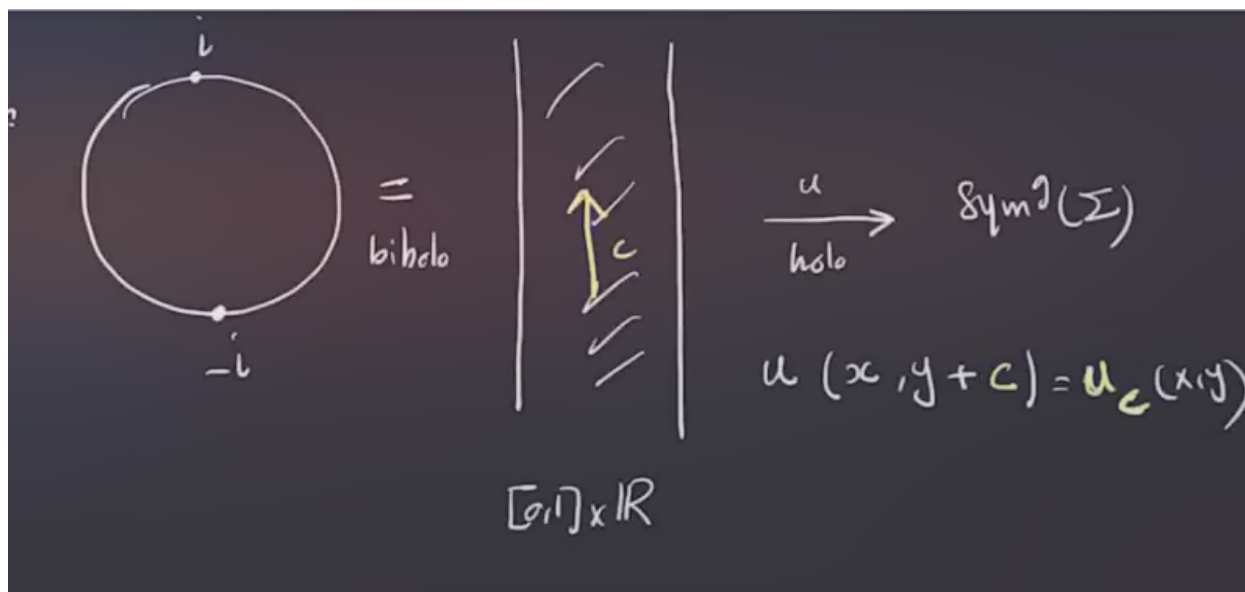
Figure 122: image_2021-02-25-12-19-15

We'll define $\widehat{\mathcal{M}}(\varphi) := \mathcal{M}(\varphi)/\mathbb{R}$. The chain complex will be defined as

$$\mathrm{HF}(\Sigma, \alpha, \beta) := \bigoplus_{x \in \mathbb{T}_\alpha \cap \mathbb{T}_\beta} \mathbb{Z}/2 \langle x \rangle$$

$$\partial x := \sum_{y \in \mathbb{T}_\alpha \cap \mathbb{T}_\beta} \sum_{\varphi \in \pi_2(x,y)?} \#\widehat{\mathcal{M}}(\varphi).$$

We'll need

- Check that ∂ is well-defined and $\partial^2 = 0$,

- Check independence of choices, e.g. the Heegard the diagram, the complex structure, the perturbations of $\mathrm{Sym}^g(j)$, etc.

Question 13.2.2
This takes a lot of work! Is the homology of this complex interesting? Is this stronger than singular homology?

Answer 13.2.3
Let $M \in \mathrm{ZHS}^3$, so the homology doesn't distinguish M from a sphere and $H_*(M; \mathbb{Z}) \cong H_*(S^3; \mathbb{Z})$. It turns out that $H_*(\mathrm{HF}(M^3)) \cong H_*(\mathrm{HF}(S^3))$, so the answer is no!

Remark 13.2.4: Osvath-Szabo picked a basepoint $z \in \Sigma \setminus (\alpha \cup \beta)$ and work with *pointed* Heegard diagrams $(\Sigma, \alpha, \beta, z)$. Perturb the differential to obtain

$$\tilde{\partial} x := \sum_{y \in \mathbb{T}_\alpha \cap \mathbb{T}_\beta} \sum_{\substack{\varphi \in \pi_2(x,y), \\ \mu(\varphi)=0, \\ n_z(\varphi)=0}} \#\widehat{\mathcal{M}}(\varphi) y.$$

where n_z denotes the coefficient of φ at the basepoint z, i.e. the number of intersection points $\#(\operatorname{im} \varphi \cap L_z)$.

Defining $\widehat{\mathrm{HF}}$ as the same chain complex with the new differential now gets interesting! We'll define $\widehat{\mathrm{HF}}$ as the homology of this new complex.

14 | The Heegard-Floer Chain Complex & Maslov Index (Tuesday, March 02)

14.1 Pointed Heegard Diagrams

Remark 14.1.1: Last time: to strengthen the homology theory, take a **pointed** Heegard diagram $(\Sigma, \alpha, \beta, z \in \Sigma \setminus \alpha \cup \beta$ and define a new chain complex

$$\widehat{\mathrm{HF}}(\Sigma, \alpha, \beta, z) = \bigoplus_{x \in \mathbb{T}_\alpha \cap \mathbb{T}_\beta} \mathbb{Z}/2 \langle x \rangle$$

$$\partial x = \sum_{y \in \mathbb{T}_\alpha \cap \mathbb{T}_\beta} \sum_{\substack{\varphi \in \pi_2(x,y), \\ \mu(\varphi)=1, \\ n_z(\varphi)=0}} \#\widehat{\mathcal{M}}(\varphi) y.$$

Note that $n_z(\varphi) = 0$ means that the coefficient attached to the region containing z is zero. Recall that we had diagram moves, how do they translate to the pointed setting?

- Allow *pointed isotopies*, which are isotopies disjoint from z.
- Allow *pointed handleslides*, where now the bounded pair-of-pants is disjoint from z:

Figure 123: image_2021-03-02-11-18-40

- Allow isotopies of the base point.

> **Lemma 14.1.2***(?).*
> Any two pointed Heegard diagrams for a 3-manifold M^3 can be connected by a sequence of the following moves:
>
> - Stabilization or destabilization,
> - Pointed isotopy,
> - Pointed handleslides,
> - Isotopes of the basepoint away from α, β.

> **Exercise 14.1.3** (?)
> Prove this lemma.

Example 14.1.4*(S^3):* Here is the simplest Heegard diagram from S^3:
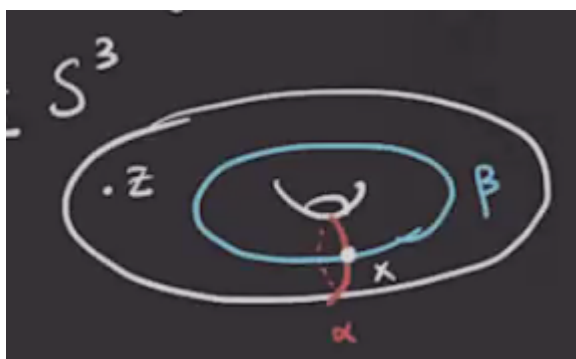
Figure 124: image_2021-03-02-11-22-54

Here there is just one one intersection point, so $\widehat{\mathrm{HF}} = \mathbb{Z}/2 \langle x \rangle$ is 1-dimensional, and $\partial x = 0$. So $\widehat{\mathrm{HF}} = \mathbb{Z}/2$.

Example 14.1.5*($\mathbb{RP}^3$):* We can write $\mathbb{RP}^3 = L(2,1)$ and produce the following Heegard diagram:
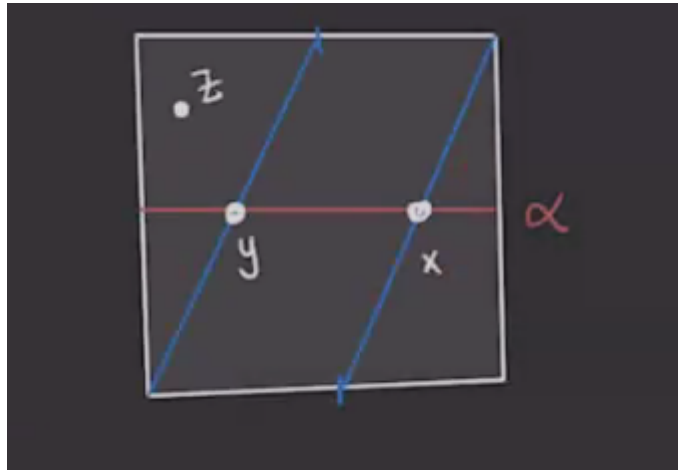
Figure 125: image_2021-03-02-11-38-42

Is there a disc between x and y? We can check the obstruction $\varepsilon(x, y)$ by labeling the generators in homology and tracing the following green path:
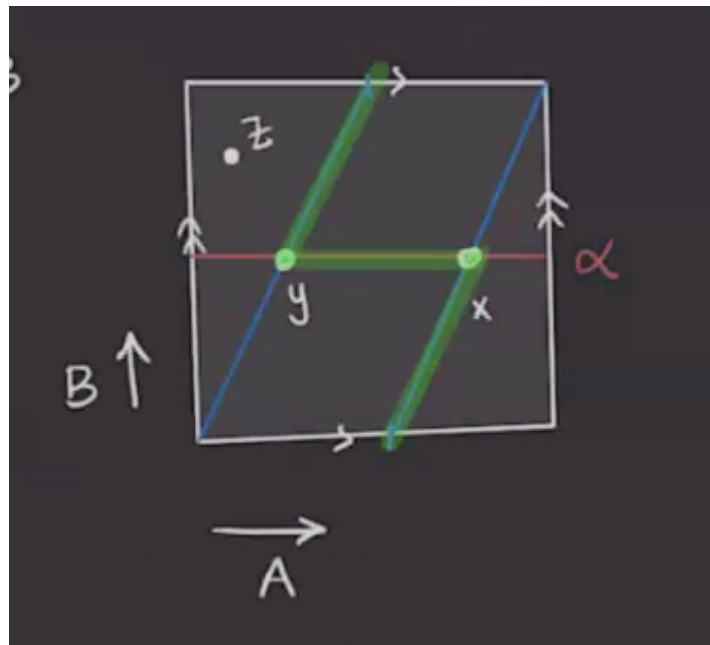
Figure 126: image_2021-03-02-11-40-13

We obtain

$$\varepsilon(x, y) = [B] \in \frac{H_1(T^2)}{\langle [\alpha] = [A], [\beta] = [A + 2B] \rangle}.$$

In this quotient, $[B] \neq 0$, and this quotient is $\mathbb{Z}/2 = \langle [B] \rangle$ so that $2B = 0$. So there are no disks in $\pi_2(x, y)$, making $\partial x = \partial y = 0$. So $\widehat{HF}(\mathbb{RP}^3) = \mathbb{Z}/2 \oplus \mathbb{Z}/2$.

> **Exercise 14.1.6** (?)
> Compute $\widehat{\mathrm{HF}}(L(p,1))$. Use that $\varepsilon(x,y) + \varepsilon(y,z) = \varepsilon(x,z)$.

14.2 Maslov Index

Remark 14.2.1: Recall that we had a natural concatenation operation on Whitney discs:

$$* : \pi_2(x,y) \times \pi_2(y,z) \to \pi_2(x,z),$$

using the identification of these discs with paths in the path space and using concatenation of paths there. Note that the domains of concatenations are given by $D(\varphi_1 * \varphi_2) = D(\varphi_1) + D(\varphi_2)$, since this amounts to adding algebraic intersection numbers.

There is an inverse

$$\pi_2(x,y) \to \pi_2(y,x)$$
$$\varphi \mapsto \varphi^{-1}(s,t) := \varphi(s,-t),$$

which reverses the parameterization on $(s,t) \in I \times \mathbb{R}$ and runs the path backward. Here $D(\varphi^{-1}) = -D(\varphi)$.

There is also a *sphere addition*

$$\pi_2(\mathrm{Sym}^g(\Sigma), x) \times \pi_2(x,y) \to \pi_2(x,y)$$
$$(\Omega, \varphi) \mapsto \Omega * \varphi.$$
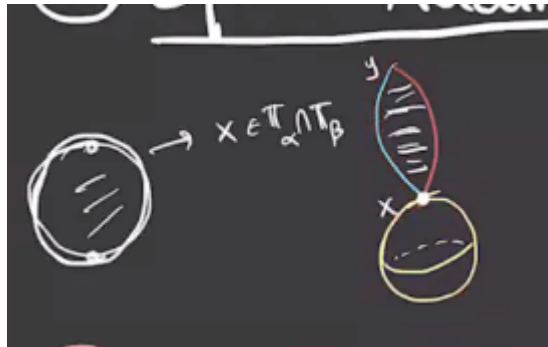
Figure 127: Maps entire boundary to a point, yielding a sphere.

Note that for $g \geq 2$, the π_2 on the left-hand side is isomorphic to $\mathbb{Z}$, which came from quotienting by the hyperelliptic involution several lectures ago. Writing the positive generator as S, we have $\Omega = kS$ for some $k \in \mathbb{Z}$.

> **Exercise 14.2.2*(?)***
> Show that
> $$D(S) = \sum_{i=1}^{m} D_i = [\Sigma].$$

> **Proposition 14.2.3*(?)*.**
> There exists a function $\mu : \pi_2(x, y) \to \mathbb{Z}$ called the **Maslov index** satisfying:
>
> 1. Additivity: $\mu(\varphi_1 * \varphi_2) = \mu(\varphi_1) + \mu(\varphi_2)$.
>
> 2. Invertibility: $\mu(\varphi^{-1}) = -\mu(\varphi)$.
>
> 3. Sphere addition: $\mu(kS * \varphi) = \mu(\varphi) + 2k$ where $k \in \mathbb{Z}$ and $S \in \pi_2(\mathrm{Sym}^g(\Sigma))$.
>
> 4. If $\varphi \in \pi_2(x, x)$ is constant, then $\mu(\varphi) = 0$.
>
> Note that $2 \implies 4$.

Remark 14.2.4: The Maslov index is the "expected" dimension of

$$\mathcal{M}(\varphi) = \left\{ u : I \to \mathbb{R} \to \mathrm{Sym}^g(\Sigma) \,\Big|\, [u] = \varphi \, du \circ i = J \circ du \right\}$$

where i is the standard complex structure on the strip and J will be a perturbation of the complex structure over the Heegard surface. This will yield an operator

$$\bar{\partial}_J : B \to \mathcal{L}$$
$$u \mapsto du \circ i - J \circ du$$

for some appropriate infinite dimensional spaces. The elements of $\mathcal{M}(\varphi)$ will be in the kernel of this operator. We want 0 to be a **regular value** (surjective derivative) for $\bar{\partial}_J$, since in finite dimensions the inverse image would be a smooth manifold. In the infinite dimensional setting, we'll have by the inverse function theorem that $\mathcal{M}(\varphi) = \bar{\partial}_J^{-1}(0)$ will be a smooth manifold. We'll want the following derivative to be surjective:

$$D_u \bar{\partial}_J : T_u B \to T_{\bar{\partial}_J u} \mathcal{L}$$

for all $u \in \bar{\partial}_J^{-1}(0)$, which is referred to as **transversality** of the operator, and can be made to hold by perturbing the complex structure. Since the dimension of a manifold is the dimension of the tangent spaces, we'll have $\mathcal{M}(\varphi)$ smooth of dimension equal to $\dim \ker D_u \bar{\partial}_J$ for any $u \in \bar{\partial}_J^{-1}(0)$. This will be an order 2 elliptic operator (or more generally a Fredholm operator), for which we have a notion of index:

$$\mathrm{ind}(D\bar{\partial}_J) = \dim(\ker D\bar{\partial}_J) - \dim(\mathrm{coker}\, D\bar{\partial}_J).$$

If surjectivity holds, the cokernel will be zero, so it will suffice to compute the dimension of the kernel to get the dimension of the moduli space. The index of this operator will be the Maslov index.

Remark 14.2.5: Take a look at *Gromov compactness* again!

15 | Maslov Index Formula (Thursday, March 04)

15.1 Review

Remark 15.1.1: Recall that for $x, y \in \mathbb{T}_\alpha \cap \mathbb{T}_\beta$, there is a map

$$\mu : \pi_2(x, y) \to \mathbb{Z}$$
$$\mu = \mathrm{ind}(D\bar{\partial}_J).$$

This index is the expected dimension of $M(\varphi)$. The following theorem can be found in the paper "A cylindrical reformulation of Heegard Floer homology":

Theorem 15.1.2 *(Lipschitz).*
Let $x = \{x_1, \cdots, x_g\}$ and $y = \{y_1, \cdots, y_g\}$ and $\varphi \in \pi_2(x, y)$. Then

$$\mu(\varphi) = e(D(\varphi)) + n_x(D(\varphi)) + n_y(D(\varphi)).$$

where $e(-)$ is the **Euler measure** and $n_x(\cdots), n_y(\cdots)$ is referred to as the **point measure**. Note that these only depend on the domain of φ.

Definition 15.1.3 (Euler Measure)
Let $D(\varphi) = \sum_{i=1}^{m} n_{z_i}(\varphi) D_i$, then

$$e(D(\varphi)) := \sum_{i=1}^{m} n_{z_i}(\varphi) e(D_i) \qquad\qquad e(D_i) := \chi(D_i) + \frac{1}{4}C_1 - \frac{1}{4}C_2.$$

Here we use the fact that all regions are polygons whose corners occur in one of two types:
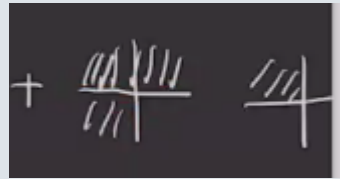
Figure 128: image_2021-03-04-11-20-25

So we define C_1 to be the number of corners of the first type and C_2 the number of the second type. The point measure is defined as

$$n_x(D(\varphi)) := \sum_{i=1}^{g} n_{x_i}(D(\varphi)) = \frac{n_1 + n_2 + n_3 + n_4}{4},$$

where the n_i are the surrounding regions' coefficients:
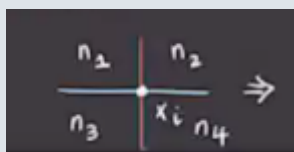
Figure 129: image_2021-03-04-11-24-27

**Example 15.1.4*(?):* Let $x = \{x_1, x_2\}, y = \{y_1, y_2\}$ and compute $\mu(\varphi)$ where $D(\varphi)$ is one of the following domains:

1. The first type:

Figure 130: image_2021-03-04-11-26-34
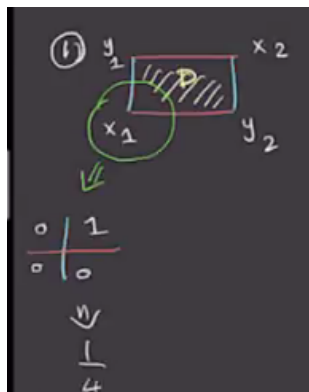
Figure 131: image_2021-03-04-11-30-34

- Here $D(\varphi) = 0$ and $e(D) = 1 + \dfrac{1}{4}(0) - \dfrac{1}{4}(0) = 0$.
- $n_x(D(\varphi)) = n_{x_1}(D) + n_{x_2}(D)F = \dfrac{1}{4} + \dfrac{1}{4} = \dfrac{1}{2}$.
- $n_y(D(\varphi)) = n_{y_1}(D) + n_{y_2}(D) + \dfrac{1}{4} + \dfrac{1}{4} = \dfrac{1}{2}$.
- So $\mu(\varphi) = 1$.

2. A second type:
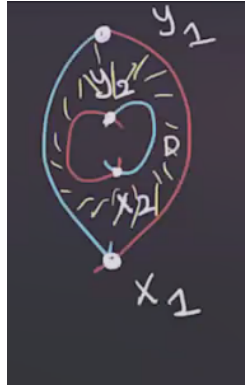
Figure 132: image_2021-03-04-11-32-08

- Here we have an annulus and $D(\varphi) = D$ implies that $e(D(\varphi)) = e(D) = \chi(D) + \cdots = 0 + \frac{1}{4}(0) - \frac{1}{4}(4) = -1$.
- $n_x(D(\varphi)) = n_{x_1}(D) + n_{x_2}(D) = \frac{1}{4} + \frac{1}{4} = \frac{1}{2}$
- $\mu(\varphi) = -1 + \frac{1}{2} + \frac{1}{2} = 0$.

3. A third type:
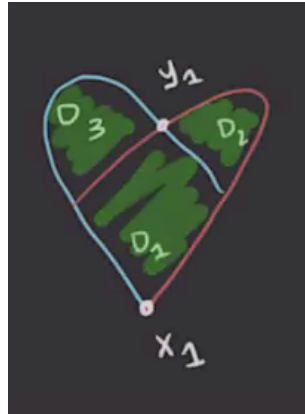
Figure 133: image_2021-03-04-11-36-09

- Here $x_2 = y_2$ and are disjoint from D_1, D_2, D_3:
- $D(\varphi) = D_1 + D_2 + D_3$.
- $e(D(\varphi)) = \sum e(D_i) = \left(1 - \frac{1}{4}(4)\right) + \left(1 - \frac{1}{4}(2)\right) + \left(1 - \frac{1}{4}(2)\right) = 0 + \frac{1}{2} + \frac{1}{2} = 1$.

    - We could have alternatively noted that $D(\varphi)$ is a disc with $\chi = 1$ and used the formula to get $1 + \frac{1}{4}(1) - \frac{1}{4}(1)$.

- $n_x(D(\varphi)) = n_{x_1}(D(\varphi)) + n_{x_2}(D(\varphi)) = \frac{1}{4} + 0 = \frac{1}{4}$.

- $n_y(D(\varphi)) = n_{y_1}(D(\varphi)) + n_{y_2}(D(\varphi)) = \dfrac{3}{4} + 0 = \dfrac{3}{4}$.
- Thus $\mu(\varphi) = 2$.

Example 15.1.5*(?)*: Another example calculation:
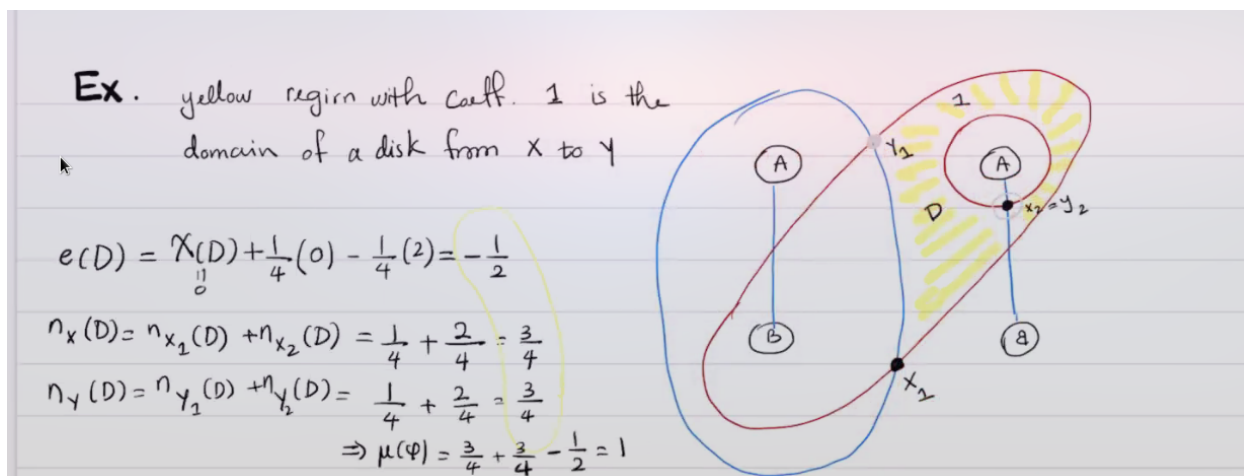
Figure 134: image_2021-03-04-11-47-57

Question 15.1.6
Does this domain have a holomorphic representative?

15.2 Positivity Principle

> **Proposition 15.2.1*(Positivity Principle)*.**
> For $\varphi \in \pi_2(x, y)$, if $\mathcal{M}(\varphi) \neq \emptyset$ then $D(\varphi) \geq 0$, i.e. $D(\varphi) = \sum n_i D_i$ where $n_i \geq 0$. This happens if and only if $n_w(\varphi) \geq 0$ for all $w \in \Sigma \setminus \alpha \cup \beta$.

> *Proof (Idea).*
> If $u \in M(\varphi)$ then $u : D \to \mathrm{Sym}^g(\Sigma)$ is holomorphic and $\mathrm{im}(u)$ is a complex submanifold. If $w \in \Sigma \setminus \alpha \cup \beta$ then $\mathcal{L}_w$ is holomorphic. ∎

Example 15.2.2*(?)*: Show that transverse complex submanifolds intersect non-negatively, i.e.

$$n_w(\varphi) := \#(\mathrm{im}(u) \cap \mathcal{L}_w) \geq 0.$$

Example 15.2.3*(?)*: Consider $S^1 \times S^2$ with the following Heegard diagram:
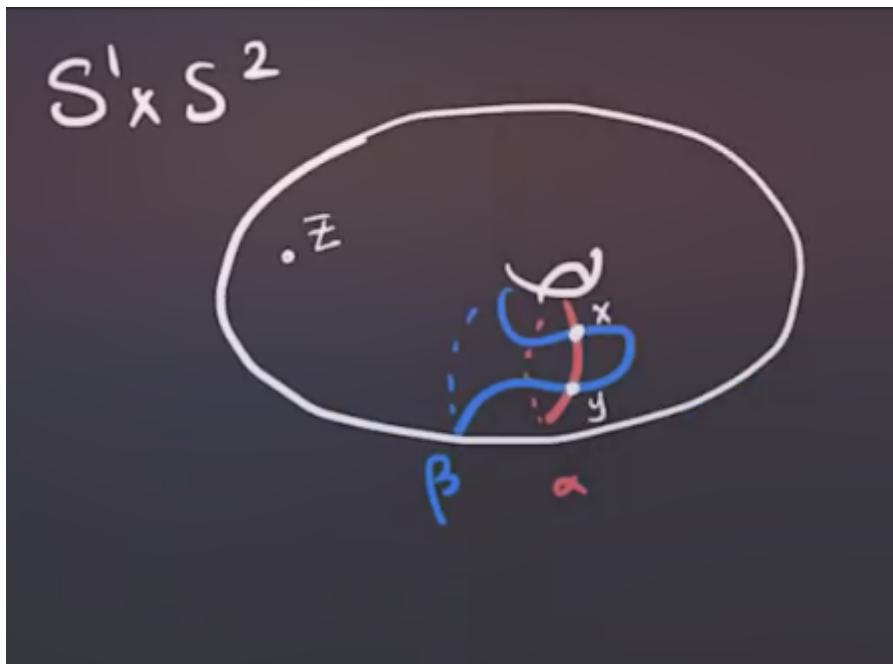
Figure 135: image_2021-03-04-12-18-25

We have $\widehat{\mathrm{HF}}(\Sigma, \alpha, \beta, z) = \mathbb{Z}/2 \langle x, y \rangle$. Then for $\varphi \in \pi_2(x, y)$ with $\mu(\varphi) = 1$ and $n_z(\varphi) = 0$, we can write $D(\varphi) = aD_1 + bD_2$. Now checking the diagonals:
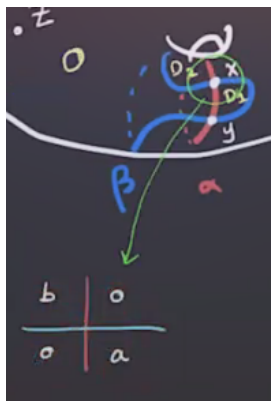
Figure 136: image_2021-03-04-12-20-40

Since the sum of multiplicities NW $\to$ SE should be 1 more than the sum NE $\to$ SW, we have $a + b = 1$ and by the positivity principle, $D(\varphi) \geq 0$ implies $a, b \geq 0$. We then obtain

$$\begin{cases} a = 0, b = 1 & \implies D(\varphi) = D_2 \ni \varphi_2 \\ a = 1, b = 0 & \implies D(\varphi) = D_1 \ni \varphi_1 \end{cases}.$$

Example 15.2.4(?): For example, if $\mu(\varphi_1) = \mu(\varphi_2) = 1$, we're looking for holomorphic maps

---
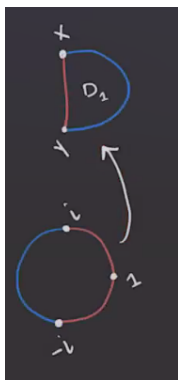
Figure 137: image_2021-03-04-12-23-52

For any p on the α circle from y to x, there exists a unique holomorphic map with $\mu(1) = p$ by the Riemann mapping theorem. After taking the quotient $\widehat{\mathcal{M}}(\varphi_1) = \mathcal{M}(\varphi_1)/\mathbb{R}$, we obtain $\#\widehat{\mathcal{M}}(\varphi_1) = 1 = \#\mathcal{M}(\varphi_2)$. Then note that

$$\partial x = \left(\#\widehat{\mathcal{M}}(\varphi_1) + \#\widehat{\mathcal{M}}(\varphi_2) \right) y = 0,$$

since we are taking coefficients mod 2. Then $\varphi \in \mu(x, y)$ implies that $a + b = -1$, so there is no non-negative disk and $\partial y = 0$.

> **Exercise 15.2.5*(?)***
> Show that there is no non-negative disc in $\pi_2(x, x)$ and $\pi_2(y, y)$ by looking at local coefficients.

So $\partial = 0$ which implies that $\widehat{\mathrm{HF}}(\Sigma, \alpha, \beta, z) = (\mathbb{Z}/2)^{\oplus 2}$.

Question 15.2.6
What if we used an isotopic diagram?
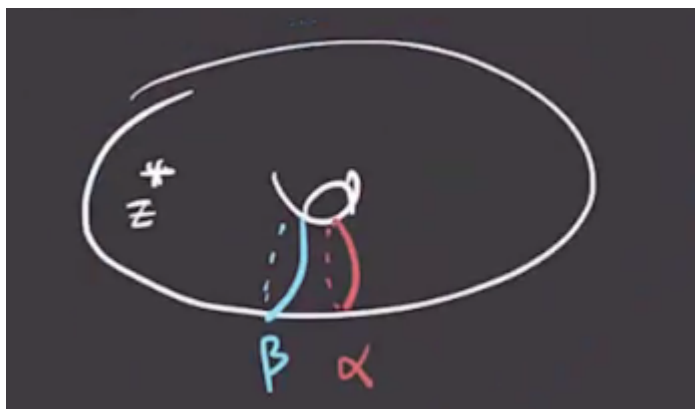
Figure 138: image_2021-03-04-12-30-18

The only difference between this and the first is an isotopy of β, and we'll see that there's an invariance and a condition called *admissibility* to help decide which to use.

16 | Tuesday, March 09

Remark 16.0.1: Recall that we were working with a diagram for $S^1 \times S^2$:
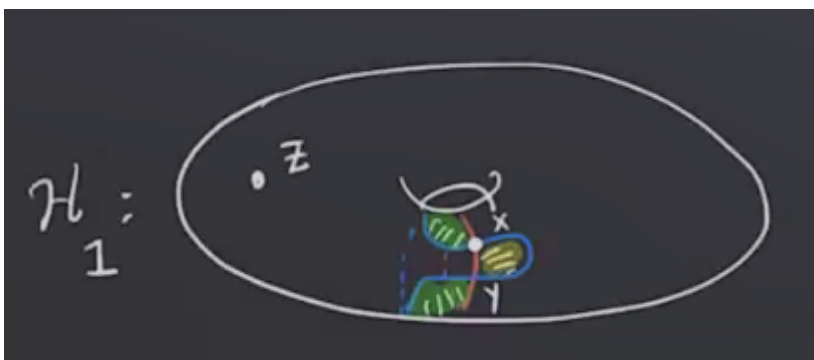
Figure 139: image_2021-03-09-11-14-10

Here we have $\partial x = 2y = 0$ since we're working mod 2, and $\partial y = 0$, so we have

$$\widehat{\mathrm{HF}}(H_1) = \frac{\ker \partial}{\operatorname{im} \partial} = \frac{\langle x, y \rangle}{1} = (\mathbb{Z}/2)^{\oplus 2}.$$

However, with a different diagram, we get a different result:
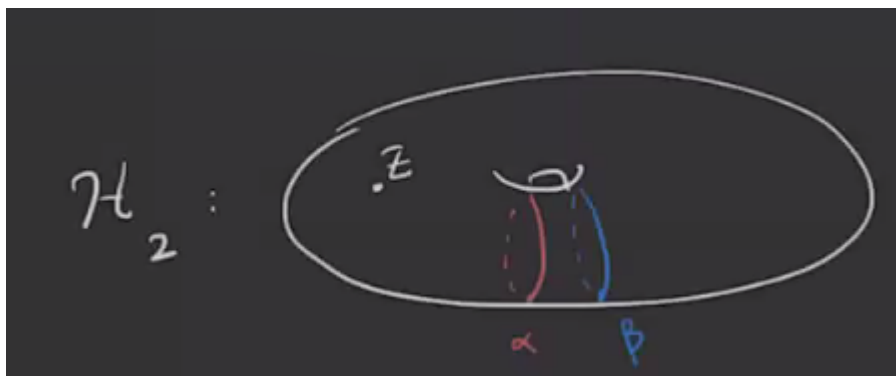
Figure 140: image_2021-03-09-11-15-46

Here $\widehat{\mathrm{HF}}(H_2) = 0$. To prevent this, we'll have some class of *admissible* diagrams.

> **Definition 16.0.2** (Periodic Domains)
>
> A 2-chain $P = \sum_{i=1}^{m} a_i D_i$ is called a **periodic domain** if and only if
>
> 1. The local multiplicity of P at z is zero, i.e. $n_z(P) = 0$, and
> 2. ∂P is a linear combination of α, β.

Remark 16.0.3: Note that for (2), the boundary could involve 1-chains, so this condition avoids corners on ∂P. The local picture is the following:
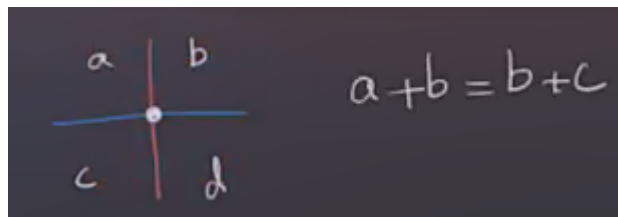
Figure 141: image_2021-03-09-11-19-12

Example 16.0.4*(?):* In this picture, $P = nD_1$ will be a periodic domain for any n;
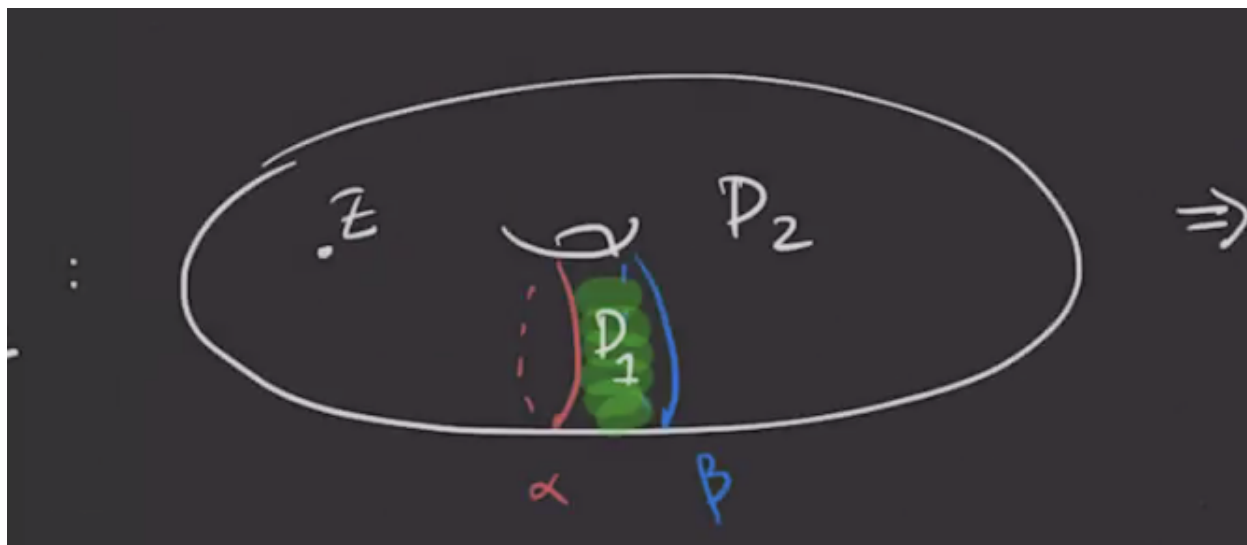
Figure 142: image_2021-03-09-11-20-54

Example 16.0.5*(?):* Labeling the first picture, we have
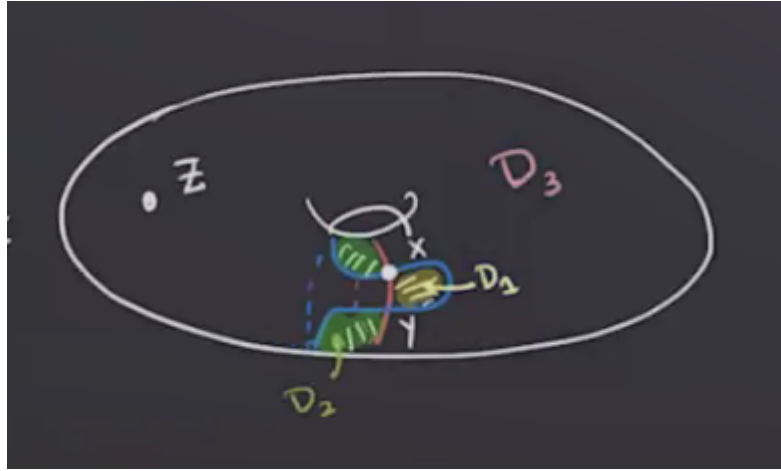
Figure 143: image_2021-03-09-11-21-32

We should have $n_1 + n_2 = 0$, so any $P = n(D_1 - D_2)$ will be a periodic domain. Checking the boundary yields $\partial P = n\alpha \pm n\beta$. In fact there is single "generator" for the periodic domains here:

Figure 144: image_2021-03-09-11-23-43

> **Definition 16.0.6** (Weakly Admissible Diagrams)
> A Heegaard diagram $H = (\Sigma, \alpha, \beta, z)$ is called **weakly admissible** if any periodic domain P has both positive and negative coefficients.

Example 16.0.7*(?):* H_1 from above is weakly admissible, but H_2 is not.

Remark 16.0.8: For any Whitney disc $\varphi \in \pi_2(x, x)$ with $n_z(\varphi) = 0$, $D(\varphi)$ is a periodic domain. For any periodic domain P, we can associate a homology class $H(P) \in H_2(M)$. Writing

$$\partial P = \sum_{i=1}^{g} a_i \alpha_i + \sum_{i=1}^{g} b_i \beta_i \xrightarrow{H} H(P) := [P + \sum_{i=1}^{g} a_i A_i + \sum_{i=1}^{g} b_i B_i].$$

using that each α_i is the boundary of some disc A_i in one handlebody, and $\beta_i = \partial B_i$ similarly. Noting that P is a boundary, this amounts to adding a number of discs to get a closed nontrivial cycle.

> **Exercise 16.0.9** (?)
> Show that if $H(P) = 0$ the $P = 0$, and that H is a bijection.

Remark 16.0.10: Let $P = \sum_{i=1}^{m} n_i D_i$ be a 2-chain that satisfies condition 2, so $\partial P = \sum_{i=1}^{m} a_i \alpha_i + \sum_{i=1}^{m} b_i \beta_i$. Then we can obtain a periodic domain:

$$P_0 := P - n_z(P) \left(\sum_{i=1}^{m} D_i \right) := P - n_z(P)[\Sigma].$$

Exercise 16.0.11 (?)
Show that if $g > 2$, then

$$\pi_2(x,x) \xrightarrow{\sim} \mathbb{Z} \oplus H_2(M)$$
$$P = P_0 + n_z(P)[\Sigma] \mapsto (n_z(P), H(P_0)).$$

Alternatively, given $\varphi \in n_z(\varphi)S$ where S is the positive generator of $\pi_2(\mathrm{Sym}^g(\Sigma)) * \varphi_0$ (i.e. the hyperelliptic involution) where $D(\varphi_0)$ is a periodic domain.

> *Use that for $g \geq 2$ there is a bijection between Whitney discs and domains, and domains of Whitney discs are domains satisfying condition (2) above.*

Exercise 16.0.12 (?)
Show that for a closed 3-manifold $M \in \mathrm{QHS}^3$, $H_2(M;\mathbb{Z}) = 0$.

Corollary 16.0.13*(?)*.
If $H_2(M) = 0$ (e.g. if $M \in \mathrm{QHS}^3$) then any Heegard diagram is weakly admissible.

Remark 16.0.14: This is because $H_2(M) = 0$ means there are no periodic domains.

Lemma 16.0.15*(?)*.
If H is weakly admissible, then for any $x,y \in \mathbb{T}_\alpha \cap \mathbb{T}_\beta$ there are *finitely* many Whitney discs $\varphi \in \pi_2(x,y)$ with $D(\varphi) \geq 0$.

Theorem 16.0.16*(?)*.
Any Heegard diagram can be made admissible using finitely many isotopies.

Example 16.0.17*(?)*: For $g = 1$, we have $\mathrm{Sym}^1(\Sigma) = \Sigma$. We'll use this in what follows.

Lemma 16.0.18*(?)*.
For any $x,y \in \alpha \cap \beta$, the 0-dimensional moduli space of holomorphic disks connecting x to y correspond to orientation-preserving immersions of the following form which satisfy:
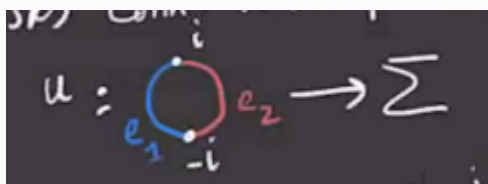
Figure 145: image_2021-03-09-12-06-12

1. $u(e_1) \subseteq \beta, u(e_2) \subseteq \alpha, u(-i) = x, u(i) = y.$
2. There are $\pi/2$ radian corners at x, y, but these are smooth immersions at other boundary points.

Exercise 16.0.19 (?)
Prove this lemma using the Riemann mapping theorem.

Example 16.0.20 *(?):* Consider the following example:
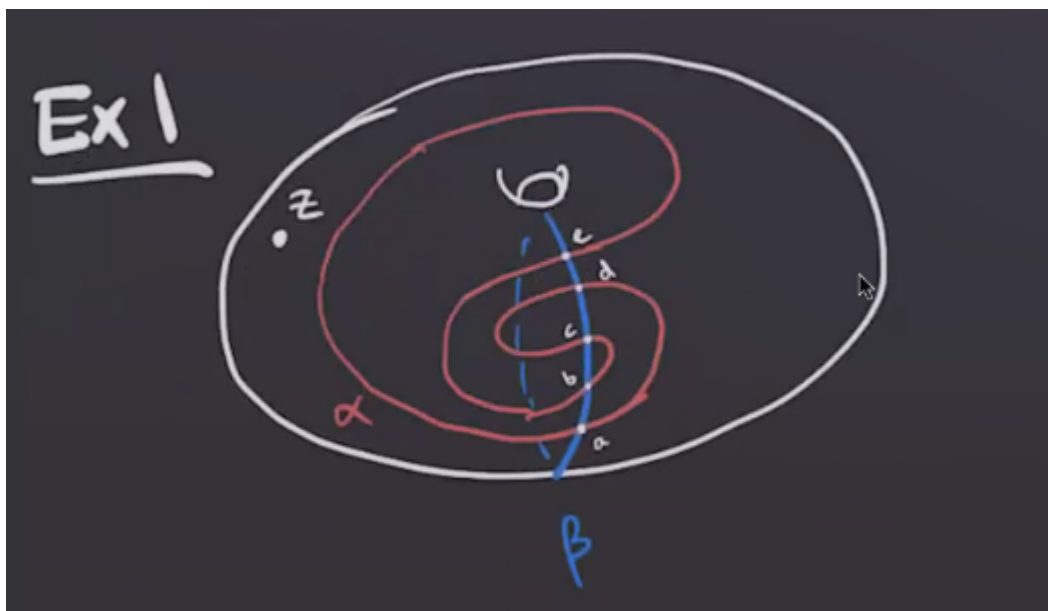
Figure 146: image_2021-03-09-12-09-05

List all of the bigons in this picture that will contribute to the differential.

17 | Thursday, March 11

Remark 17.0.1: Recall the example from last time: we are trying to show that changing a diagram by isotopy doesn't change the homology.
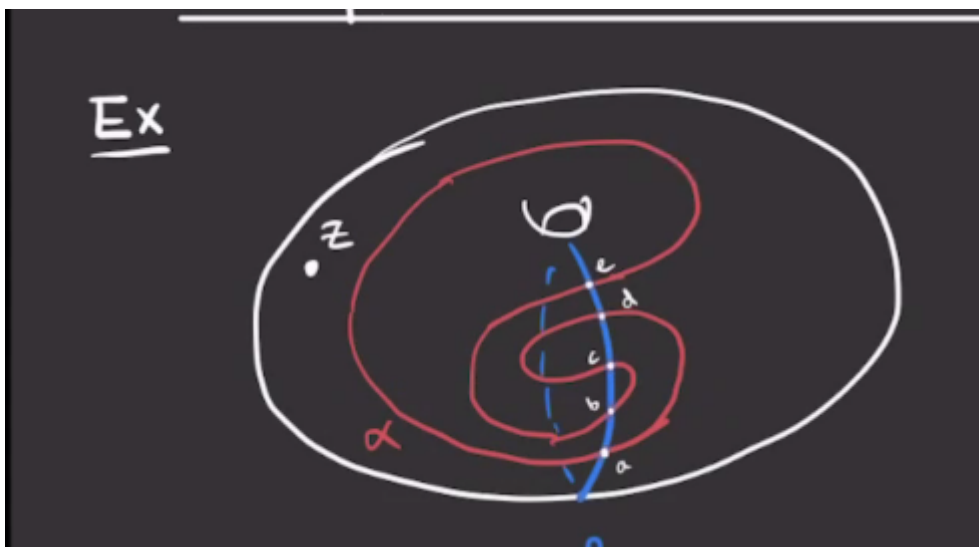
Figure 147: image_2021-03-11-11-16-15

Here we have $g = 1$ and so $\mathrm{Sym}^1(T^2) = T^2$, and $\alpha \cap \beta = \{a, b, c, d, e\}$. So $\widehat{\mathrm{HF}}(\Sigma, \alpha, \beta, z) = \mathbb{Z}/2 \langle a, b, c, d, e \rangle$.

First mark the component that contains the base point z and give it a coefficient of zero:
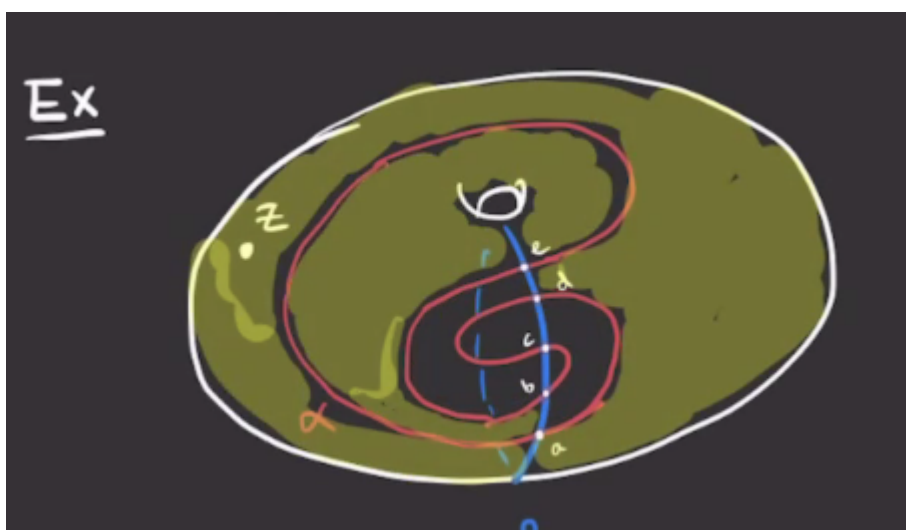
Figure 148: image_2021-03-11-11-18-34

We can make this part bigger, and find that there are only two bigons involving a.
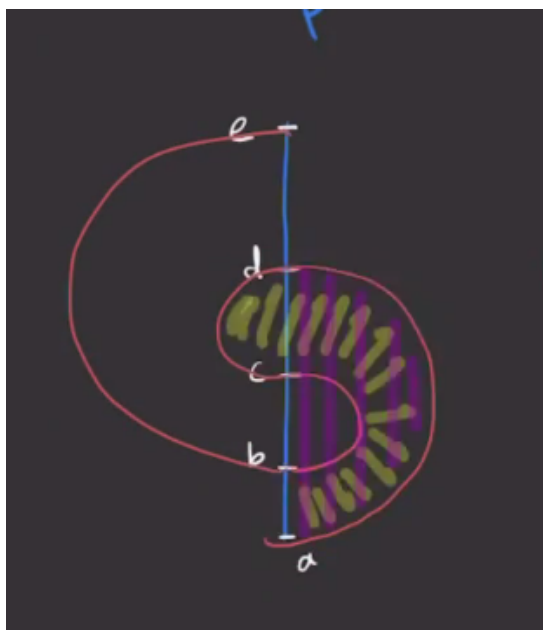
Figure 149: image_2021-03-11-11-23-41

This is because starting at a point and following the orientation should yield red first and then blue, matching up with the orientation on the disc.
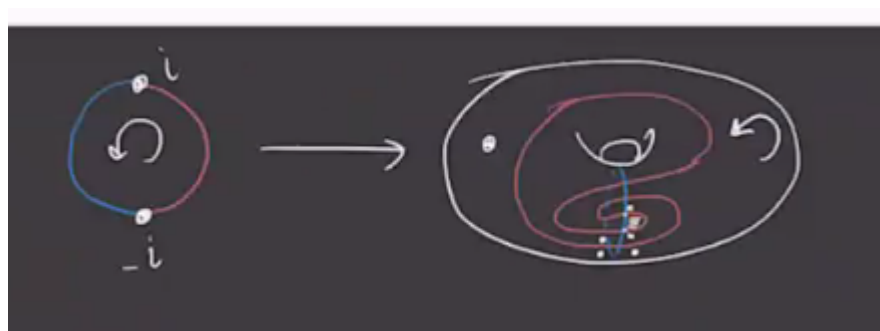
Figure 150: image_2021-03-11-11-35-44

So $\partial a = b + d$, since we require 90 degree corners. Similarly,

- $\partial e = b + d$
- $\partial b = c$
- $\partial d = c$
- $\partial c = 0$

We can simplify this information with a graph with arrows pointing toward boundaries:
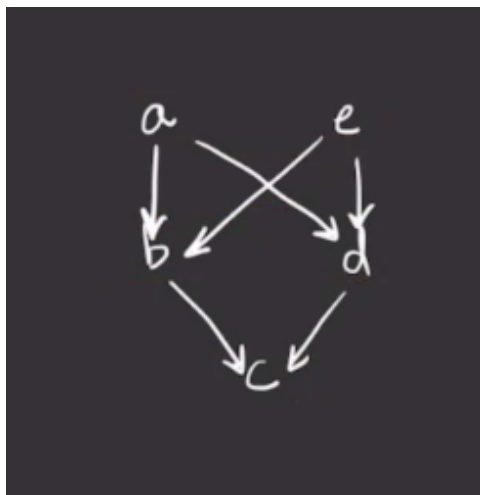
Figure 151: image_2021-03-11-11-29-41

Then any linear combination with the same image will have zero boundary, so we have

$$\ker \partial = \langle a + e, b + d, c \rangle$$
$$\operatorname{im} \partial = \langle b + d, c \rangle,$$

and thus $\widehat{\mathrm{HF}}(\Sigma, \alpha, \beta, z) = \mathbb{Z}/2$.
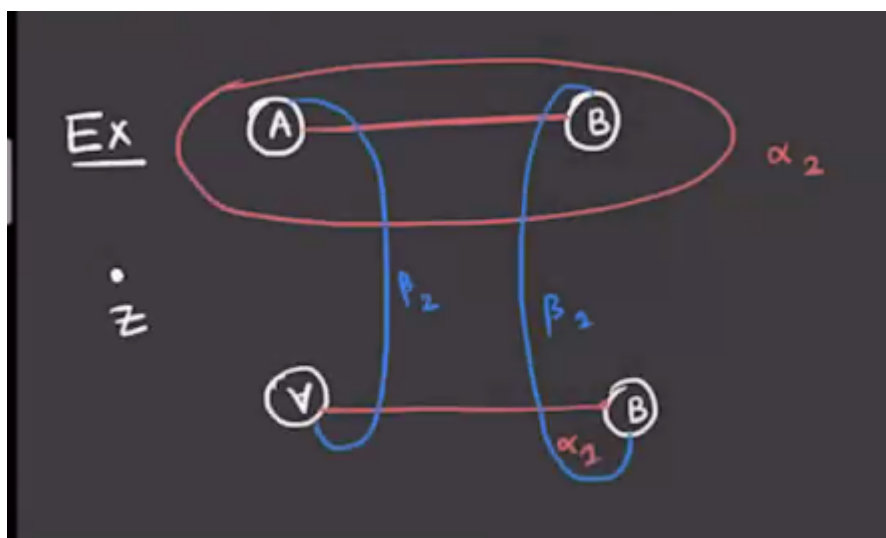
Figure 152: image_2021-03-11-11-37-28

Example 17.0.2*(?):* Drawing this on a surface yields the following:
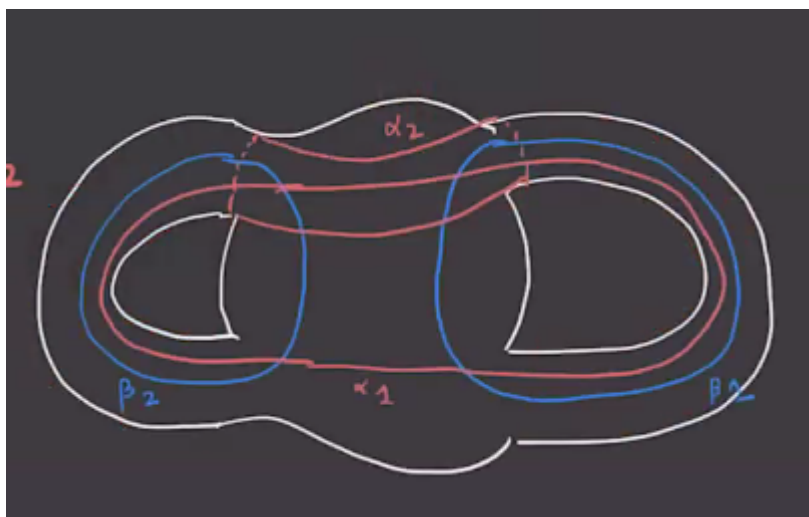
Figure 153: image_2021-03-11-12-01-09

One useful trick here is labeling the points along one curve with letters and the other with numbers. Another is making a table like the following:

Figure 154: image_2021-03-11-12-05-41

From this it's easy to read off the 4 possible generators $\{ae, ce, bf, bd\}$. The regions the contain z can be seen in the latter picture:
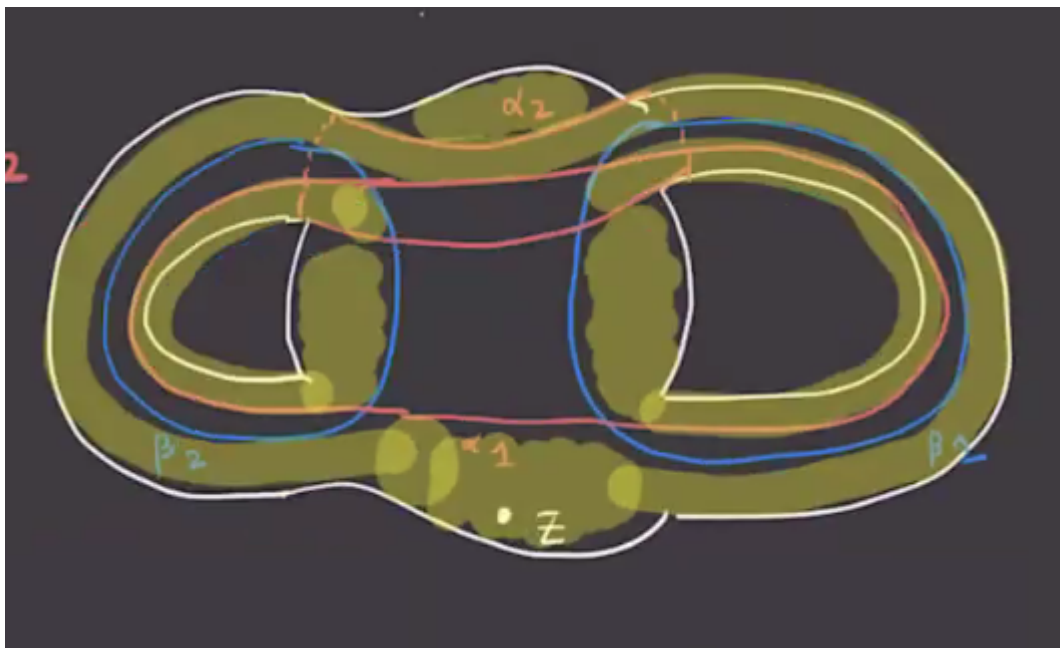
Figure 155: image_2021-03-11-12-07-48

Translating this to the original picture yields these regions:
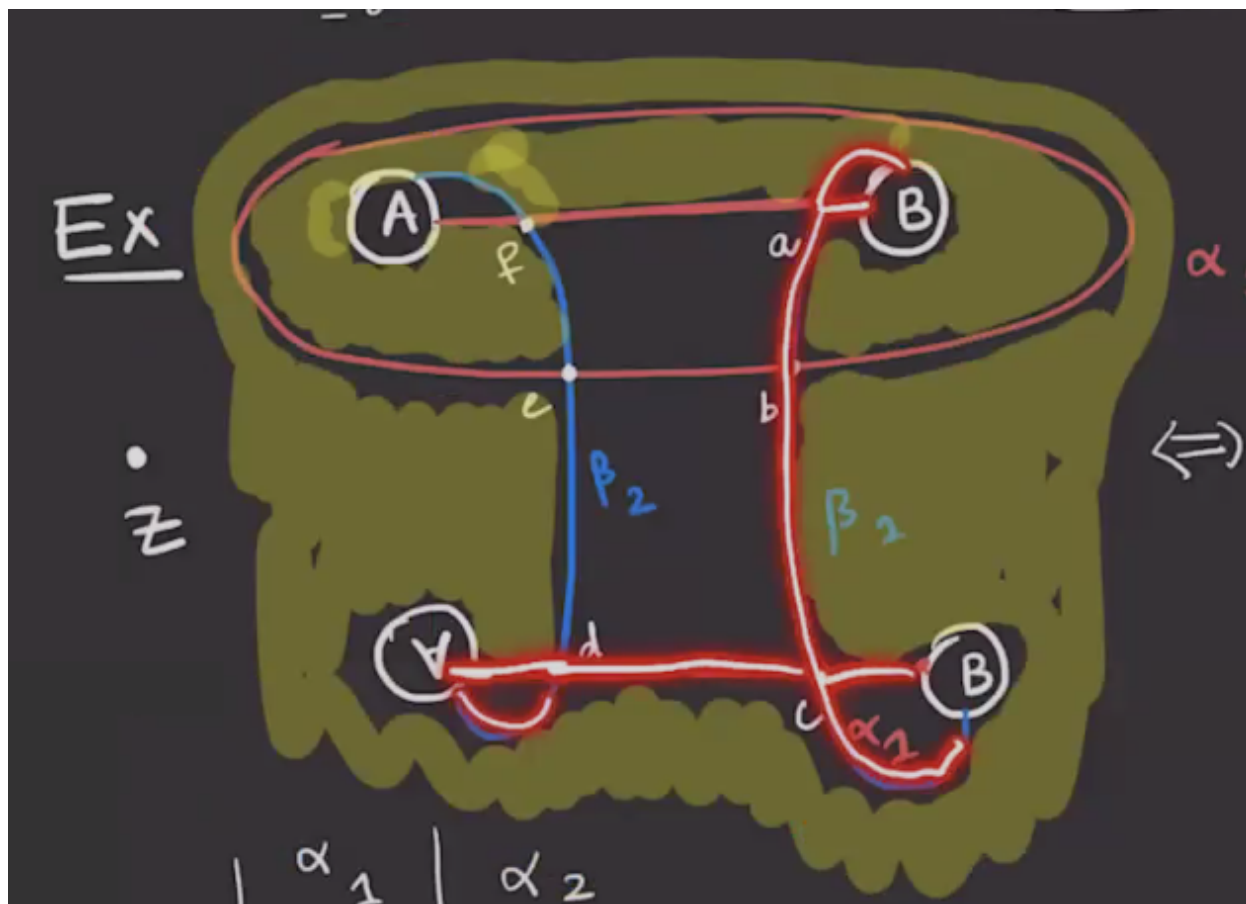
Figure 156: image_2021-03-11-12-09-26

Note that the half-bigons in the diagram actually pair to a bigon on the surface, so consider this simplified drawing of the surface:
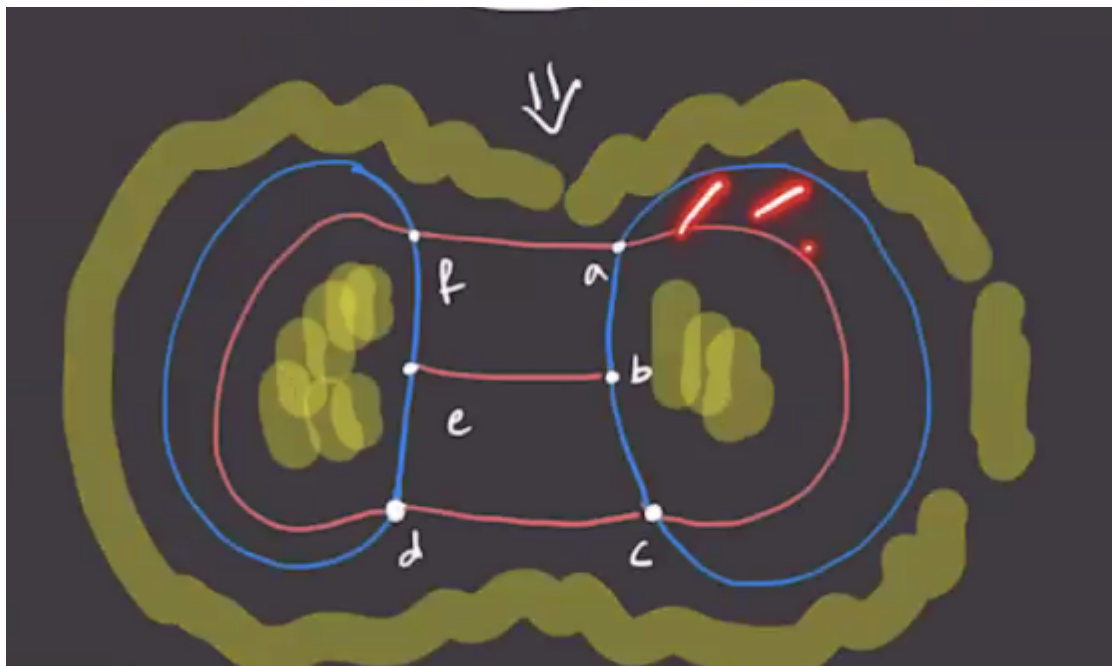
Figure 157: image_2021-03-11-12-11-38

- For the bigon from $a \to c$, we can get $ae \to ce$ using the embedding

$$\mathbb{D} \xrightarrow{u} \Sigma \hookrightarrow \mathrm{Sym}^2(\Sigma).$$

- For the bigon $d \to f$, we get $bd \to bf$.

Setting $D_1 = D(\varphi)$ for $\varphi \in \pi_2(ae, bf)$, we have $\mu(\varphi) = 1$ since we showed that rectangular regions have Maslov index 1. Are there any holomorphic representatives? The claim is that $\#\widehat{\mathcal{M}}(\varphi)$. Checking boundaries yields the following:
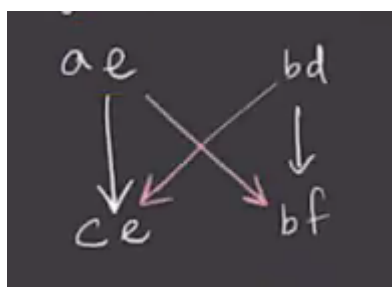
Figure 158: image_2021-03-11-12-19-43

Then

$$\ker \partial = \langle ce, bf \rangle$$
$$\operatorname{im} \partial = \langle ce + bf \rangle$$
$$\implies \widehat{HF}(\Sigma, \alpha, \beta, z) \cong \mathbb{Z}.$$

This is good, since some valid moves will make this into a standard diagram for S^3 (?).

Remark 17.0.3: Recall that given a rectangle, there is a 2-to-1 branched cover:
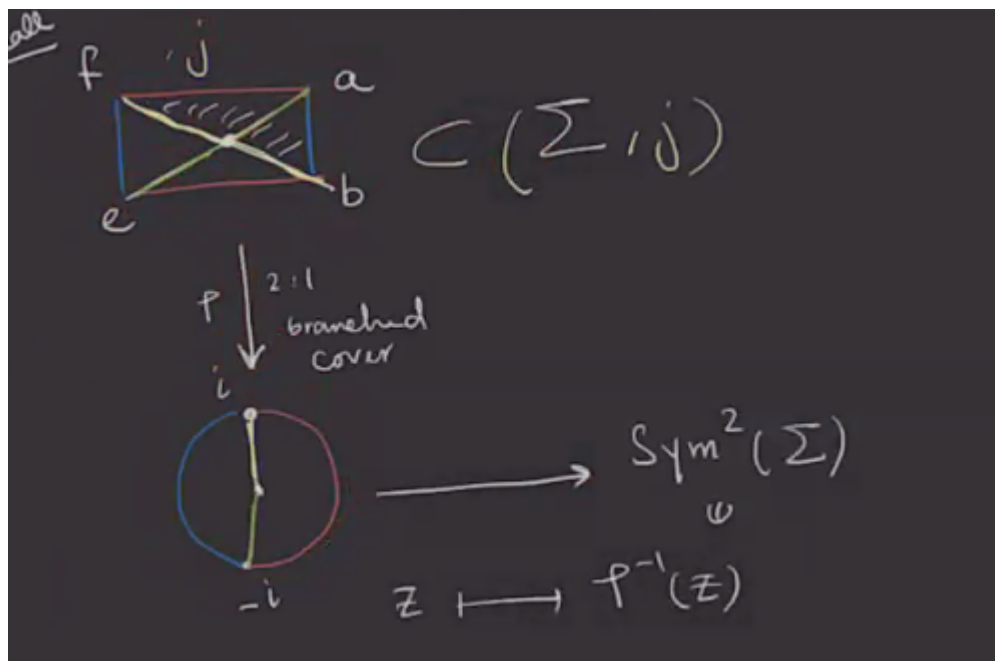
Figure 159: image_2021-03-11-12-25-02

Such branched coverings bijectively correspond to biholomorphic involutions

$$a \rightleftharpoons e$$
$$b \rightleftharpoons f.$$

This is because there is a unique involution exchanging them by the Schwarz lemma, since any pole of the involution must lie along the line connecting points it exchanges, and exchanging each pair of corners in the rectangle forces to pole to be precisely the point in the center of the rectangle. So these correspond got biholomorphic involutions of $\mathbb{D}$ using complex analysis.

Remark 17.0.4: Next week: more about the Maslov index and $\mathrm{Spin}^{\mathbb{C}}$ structures, then invariance under diagram moves.

18 | Maslov Grading and Spin$^{\mathbb{C}}$ Structures (Tuesday, March 16)

Remark 18.0.1: Let $M \in \mathsf{Mfd}^3(\mathbb{R})$ be a closed oriented 3-manifold and $\mathcal{H} = (\Sigma, \alpha, \beta, z)$ a Heegaard diagram for M. Letting b_i be the Betti numbers, note that $b_1 = 0 \iff M \in \mathrm{QHS}^3$ is a rational homology 3-sphere, i.e. $H_i(M; \mathbb{Q}) \cong H_i(S^3; \mathbb{Q})$ for all i. This also implies that $H_2(M; \mathbb{Z}) = 0$. Under this condition, we can define a **relative $\mathbb{Z}$-grading** (i.e. we have a difference of grading between any two elements) on $\widehat{CF}$ in the following way: for x, y two generators, we set

$$\mathsf{gr}\,(x) - \mathsf{gr}\,(y) := \mu(\varphi) - 2n_z(\varphi) \qquad\qquad \text{for some } \varphi \in \pi_2(x, y).$$

Recall that $\mu(-)$ denotes the Maslov index, $n_z(-)$ is the local multiplicity of a Whitney disc at z, and x, y denote tuples of points.

Remark 18.0.2: This involves a choice of disc, so why is it well-defined? We'll also see why we need $M \in \mathrm{QHS}^3$.

> *Proof (of well-definedness).*
> Let $\varphi, \varphi' \in \pi_2(x, y)$. We have
>
> $$\varphi * (-\varphi') \in \pi_2(x, x) = \mathbb{Z} \oplus H_2(M) = \mathbb{Z} \oplus 0,$$
>
> so this is some multiple kS where S is the positive generator of $\pi_2 \,\mathrm{Sym}^g \Sigma$. So
>
> $$\mu(\varphi * (-\varphi')) = \mu(\varphi) - \mu(\varphi') = k\mu(S) = 2k.$$
>
> Similarly,
>
> $$n_z(\varphi * (-\varphi')) = n_z(\varphi) - n_z(\varphi') = kn_z(S) = k,$$
>
> where we've used $\mu(S) = 2, n_z(S) = 1$. Then
>
> $$\mu(\varphi) - \mu(\varphi') = 2(n_z(\varphi) - n_z(\varphi'))$$
> $$\implies \mu(\varphi) - 2n_z(\varphi) = \mu(\varphi') - 2n_z(\varphi').$$
>
> ∎

Remark 18.0.3: Note that the relative grading is only defined if $\pi_2(x, y) \neq \emptyset \iff \varepsilon(x, y) = 0 \in H_1(M; \mathbb{Z})$. This generated an equivalence relation of elements in $\mathbb{T}_\alpha \cap \mathbb{T}_\beta$ by $x \sim y \iff \varepsilon(x, y) = 0$, so we have a decomposition

$$\widehat{CF}(\mathcal{H}) = \bigoplus_? \widehat{CF}(\mathcal{H}, ?).$$

which is preserved by ∂, so $\widehat{HF}(\mathcal{H})$ will split similarly as

$$\widehat{HF}(\mathcal{H}) = \bigoplus_? \widehat{CF}(\mathcal{H}, ?).$$

It turns out that the right thing to replace the "?" with will be Spin$^{\mathbb{C}}$ structures.

18.1 Spin$^{\mathbb{C}}$ Structures

Remark 18.1.1: We'll discuss Turaev's (?) reformulation of Spin$^{\mathbb{C}}$ structure for Mfd^3. Note that $\chi(M) = 0$, so there exists nowhere vanishing vector fields on M by Poincaré-Hopf.

Definition 18.1.2 (?)
Let v_1, v_2 be nowhere vanishing vector fields on M. We say

$$v_1 \sim v_2 \iff v_1|_{M \setminus B} \simeq v_2|_{M \setminus B},$$

i.e. their restrictions to $M \setminus B$ are homotopic, and here B is a 3-ball in M. Equivalently, $v_1 \sim v_2 \iff v_1, v_2$ are homotopic in the complement of finitely many 3-balls in M.

Definition 18.1.3 (Spin$^{\mathbb{C}}$ Structures)

$$\text{Spin}^{\mathbb{C}}(M) \coloneqq \{\text{Nowhere vanishing vector fields on } M\}_{/\sim}.$$

Definition 18.1.4 (?)
Let $\mathcal{H} = (\Sigma, \alpha, \beta, z)$ be a Heegard diagram for M, then define a map

$$S_z : \mathbb{T}_\alpha \cap \mathbb{T}_\beta \to \text{Spin}^{\mathbb{C}}(M).$$

Step 1: Choose a self-indexing Morse function f with $\# \text{Crit}^0(f) = \# \text{Crit}^3(f) = 1$ such that its corresponding Heegaard diagram is $\mathcal{H}$:
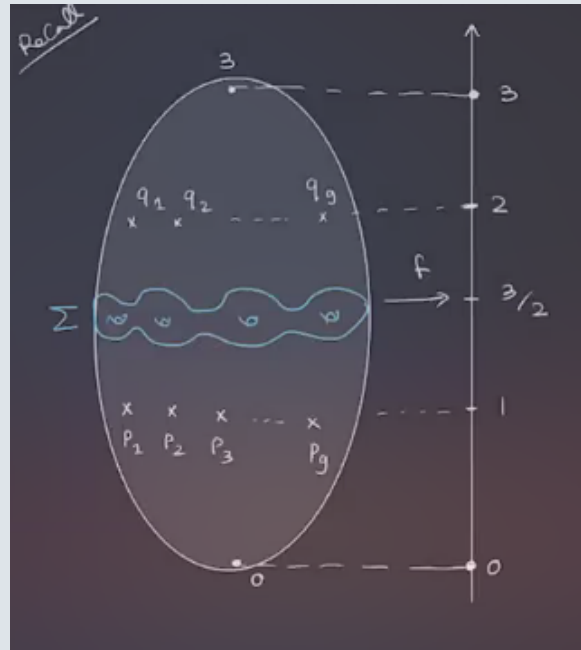
Figure 160: image_2021-03-16-11-47-19

Note that we have a surface in $f^{-1}(3/2)$ and there are exactly q critical points along each of $f^{-1}(1), f^{-1}(2)$. For each $x = \{x_1, x_2, \cdots, x_g\} \cap \mathbb{T}_\alpha \cap \mathbb{T}_\beta$, we have $x_i \in \alpha_i \cap \beta_{\sigma(i)}$ for some permutation $\sigma \in S_g$ Then $\alpha \mapsto p_i$ and $\beta_{\sigma(i)} \mapsto q_{\sigma(i)}$:
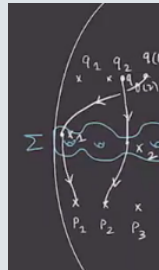
Figure 161: image_2021-03-16-11-49-42

Trajectories of $-\nabla f$ that pass through $x_1, x_2, \cdots, x_g$ are g pairwise disjoint arcs connecting $q_1, q_2, \cdots, q_g$ to $p_1, p_2, \cdots, p_g$, so there is a one-to-one correspondence between these intersection points.

Now taking tubular neighborhoods of the $g+1$ disjoint arcs yields $g+1$ pairwise disjoint 3-balls in M, so write this as $B := B_1 \coprod \cdots \coprod B_{g+1}$.
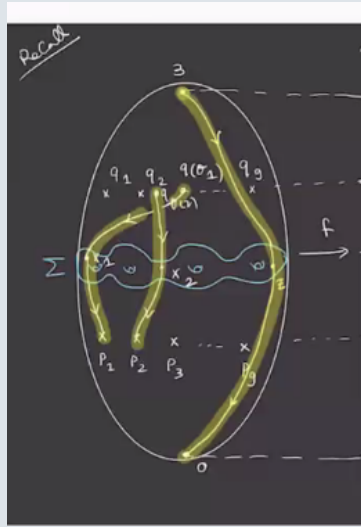
Figure 162: image_2021-03-16-11-53-04

Note that

- $-\nabla f$ does not vanish in $M \setminus B$.

- $-\nabla f$ can be extended to a nowhere vanishing vector field on M

> **Exercise 18.1.5** (?)
> Show this!
> *Hint: the trajectories of $-\nabla f$ in each ball connect critical points of different parities, and so each $-\nabla f|_{\partial B_i}$ has index zero.*

Define $S_z(x) \in \mathrm{Spin}^{\mathbb{C}}(M)$ to be the equivalence class represented by this vector field. This is well-defined since outside of the finitely many balls, this vector field is just equal to $-\nabla f$.

> **Exercise 18.1.6** (?)
> Show that this does not depend on which Morse function is chosen.

> **Proposition 18.1.7***(?).*
> There is a one-to-one correspondence
>
> $$\mathrm{Spin}^{\mathbb{C}}(M) \rightleftharpoons H^2(M; \mathbb{Z}).$$
>
> Picking a trivialization $\tau : TM \to M \times \mathbb{R}^3$ and a Riemannian metric on M, then
>
> $$\left\{ \substack{\text{Nowhere vanishing vector fields} \\ \text{on } M} \right\} \rightleftharpoons \left\{ \text{functions } f : M \to S^2 \right\}$$
>
> $$v : M \to \mathbb{R}^3 \setminus \{0\} \mapsto x \xrightarrow{f_v} \widehat{\mathbf{v}_x}$$

Definition 18.1.8 (?)
Let $\alpha \in H^2(S^2; \mathbb{Z})$ be the positive generator, then define

$$\delta^\tau(v) := f_v^*(\alpha) \in H^2(M; \mathbb{Z}).$$

Note that if $v_1 \sim v_2$, we have $\delta^\tau(v_1) = \delta^\tau(v_2)$ since they are homotopic on the complement of a ball:

$$M \setminus B \overset{i}{\hookrightarrow} M \overset{f_v}{\longrightarrow} S^2.$$

Conclude that

$$(f_{v_1} \circ i)^*(\alpha) = (f_{v_2} \circ i)^*(\alpha),$$

i^* is an isomorphism, so $f_{v_1}^*(\alpha) = f_{v_2}^*(\alpha)$, yielding the identification.

Exercise 18.1.9 (?)

1. Show that δ^τ is a bijection.

2. $\delta(v_1, v_2) := \delta^\tau(v_1) - \delta^\tau(v_2) \in H^2(M; \mathbb{Z})$ is well-defined and independent of the choice of τ, and satisfies

$$\delta(v_1, v_2) + \delta(v_2, v_3) = \delta(v_1, v_3).$$

Thus we also have a relative map

$$\mathrm{Spin}^{\mathbb{C}}(M) \rightleftharpoons H^2(M; \mathbb{Z})$$
$$s_1, s_2 := [v_1] - [v_2] \mapsto s_1 - s_2 := \delta(v_1, v_2).$$

19 | **Thursday, March 18**

19.1 $\mathrm{Spin}^{\mathbb{C}}$ **Structures and Invariance**

Remark 19.1.1: Recall that given a Heegard diagram $(\Sigma, \alpha, \beta, z)$ gives an equivalence relation

$$x \sim y \iff \varepsilon(x, y) = 0 \in H_1(M) \overset{\mathrm{PD}}{=} H^2(M).$$

This yields a decomposition of $\widehat{\mathrm{HF}}$ into a direct sum over equivalence classes of subcomplexes defined by $\mathrm{Spin}^{\mathbb{C}}$ structures. Note that the differential will preserve each direct summand. We defined $\mathrm{Spin}^{\mathbb{C}}(M)$ as the set of nowhere vanishing vector fields on M modulo being homotopic outside finitely many 3-balls in M. We had a map

$$\mathbb{T}_\alpha \cap \mathbb{T}_\beta \overset{s_z}{\longrightarrow} \mathrm{Spin}^{\mathbb{C}}(M),$$

recalling that the left-hand side are the generators of $\widehat{\mathrm{HF}}$. We took a self-indexing Morse function on M, took the inverse image of $3/2$ to get the Heegard surface, and each intersection point x_i gave a flow line from an index 2 critical point to an index 1 critical point passing through x_i:
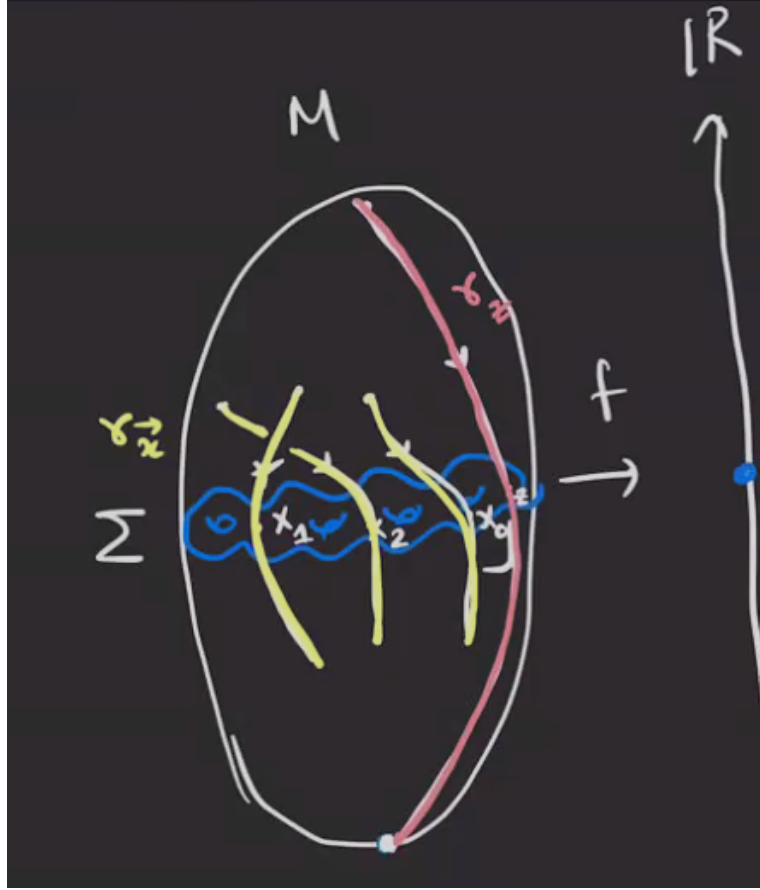
Figure 163: Trajectories of negative gradient flow

We proceeded by cancelling adjacent flow lines (at the level of vector fields), and then modifying γ_z (the flow line passing through the basepoint z connecting the index 0 to the index 3) to get a nowhere vanishing vector field. We then took a trivialization $\tau : TM \to M \times \mathbb{R}^3$ defined a map

$$\mathrm{Spin}^{\mathbb{C}}(M) \xrightarrow{\gamma^{\tau}} H^2(M)$$
$$s = [v] \mapsto f_v^*(\alpha).$$

where α is the volume form of S^2 and

$$f_v : M \to S^2$$
$$x \mapsto \widehat{v_x} := \frac{v_x}{\|v_x\|}.$$

Note that δ^{τ} a priori depends on τ, but

$$\delta(s_1, s_2) = \delta^{\tau}(s_1) - \delta^{\tau}(s_2) \in H^2(M),$$

and the difference is independent of τ.

> **Lemma 19.1.2*(?).***
> For $x, y \in \mathbb{T}_\alpha \cap \mathbb{T}_\beta$, defining $s_1 - s_2 = \delta(s_1, s_2) \in H^2(M)$, we have
>
> $$s_z(y) - s_z(x) = \mathrm{PD}[\varepsilon(x, y)].$$
>
> As corollaries,
>
> 1. If $x \sim y$ then $s_z(y) = s_z(x)$, and
> 2. If $x \not\sim y$ then the above equation holds.

> **Exercise 19.1.3** (?)
> Prove this!
> *Hint, take the Poincaré dual of the link below to get the formula:*
>
> $$s_z(y) - s_z(x) = \mathrm{PD}[\gamma_y \cup (-\gamma_x)].$$
>
> *This implies that the two vector fields are equal everywhere outside of a tubular neighborhood of the link. Then show that $[\gamma_x \cup (-\gamma_x)] = [\varepsilon(x, y)]$.*

Remark 19.1.4: We thus have

$$\widehat{\mathrm{HF}}(\Sigma, \alpha, \beta, z) = \bigoplus_{\mathfrak{s} \in \mathrm{Spin}^{\mathbb{C}}(M)} \widehat{\mathrm{HF}}(\Sigma, \alpha, \beta, z, \mathfrak{s}).$$

Remark 19.1.5: We have several properties of $\mathrm{Spin}^{\mathbb{C}}$ structures. There is a map

$$J : \mathrm{Spin}^{\mathbb{C}}(M) \to \mathrm{Spin}^{\mathbb{C}}(M)$$
$$s = [v] \mapsto \overline{s} := [-v].$$

There is also a first Chern class

$$c_1 : \mathrm{Spin}^{\mathbb{C}}(M) \to H^2(M)$$
$$s \mapsto s - \overline{s},$$

i.e. $c_1(s) = \delta(s, \overline{s})$.

> **Theorem 19.1.6*(Topological Invariance).***
> The association
>
> $$(\Sigma, \alpha, \beta, z), J \rightsquigarrow \widehat{\mathrm{HF}}(\Sigma, \alpha, \beta, z)$$
>
> does not depend on the choice of Heegard diagram or the almost complex structure J, so this yields a well-defined invariant of M which we'll denote $\widehat{\mathrm{HF}}(M)$ for $M \in \mathsf{Mfd}^3(\mathbb{R})$.

Remark 19.1.7: There are few things to discuss:

1. The almost complex structure J:

2. Isotopies

3. Handle slides

4. Stabilization

Remarks on these:

1. This involves a standard argument from Lagrangian Floer homology.
2. There are two cases:

   - If the isotopy doesn't create a new intersection, we have a 1-to-1 correspondence between generators for any two choices, and changing J to J' will give a correspondence between the differentials. This just involves picking a diffeomorphism that maps α circles to α' circles, and so on. So this reduces to showing 1.
   - If is *does* create new intersection points, there are again standard arguments in Lagrangian Floer homology for this.

3. This involves the following situation, which induces a map
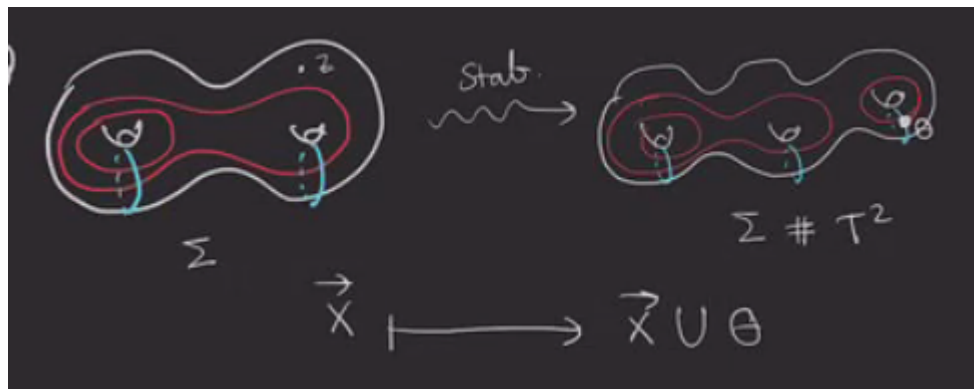
Figure 164: image__2021-03-18-11-51-38

For an appropriate choice of J on $\Sigma \# T^2$, the map f above will induce a chain homotopy equivalence

$$\tilde{f} : \widehat{\mathrm{HF}}(\Sigma, \alpha, \beta, z) \xrightarrow{\sim} \widehat{\mathrm{HF}}(\Sigma \# T^2, \alpha', \beta', z).$$

4. What's the picture?
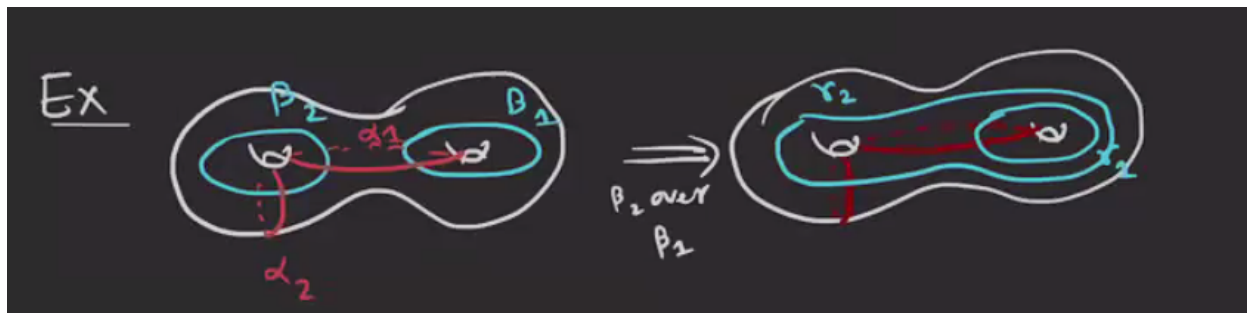
Figure 165: image_2021-03-18-11-56-59

This will yield a map

$$(\Sigma, \alpha, \beta, z) \rightsquigarrow (\Sigma, \alpha, \gamma, z).$$

For $i = 1, \cdots, g-1$, we'll have γ_i isotopic to β_i, and for $i = g$, γ_g is obtained by sliding β_g over β_{g-1}. We'll combine these into the same diagram with different colors to compare them, yielding a **Heegard triple**:

$$(\Sigma, \alpha, \beta, \gamma, z).$$

We can think of this as three separate diagrams:

$$(\Sigma, \alpha, \beta, z) \rightsquigarrow M$$
$$(\Sigma, \beta, \gamma, z) \rightsquigarrow ?$$
$$(\Sigma, \alpha, \gamma, z) \rightsquigarrow M.$$

What does the middle one represent?

Figure 166: Heegard diagram

Here this is a diagram for $(S^1 \times S^2)^{\# 2}$.

Note that we draw γ_i such that it intersects β_i in two transverse intersection points to make sure the diagram is admissible.

Remark 19.1.8: Give a Heegard triple $(\Sigma, \alpha, \beta, \gamma, z$, pick three intersection points

$$x \in \mathbb{T}_\alpha \cap \mathbb{T}_\beta$$
$$y \in \mathbb{T}_\beta \cap \mathbb{T}_\gamma$$
$$w \in \mathbb{T}_\gamma \cap \mathbb{T}_\alpha.$$

We can use **Whitney triangles** to connect x, y, w:
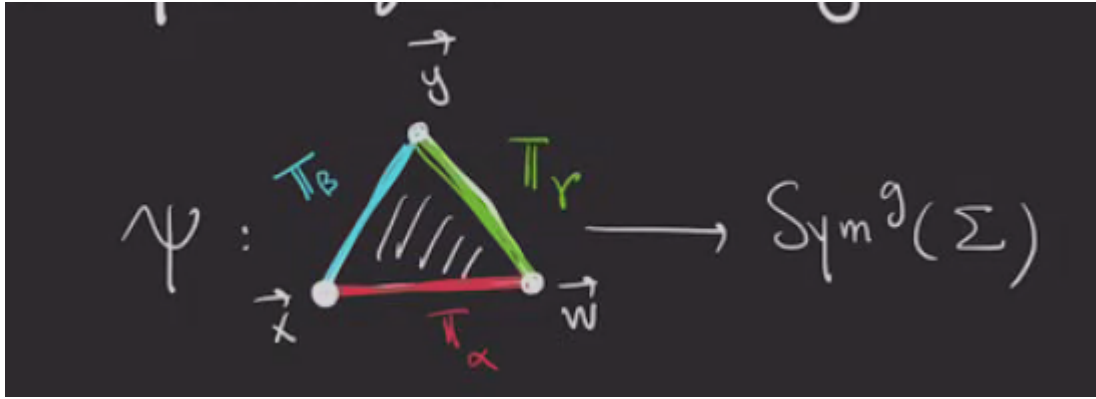
Figure 167: image_2021-03-18-12-23-07

We then define $\pi_2(x, y, z)$ to be the homotopy class of Whitney triangles connecting x, y, w. We can similarly define $\mathcal{M}(\psi)$ to be the moduli space of J-holomorphic representatives of $\psi \in \pi_2(x, y, w)$, along with a chain map

$$f_{\alpha\beta\gamma} : \widehat{\mathrm{HF}}(\Sigma, \alpha, \beta, z) \otimes \widehat{\mathrm{HF}}(\Sigma, \beta, \gamma z) \to \widehat{\mathrm{HF}}(\Sigma, \alpha, \gamma, z)$$
$$x \otimes y \mapsto \sum_{w \in \mathbb{T}_\alpha \cap \mathbb{T}_\beta} \sum_{\substack{\psi \in \pi_2(x,y,w) \\ \mu(\psi)=0 \\ n_z(\psi)=0}} \#\mathcal{M}(\psi) \cdot w.$$

> **Theorem 19.1.9*(?)*.**
> $f_{\alpha\beta\gamma}$ is a chain map.

Remark 19.1.10: Next time: we'll show how to get a chain homotopy equivalence from the first tensor term above to the codomain. We'll also see surgery exact triangles.

20 | **Thursday, March 25**

Remark 20.0.1: Recall that we have several variants: namely $\widehat{\mathrm{HF}}, \mathrm{HF}^-, \mathrm{HF}^+, \mathrm{HF}^\infty$. Let $M \in \mathsf{Mfd}^3$ and take a Heegard diagram $(\Sigma, \alpha, \beta, z)$. Note that $\mathrm{HF}^-(\Sigma, \alpha, \beta, z)$ is the free $\mathbb{Z}/2[u]$-module generated by $\mathbb{T}_\alpha \cap \mathbb{T}_\beta$ with differential given by ?.

Missing some stuff.

> **Definition 20.0.2** (Nice Diagrams)
> A Heegaard diagram is called **nice** if every connected component of $\Sigma \setminus \alpha \cup \beta$ that does not contain z is either a bigon or a rectangle.

Remark 20.0.3: For nice Heegaard diagrams, the Maslov index 1 holomorphic discs with $n_z(\varphi) = 0$ are embedded bigons and rectangles.

> **Lemma 20.0.4***(?).*
> Any 3-manifold has a nice Heegaard diagram, so computing $\widehat{\mathrm{HF}}$ is combinatorial.

Remark 20.0.5: Some properties:

1. $\mathrm{Spin}^{\mathbb{C}}$ structures: we have a decomposition

$$\mathrm{HF}^-(M) = \bigoplus_{s \in \mathrm{Spin}^{\mathbb{C}}(M)} \mathrm{HF}^-(M, s)$$

    which induces

$$\mathrm{HF}^{\star}(M) = \bigoplus_{s \in \mathrm{Spin}^{\mathbb{C}}(M)} \mathrm{HF}^{\star}(M, s)$$

    where $\star = +, -, \infty$.

2. Maslov grading: For a QHS^3, $\mathrm{HF}^-(M)$ is relatively $\mathbb{Z}$-graded. The degree of u is -2, and this grading can be lifted to an absolute $\mathbb{Q}$-grading.

3. There is a SES

$$0 \to \mathrm{HF}^-(M, s) \xrightarrow{\cdot u} \mathrm{HF}^-(M, s) \to \widehat{\mathrm{HF}}(M, s) \to 0.$$

This yields an exact triangle

$$
\begin{array}{ccc}
\mathrm{HF}^-(M, s) & \xrightarrow{\;\;\;\;\cdot u\;\;\;\;} & \mathrm{HF}^-(M, s) \\
& \searrow \qquad \swarrow & \\
& \widehat{\mathrm{HF}}(M, s) &
\end{array}
$$

Link to Diagram

4. There is a short exact sequence

$$0 \to \mathrm{HF}^-(M) \to \mathrm{HF}^\infty(M) \to \mathrm{HF}^+(M) \to 0.$$

yielding an exact triangle

5. $\mathbb{Z}/2[u]$ is a PID, so by the structure theorem, any module over it will decompose and we have

$$\mathrm{HF}^-(M,s) = \bigoplus_i \mathbb{Z}/2[u] \oplus \bigoplus_j \frac{\mathbb{Z}/2[u]}{\langle u^{n_j} \rangle}.$$

Supposing that $M \in \mathrm{QHS}^3$, then by Osvath-Szabo, for any $s \in \mathrm{Spin}^{\mathbb{C}}(M)$ there is exactly one free summand. Let d be the Maslov grading of the free generator, and c_j be the grading of the torsion part. We write the u-torsion part as $\mathrm{HF}_{\mathrm{red}}(M,s)$.

> **Definition 20.0.6** (d-invariant)
> The Maslov grading of the free summand $d = d(M,s)$ is referred to as the d-**invariant** or correction term, and
> $$d(M,s) = \max \left\{ \mathsf{gr}\,(\alpha) \ \middle| \ \alpha \in \mathrm{HF}^-(M,s),\ u^n \alpha \neq 0 \forall n \right\}.$$

> **Definition 20.0.7** (Rational Homology Cobordism Group)
> The **rational homology cobordism group** is denoted
> $$\left(\Theta^3_{\mathbb{Q}} := \left\{ M \in \mathrm{QHS}^3 \right\} / \sim, \# \right)$$
> where $M_1 \sim M_2$ if and only if they are *rationally homology cobordant*, i.e.
>
> 1. There exists an $W \in \mathsf{Mfd}^4$ (connected, oriented) such that $\partial W = -M_1 \coprod M_2$, i.e. W is a cobordism from M_1 to M_2.
>
> 2. $H_i(W; \mathbb{Q}) = 0$ for $i = 1, 2$, so W is a rational homology cylinder.

Remark 20.0.8: Note that this is only a monoid without the equivalence relation, but this equivalence creates inverses.

> **Definition 20.0.9** (?)
> Define the *d*-**invariant** of M as
> $$d(M) = \sum_{s \in \mathrm{Spin}^{\mathbb{C}}(M)} d(M, s).$$

Remark 20.0.10: This induces a homomorphism

$$d : \Theta^3_{\mathbb{Q}} \to \mathbb{Q}.$$

21 | **Tuesday, March 30**

21.1 *L*-spaces

Missing lecture

Remark 21.1.1: Today: *L*-spaces and the surgery exact triangle. We've been loosely following [**OS-1**], references for upcoming topics include [**OS-2**] and Jen Hom's survey [**H**].

Remark 21.1.2: Recall that we were discussing $\mathrm{HF}^-(M, s)$ for $M \in \mathsf{Mfd}^3(\mathbb{R})$ and s a $\mathrm{Spin}^{\mathbb{C}}$ structure, and if $M \in \mathrm{QHS}$ this decomposes as $\mathbb{Z}/2[u] \oplus \left(\bigoplus_i \dfrac{\mathbb{Z}/2[u]}{\langle un_i \rangle} \right) := \mathbb{Z}/2[u] \oplus \mathrm{HF}_{\mathrm{red}}(M, s)$. The Maslov grading of 1 in the first summand is the *d*-**invariant**, $d(M, s)$. If one defines $d(M) := \sum_{s \in \mathrm{Spin}^{\mathbb{C}}(M)} d(M, s)$, then $d : \Theta^3_{\mathbb{Q}} \to \mathbb{Q}$ is a group homomorphism. We want to talk about $X \in \mathsf{Mfd}^3$ which have the "simplest" Floer theory, in the sense that the torsion summand above vanishes.

> **Definition 21.1.3** (?)
> A manifold $M \in \mathrm{QHS}^3$ is an *L*-**space** if $\mathrm{HF}_{\mathrm{red}}(M, s) = 0$, which happens if and only if $\mathrm{HF}^-(M, s) = \mathbb{Z}/2[u]$.

Remark 21.1.4: Recall that there is an exact triangle

$$\mathrm{HF}^-(M, s) \xleftarrow{\quad \cdot u \quad} \mathrm{HF}^-(M, s)$$

with maps 0 and p to $\widehat{\mathrm{HF}} - (M, s)$.

Since multiplication by u is injective, we obtain

$$\widehat{\mathrm{HF}} = \operatorname{im} p \cong \frac{\mathrm{HF}^-(M,s)}{\ker p} \cong \frac{\mathbb{Z}/2[u]}{u\mathbb{Z}/2[u]} \cong \mathbb{Z}/2.$$

> **Exercise 21.1.5** (?)
> So $\mathrm{HF}^-(M,s) \cong \mathbb{Z}/2[u] \implies \widehat{\mathrm{HF}}(M,s) \cong \mathbb{Z}/2$. Show the converse is also true.

> **Corollary 21.1.6***(?)*.
> M is an L-space if and only if $\widehat{\mathrm{HF}}(M,s) \cong \mathbb{Z}/2$ for all $s \in \mathrm{Spin}^{\mathbb{C}}(M)$. This happens if and
> only if $\mathrm{rank}_{\mathbb{Z}[u]}\widehat{\mathrm{HF}}(M,s) = 1$, if and only if $\#\mathrm{Spin}^{\mathbb{C}}(M) = \#H^2(M) \overset{\mathrm{PD}}{=} \#H^1(M)$, which is
> finite for QHS.

> **Corollary 21.1.7***(?)*.
> Any $M \in \mathrm{QHS}^3$ is an L-space if and only if $\mathrm{rank}_{\mathbb{Z}[u]}\widehat{\mathrm{HF}}(M) = \#H^1(M)$.

Remark 21.1.8: Note that we've proved the forward implication but not the reverse. This is sometimes used as a definition in talks!

Sketch of the proof ($\impliedby$): A computation will show that $\chi\widehat{\mathrm{HF}}(M,s) = \pm 1$ for all s, since the grading can be shifted. This is proved in [**OS-2**], and is the main ingredient in this proof. This implies that $\mathrm{rank}\widehat{\mathrm{HF}}(M,s) \geq 1$, and so adding all summands yields $\mathrm{rank}\widehat{\mathrm{HF}}(M) \geq \#H_1(M)$. This implies that $\widehat{\mathrm{HF}}(M,s) \cong \mathbb{Z}/2$ for all s, making M an L-space.

Remark 21.1.9: Here note that C_* is $\mathbb{Z}/2$-graded, as is $(\widehat{\mathrm{HF}}(M), \partial)$, so we define $\chi(C_*) = \mathrm{rank}C_0 - \mathrm{rank}C_1$. Since we have a relative $\mathbb{Z}$-grading given by μ, we get a relative $\mathbb{Z}/2$-grading given by $\mathsf{gr}_{\mathbb{Z}/2}(x,y) = \mathsf{gr}_{\mathbb{Z}}(x,y)$, which gives us $\chi\widehat{\mathrm{HF}}(M)$ up to sign.

Example 21.1.10*(?):* We have seen lens spaces, here's an example of $L(2,3)$:
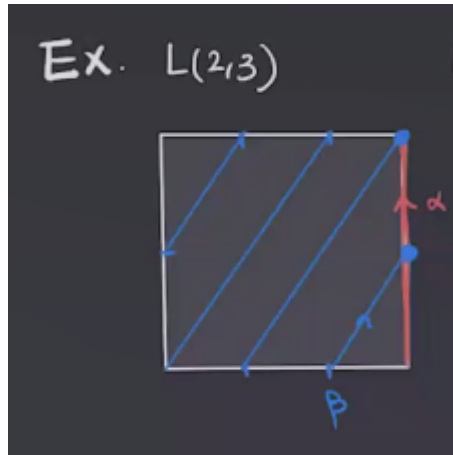
Figure 168: image_2021-03-30-11-46-39

Here $\widehat{\mathrm{HF}}L(2,3) \cong (\mathbb{Z}/2)^{\oplus 2}$ and $\mathrm{rank}\widehat{\mathrm{HF}}L(2,3) = 2 = \#H_1(L(2,3);\mathbb{Z}/2)$.

Example 21.1.11 *(?):* In general, every $L(p,q)$ is a lens space, hence the name! Note that $H_1(L(p,q)) \cong \mathbb{Z}/p$ is not a ZHS^3.

Example 21.1.12 *(?):* A Poincaré homology sphere $\pm P^3$ (with either the standard orientation or its reverse) will be an L-space.

> **Conjecture 21.1.13.**
> Poincaré-type conjecture in Heegard Floer homology: the only irreducible ZHS^3 L-spaces are S^3 and $\pm P^3$. Still open!

Remark 21.1.14: So $\widehat{\mathrm{HF}}$ can detect these two among all integral homology spheres using $\widehat{\mathrm{HF}}$.

21.2 Surgery

> **Definition 21.2.1** (Dehn Surgery)
> Let $K \subseteq M \in \mathsf{Mfd}^3$ be a knot, i.e. the image of an embedding $S^1 \hookrightarrow M$. Remove a tubular neighborhood of K, and set $X = M \setminus \nu(K)$. Fill in the torus boundary with a solid torus $S^1 \times \mathbb{D}^2$ using a diffeomorphism
>
> $$\varphi : \partial(S^1 \times \mathbb{D}^2) \xrightarrow{\text{diffeo}} \partial X.$$
>
> Any surgery will be determined by the image of the red circle $\gamma := \mathrm{pt} \times \partial\mathbb{D}^2$ in the following:
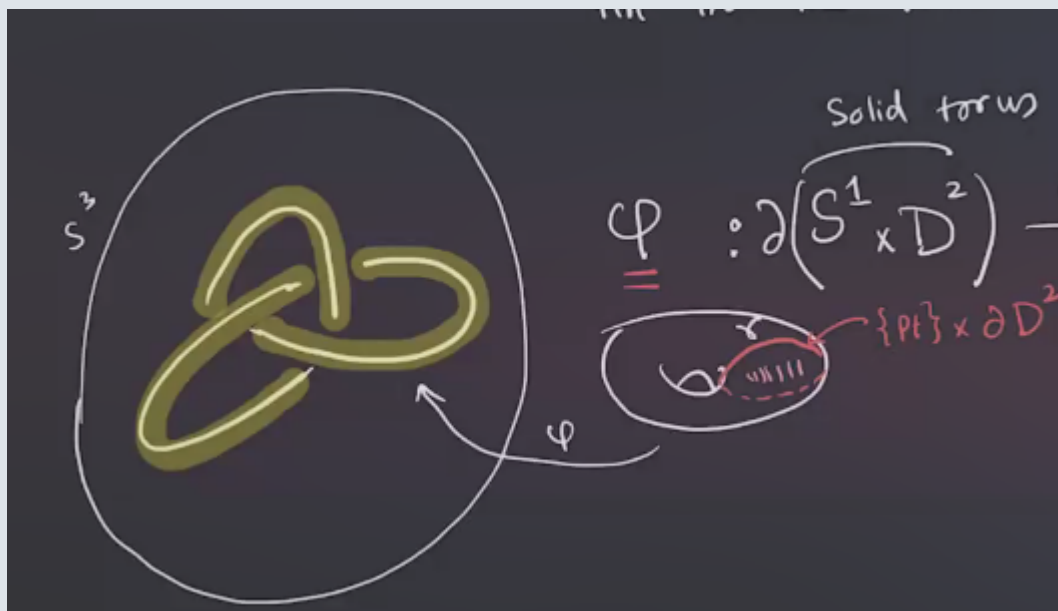
Figure 169: image_2021-03-30-12-01-24

So φ is determined by $\varphi(\gamma)$, and in fact only depends on its class in homology since $\pi_1 T^2 = H_1 T^2$. If $\varphi(\gamma) = \lambda$, we denote the resulting manifold as $M_\lambda(K)$, the **Dehn surgery on** K.

Definition 21.2.2 (Meridian and Longitude)

A **meridian** μ of K will be a simple closed curve on ∂X that bounds a disk in the tubular neighborhood $\nu(K)$:
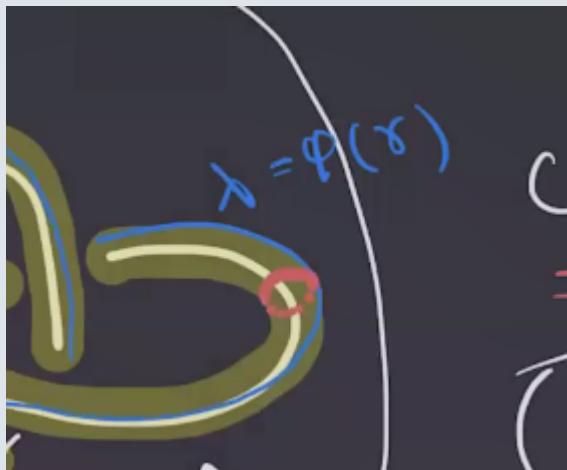
Figure 170: image_2021-03-30-12-05-02

Here we orient μ on the boundary of this disk.

A **longitude** will be a nullhomotopic simple closed curve such that $\#(\mu \cap \lambda) = -1$. For example:

?
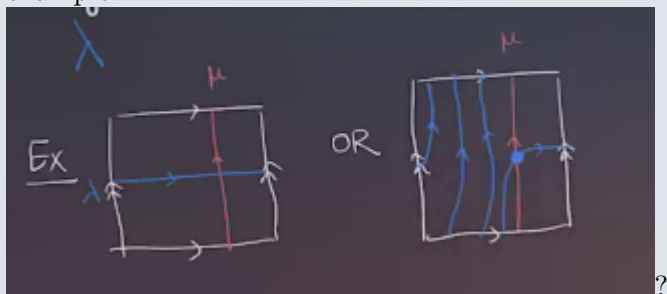
Observation 21.2.3

- λ is not unique, i.e. $\lambda + n\mu$ will again be a longitude for all $n \in \mathbb{Z}$.

- μ, λ is a basis for $H_1(\partial X)$, so any simple closed curve γ is a $\mathbb{Z}$-linear combination of them:

$$[\gamma] = a[\mu] + b[\lambda], \qquad\qquad a, b \in \mathbb{Z}.$$

Definition 21.2.4 (?)

A knot K along with a choice of longitude λ is called a **framed knot**.

Remark 21.2.5: This allows us to specify Dehn surgeries by a rational number.

> **Definition 21.2.6** (?)
> Let K be a framed knot, then $M_{\frac{p}{q}}(K) = M_\gamma(K)$ where $[\gamma] = p[\mu] + q[\lambda]$. We'll use the notation $\gamma = p\mu + q\lambda$.

> **Definition 21.2.7** (?)
> If K is nullhomologous, for example when $M = S^3$ since $H^1 S^3 = 0$, there is a canonical choice for λ by assuming that
>
> - λ is nullhomologous in $X = M \setminus \nu(K)$
> - Equivalently, $\mathrm{lk}(K, \lambda) = 0$.
>
> This longitude is called the **Seifert framing**.

> **Exercise 21.2.8** (?)
> Show this equivalence, and find the Seifert framing for the trefoil in S^3.

Example 21.2.9*(?):*   • $S^3_{p/q}(U) = L(p, q)$ for U the unknot.
- $S^3_\infty(K) := S^3_{\frac{1}{0}}(K) = S^3$.
- $S^3_0 := S^3_{\frac{0}{1}} = S^1 \times S^2$
- $S^3_{+1}(T_{2,3}) = P^3$ (torus knot).

> **Theorem 21.2.10***(Gordan-Leuke, '80s).*
> IF $K \neq U$ and $\dfrac{p}{q} \neq \infty$, then $S^3_{\frac{p}{q}}(K) \neq S^3$.

Remark 21.2.11: Can we get everything 3-manifold this way, as surgery on a knot? The answer is no, but yes if you allow *links*!

> **Theorem 21.2.12***(Lickorish-Wallace).*
> There is a bijection
>
> $$\left\{ M \in \mathsf{Mfd}^3 \;\middle|\; \text{closed, oriented, connected} \right\} \rightleftharpoons \left\{ \text{Integer } \pm 1 \text{ surgeries on links in } S^3 \right\}$$

22 | **Tuesday, April 06**

22.1 Surgery Exact Triangle

Definition 22.1.1 (Surgery on a Knot)
Recall that for $K \subseteq M^3$ a knot, surgery on K involves the following: take a tubular neighborhood of K, $\mathrm{nd}(K)$, and set $X := M \setminus \mathrm{nd}(K)$, whose boundary is a solid torus $S^1 \times \mathbb{D}^2$:
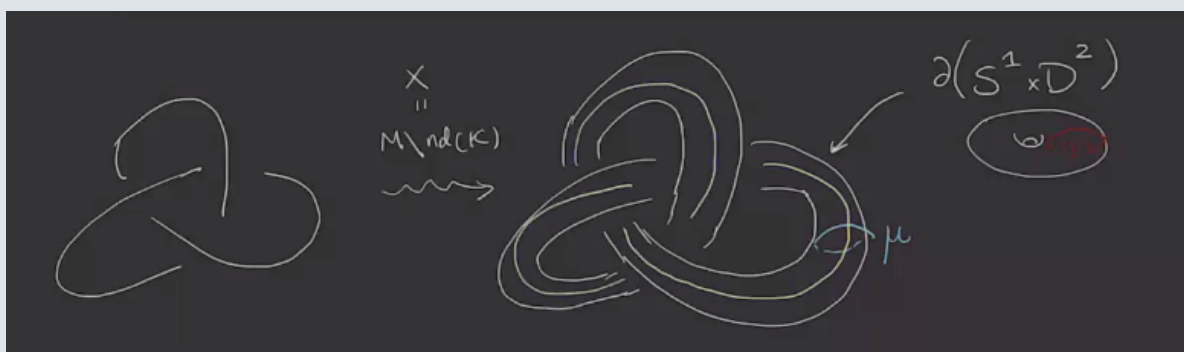
Figure 171: image_2021-04-06-11-18-17

Take a basis for its homology:

- μ to be a meridian of K, which bounds a disc in M^3.
- λ to be a meridian of K with $\#(\mu \cap \lambda) = -1$. Note that there are many choices, we can wind many times:
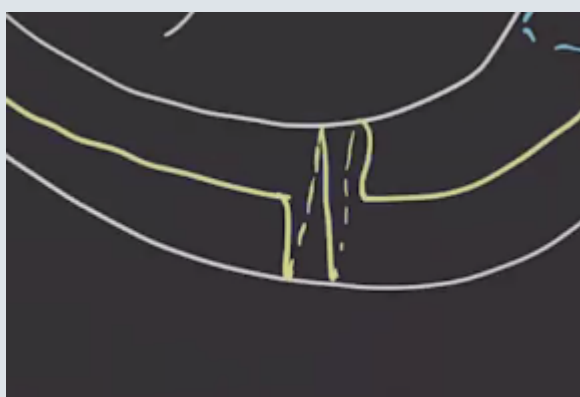
Figure 172: image_2021-04-06-11-19-05

We can then write any simple closed curve γ as $[\gamma] = p[\mu] + q[\lambda]$, where for shorthand we'll just write $\gamma = p\mu + q\lambda$. We'll refer to the pair (K, λ) as a **framed knot** and the corresponding

surgery as $M_{\frac{p}{q}}(K)$, which is surgery on K such that the following curve is $p\mu + q\lambda$:
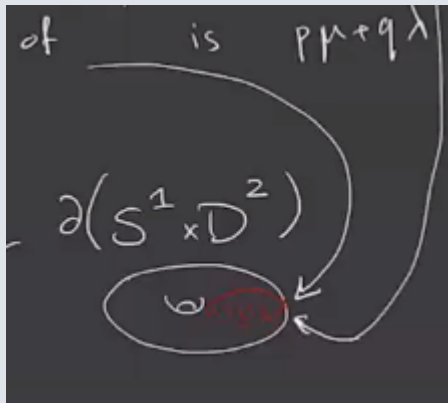
Figure 173: image_2021-04-06-11-22-32

We'll write $M_\lambda(L) = M_0(K)$ for the surgery that sends λ to this curve instead, since this corresponds to $p = 0, q = 1$.

Definition 22.1.2 (Triad of 3-Manifolds)
Suppose $\gamma_0, \gamma_1, \gamma_\infty$ are oriented simple closed curves on $\partial X = M - \operatorname{nd}(K)$ such that

$$-1 = \#(\gamma_0 \cap \gamma_1) = \#(\gamma_1 \cap \gamma_\infty) = \#(\gamma_\infty \cap \gamma_0),$$

and we have a cyclic ordering
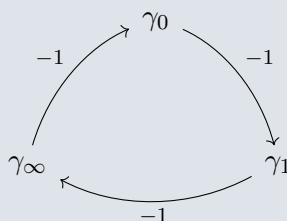
Link to Diagram

Then writing $M_i := M_{\gamma_i}(K)$, the triple (M_∞, M_0, M_1) is a **tried of 3-manifold**.

Example 22.1.3*(?):* Let $\gamma_\infty = \mu, \gamma_0 = \lambda, \gamma_1 = a\mu - b\lambda$, and the punch line is that the third is determined by the other two. What are a and b? We have

$$\#(\gamma_0, \cap \gamma_1) = \#(\lambda, a\mu + b\lambda) = -a\#(\mu \cap \lambda) = (-1)a \implies a = -1$$

$$\#(\gamma_1 \cap \gamma_\infty) = \#(a\mu + b\lambda, \mu) = b\#(\lambda \cap \mu) = b(1) = b \implies b = -1.$$

We thus obtain the following picture, which has the curves arrange in a clockwise fashion:
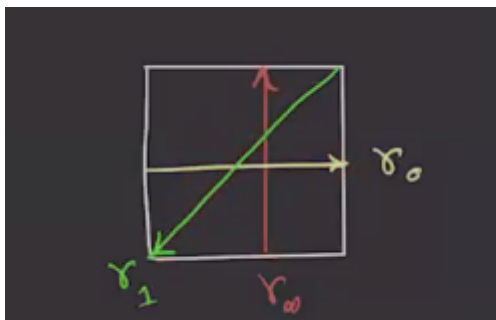
Figure 174: image_2021-04-06-11-32-35

Here we get the triad $(M_\infty(K) = M, M_0(K), M_1(K)$.

> **Exercise 22.1.4** (?)
> Show that $(M, M_{-1}(K), M_0(K))$ is also a triad.

Example 22.1.5(?): Let $\lambda_\infty = p\mu + q\lambda$ and $\lambda_0 = r\mu + s\lambda$, then

$$
\begin{aligned}
-1 &= \#(\gamma_\infty \cap \gamma_0) \\
&= \#(p\mu + q\lambda, r\mu + s\lambda) \\
&= ps\#(\mu \cap \lambda) + qr\#(\lambda \cap \mu) \\
&= -ps + qr \\
&\implies qr - ps = 1.
\end{aligned}
$$

Similarly,

$$
-1 = \#(\gamma_0 \cap \gamma_1) = sa - rb = -1\#(\gamma_1 \cap \gamma_\infty) \qquad = bp - aq = -1.
$$

Example 22.1.6(?): Pick a framed knot K (or really just a fixed longitude), then pick $\gamma_\infty = \mu, \gamma_0 = p\mu + \lambda$. Then $\gamma_1 = (p+1)\mu + \lambda$, and we get the triad $M_\mu(K) = M, M_{\gamma_0}(K) = M_p(K), M_{p+1}(K)$.

> **Theorem 22.1.7(?).**
> Suppose (M, M_0, M_1) is a triad, then there exist exact triangles:
>
> $$
> \widehat{\mathrm{HF}}(M_0) \xrightarrow{\quad \widehat{F}_0 \quad} \widehat{\mathrm{HF}}(M_1)
> $$
>
> with maps $\widehat{F}_\infty$ and $\widehat{F}_1$ to $\widehat{\mathrm{HF}}(M_\infty)$.
>
> *Link to Diagram*

Remark 22.1.8: Here exactness means that e.g. $\ker(\widehat{F}_1 = \operatorname{im}(\widehat{F}_0)$. There is a similar triangle for HF^+, as well as HF^∞ and HF^-, although these are more complicated. However, HF^- becomes easier to work with when one is looking at knot invariants instead.

Example 22.1.9*(?):* Let K be the unknot in S^3, and take as before $(S^3, S^3_0(K) = S^1 \times S^2, S^3_{+1}(K) = S^3$. We get the exact triangle

$$\widehat{\mathrm{HF}}(S^3) = \mathbb{Z}/2 \xrightarrow{\quad\widehat{F}_0\quad} \widehat{\mathrm{HF}}(S^1 \times S^2) = (\mathbb{Z}/2)^{\oplus 2}$$

$$\widehat{F}_\infty = 0 \qquad\qquad \widehat{F}_1$$

$$\widehat{\mathrm{HF}}(S^3) = \mathbb{Z}/2$$

Lemma 22.1.10*(?).*
Suppose the following is an exact triangle of vector spaces for some cyclic ordering:

$$V_0 \xrightarrow{\quad f_0 \quad} V_1$$

$$f_\infty \qquad\qquad f_1$$

$$V_\infty$$

Then

$$V_\infty = V_0 \oplus V_1 \iff \operatorname{rank} V_\infty = \operatorname{rank}(V_0) + \operatorname{rank}(V_1),$$

and if $f_0 = 0$ then f_1 is injective and f_∞ is surjective.

Proof (?).

$$\operatorname{rank} V_\infty \cong \operatorname{rank} \ker f_\infty \bigoplus \operatorname{rank} \operatorname{im} f_\infty$$
$$= \operatorname{rank} \operatorname{im} f_1 \oplus \operatorname{im} f_\infty$$
$$\leq \operatorname{rank} V_1 + \operatorname{rank} V_0.$$

Equality holds if and only if $\operatorname{rank} V_1 = \operatorname{rank} \operatorname{im} f_1$, which implies f_1 is injective, and similarly $\operatorname{rank} V_0 = \operatorname{rank} \operatorname{im} f_\infty \implies f_\infty$ is surjective. These together would imply that $f_0 = 0$. ∎

Example 22.1.11*(?):* For K the unknot in S^3, take the triad $(S^3, S^3_p(K) = L(p,1), L(p+1,1)$. This yields the exact triangle

$$\widehat{\mathrm{HF}}(S^3) = \mathbb{Z}/2 \xrightarrow{\quad\quad f_0 = 0 \quad\quad} \widehat{\mathrm{HF}}(L(p,1)) = (\mathbb{Z}/2)^{\oplus p}$$

with f_∞ and f_1 pointing to:

$$\widehat{\mathrm{HF}}(L(p+1,1)) = (\mathbb{Z}/2)^{\oplus p+1}$$

Link to Diagram

Remark 22.1.12: Note that this gives a way to produce L-spaces.

> **Definition 22.1.13** (L-spaces)
> Any $M \in \mathrm{QHS}^3$ is called an **L-space** if
> $$\mathrm{rank}\widehat{\mathrm{HF}}(M) = |H_1(M;\mathbb{Z})|.$$

Example 22.1.14*(?):* If p, q are coprime then $\widehat{\mathrm{HF}}L(p,q) = (\mathbb{Z}/2)^{\oplus p}$ since there is one $\mathrm{Spin}^{\mathbb{C}}$ class for each element of H^1. So $\mathrm{rank}\widehat{\mathrm{HF}} = p$, and on the other hand, $|H_1| = |\mathbb{Z}/p| = p$.

> **Exercise 22.1.15** (?)
> For any triad (M_∞, M_0, M_1) there exists a cyclic reordering such that
> $$|H_1(M_\infty)| = |H_1(M_0)| = |H_1(M_1)|,$$
> where we define
> $$|H_1(M)| = \begin{cases} \#H_1(M) & \text{if this is a finite group} \\ 0 & \text{otherwise.} \end{cases}$$

Example 22.1.16*(?):* For the triad $(S^3, L(p,1), L(p+1,1))$ we have
$$p + 1|H_1(L(p+1,1))| = \left|H_1(S^3)\right| + |H_1(L(p,1))| = 1 + p.$$

Remark 22.1.17: This exercise is useful because it can be used to prove the following:

> **Lemma 22.1.18*(?).***
> Suppose (M, M_0, M_1) is a triad with an ordering fixed such that
> $$|H_1 M| = |H_1 M_0| + |H_1 M_1|.$$
> If M_0, M_1 are L-spaces, then M is also an L-space.

> *Proof (?).*
> We have the exact triangle

$$|H_1 M_0| = \operatorname{rank}\widehat{\mathrm{HF}}(M_0) \longrightarrow |H_1 M_1| = \operatorname{rank}\widehat{\mathrm{HF}}(M_1)$$

$$f_\infty \qquad\qquad f_1$$

$$\widehat{\mathrm{HF}}(M_{)}$$

Link to Diagram

Thus

$$\operatorname{rank}\widehat{\mathrm{HF}}M \leq \operatorname{rank}\widehat{\mathrm{HF}}M_0 + \operatorname{rank}\widehat{\mathrm{HF}}M_1$$
$$\leq |H_1 M_0| + |H_1 M_1|$$
$$= |H_1 M|.$$

In general, $|H_1 M| \leq \operatorname{rank}\widehat{\mathrm{HF}}M$, so we get an equality $\operatorname{rank}\widehat{\mathrm{HF}}M = |H_1 M|$.

∎

Example 22.1.19*(?):* Let $K \subseteq S^3$ be a knot, and take the triad $(S^3, S_p^3(K), S_{p+1}^3(K))$. So if $S_p^3(K)$ is an L-space, so is $S_{p+1}^3(K)$. Inductively this shows that $S_n^3(K)$ is an L-space for all $n \geq p$.

Example 22.1.20*(?):* For $K = T_{p,q}$, the surgery $S_{pq-1}^3(T_{p,q})$ is a lens space. Thus $S_n^3(T_{p,q})$ is an L-space for all $n \geq pq - 1$.

23 | Surgery Exact Triangle and Knot Diagrams (Thursday, April 15)

Remark 23.0.1: Recall: let (M, M_0, M_1) be a triple of 3-manifolds corresponding to a knot $K \subseteq M$, where M_0 is 0-surgery, M_1 is 1-surgery, and M_∞ is ∞-surgery. Here M can be chosen such that M

- γ_∞ is a meridian of K,
- γ_0 is a longitude of K,
- $\gamma_1 = -\gamma_\infty - \gamma_0$

Then there exists an exact triangle:

$$\widehat{\mathrm{HF}}(M_0) \xrightarrow{\quad f_0 \quad} \widehat{\mathrm{HF}}(M_1)$$

$$f=f_\infty \qquad\qquad f_1$$

$$\widehat{\mathrm{HF}}(M)$$

Our goal is to define $f : \widehat{\mathrm{HF}}(M) \to \widehat{\mathrm{HF}}(M_0)$.

Remark 23.0.2: Note that M admits a Heegard diagram

$$(\Sigma_g, \vec{\alpha} = [\alpha_1, \cdots, \alpha_g], \vec{\beta} = [\alpha_1, \cdots, \alpha_g])$$

such that $(\Sigma_g, \vec{\alpha}, [\beta_1, \cdots, \beta_{g-1}]$ is a "diagram" for $M - \mathrm{nd}(K)$. Recall the notion of handlebodies, where each handle bounds a disc:
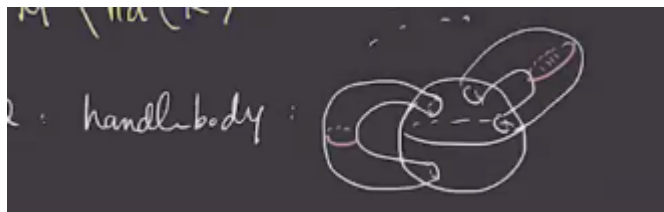
Figure 175: image_2021-04-15-11-20-29

We can generalize this to a **compression body**:
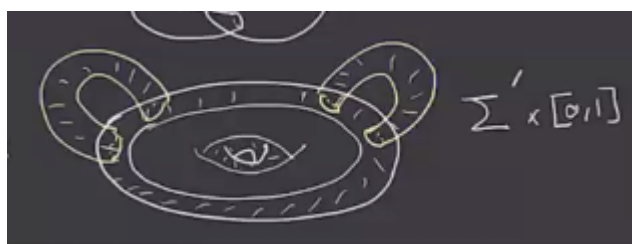
Figure 176: image_2021-04-15-11-22-13

- Start with $\Sigma'_{g'} \times [0, 1]$.
- Attach a solid handle K to $\Sigma' \times \{1\}$

This yields a cobordism from $\Sigma'_{g'} \times \{0\}$ to $\Sigma_{g'+k}$. So we can write $\partial C = \Sigma' \times \{0\} \coprod \Sigma$. Label the curves bounding the embedded discs as γ_i:
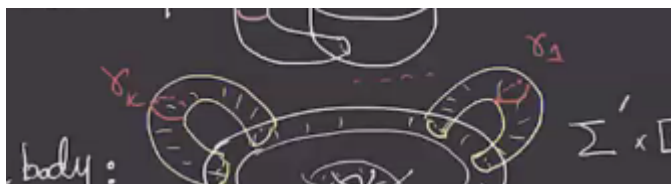
Figure 177: image_2021-04-15-11-24-22

Then we can form a diagram $(\Sigma_g, \{\gamma_1, \cdots, \gamma_k\}$ where $k \le g$ will specify the compression body. If

these are pairwise disjoint simple closed curves that are linearly independent in $H_1(\Sigma)$, this will be a compression body from a surface with genus $g - k$ to Σ_g.
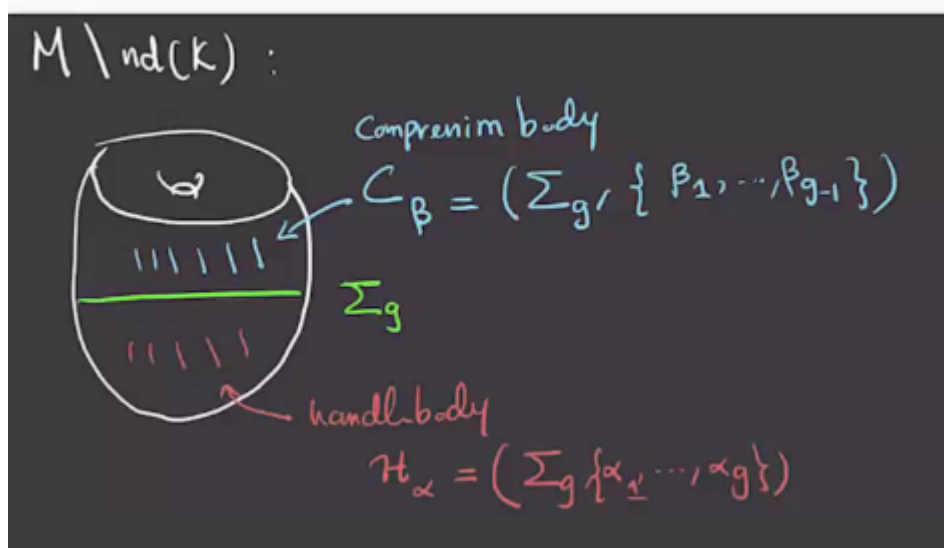
Figure 178: image_2021-04-15-11-31-50

In this case, $(\Sigma, \vec{\alpha}, \{\beta_1, \cdots, \beta_{g-1}\}$ will be a diagram for $M \setminus \mathrm{nd}(K)$.
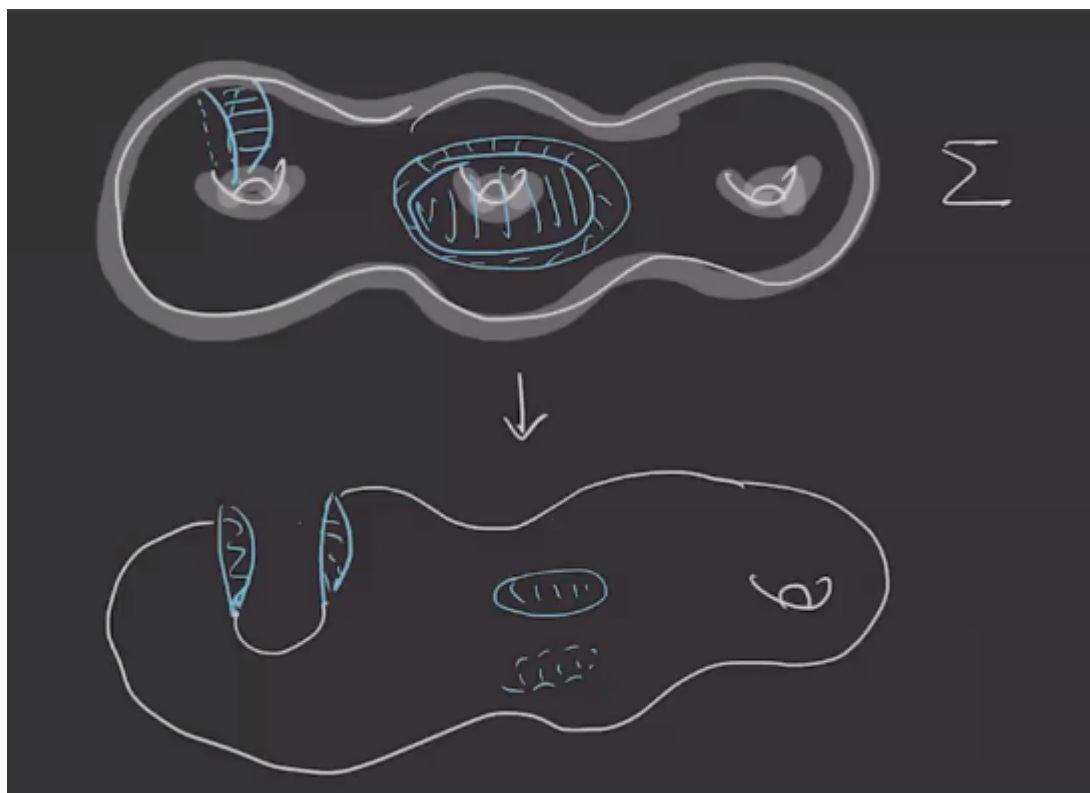
Figure 179: The cobordism from Σ to the compressionbody

Example 23.0.3*(?):* Consider $S^3 \setminus \mathrm{nd}(T)$ for T the trefoil. Behold the beautiful trefoil:

Figure 180: image_2021-04-15-11-37-56

After thickening, we obtain the following:
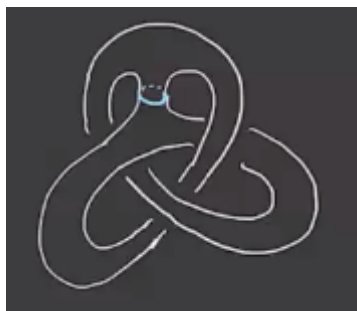
Figure 181: image_2021-04-15-11-39-41

We can push the top down:

Figure 182: image_2021-04-15-11-40-24

And wrap part of it around:
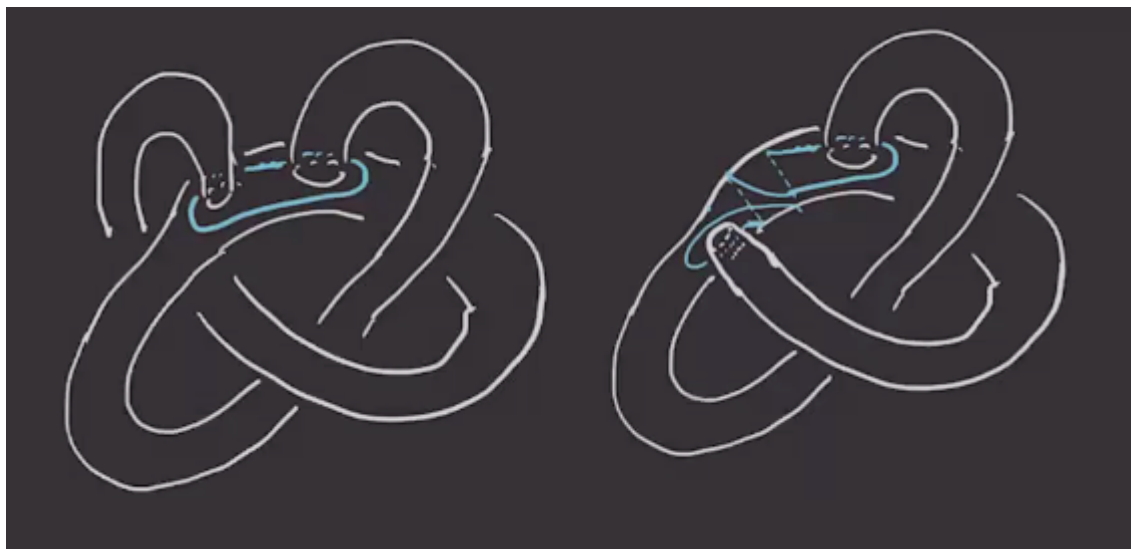
Figure 183: image__2021-04-15-11-43-42

We can keep moving this to undo the crossing:
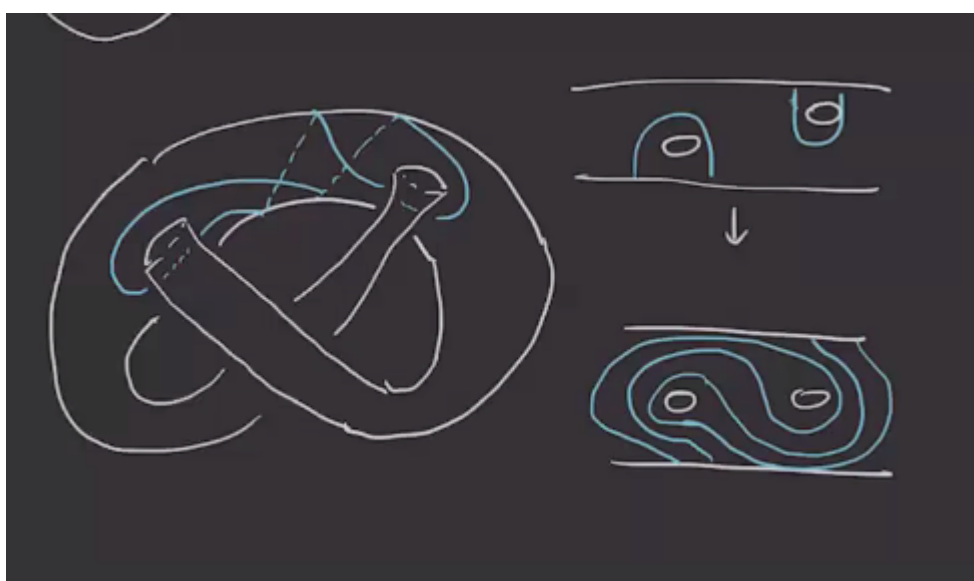
Figure 184: image__2021-04-15-11-45-58
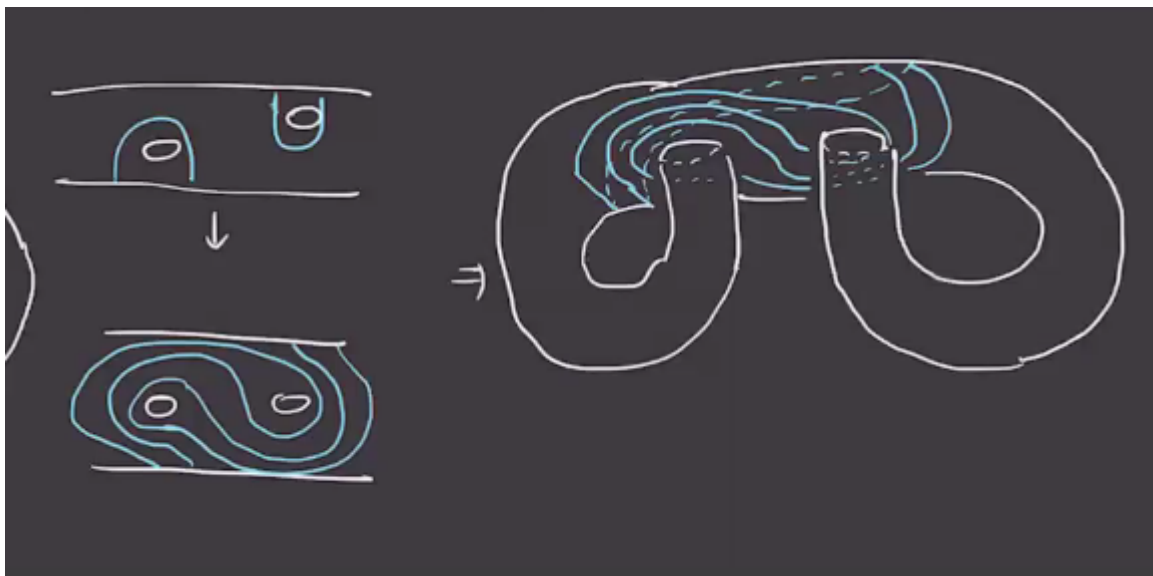
Figure 185: image_2021-04-15-11-47-36

So the blue curve gets complicated, but the neighborhood of T is a genus 2 surface, since the outer two circles bound discs. So in summary, we have the following process:
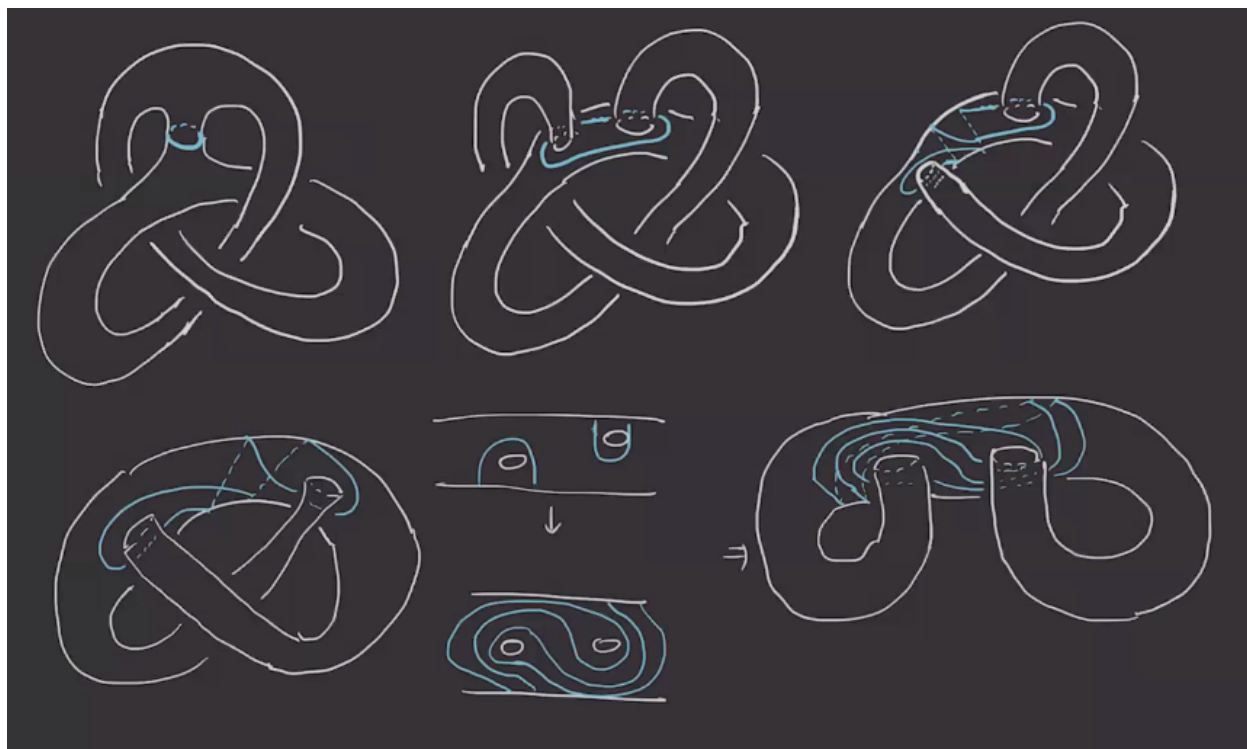
Figure 186: image_2021-04-15-11-50-12

We can represent this with a planar picture:

Figure 187: image_2021-04-15-11-56-01

Following the longitude, we obtain:
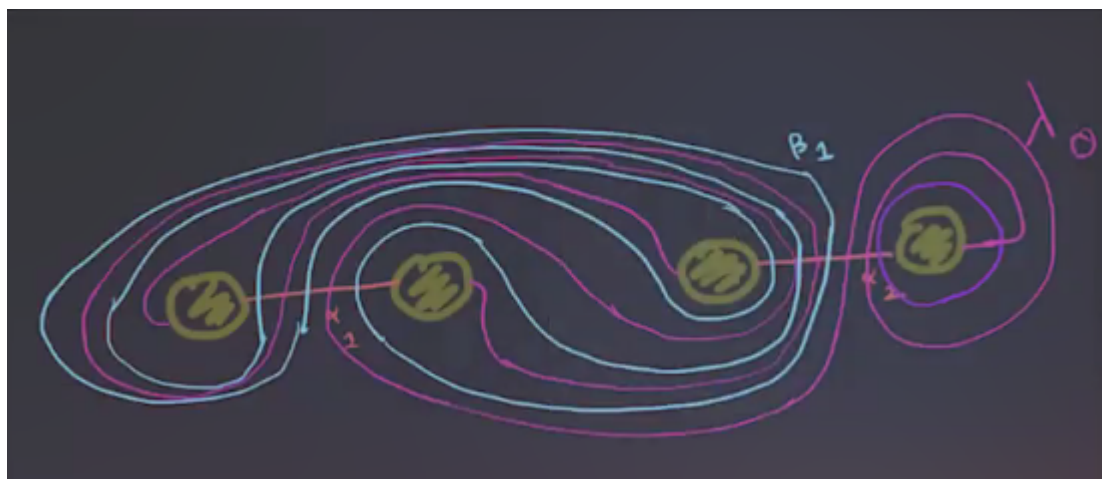
Figure 188: image_2021-04-15-12-15-41

Here λ has been wrapped twice, and to do n-surgery, we wrap n times.

Figure 189: image_2021-04-15-12-16-46

Exercise 23.0.4 (?)
Draw a diagram for S_n^3 (the figure eight).

ToDos

List of Todos

23

Definitions

Theorems

23

Exercises

Figures

List of Figures